NATIONAL TRANSPORTATION SAFETY BOARD

Office of Research and Engineering
Washington, D.C. 20594

December 21, 2021

Cockpit Visibility Study

by John O'Callaghan

Location:	Soldotna, Alaska
Date:	July 31, 2020
Time:	08:27 Alaska Daylight Time (ADT) / 16:27 Coordinated Universal Time (UTC)
Aircraft:	De Havilland DHC-2 Beaver, registration N4982U Piper PA-12, registration N2587M
NTSB#:	ANC20LA074A (Beaver) ANC20LA074B (Piper)

CONTENTS

NATIONAL TRANSPORTATION SAFETY BOARD

Office of Research and Engineering
Washington, D.C. 20594

December 21, 2021

Cockpit Visibility Study

by John O'Callaghan

A. ACCIDENT

Location:	Soldotna, Alaska
Date:	July 31, 2020
Time:	08:27 Alaska Daylight Time (ADT) / 16:27 Coordinated Universal Time (UTC)
Aircraft:	De Havilland DHC-2 Beaver, registration N4982U
	Piper PA-12, registration N2587M
NTSB#:	ANC20LA074A (N4982U)
	ANC20LA074B (N2587M)

B. GROUP

Not Applicable

C. SUMMARY

On July 31, 2020, at about 08:27 ADT, a de Havilland DHC-2 (Beaver) airplane, N4982U, and a Piper PA-12 airplane, N2587M, were destroyed when they collided in midair near Soldotna, Alaska. The pilots of both airplanes and the five passengers on the DHC-2 were fatally injured. The DHC-2 was operated as a Title 14 Code of Federal Regulations (CFR) Part 135 on demand charter flight. The PA-12 was operated as a Title 14 CFR Part 91 personal flight.

The float-equipped DHC-2, operated by High Adventure Charter, departed Longmere Lake, Soldotna, at about 08:24 bound for a remote lake on the west side of Cook Inlet. The purpose of the flight was to transport the passengers to a remote fishing location. The PA-12, operated by a private individual, departed Soldotna Airport, Soldotna, Alaska, at about 08:24 bound for Fairbanks, Alaska.

The *Aircraft Performance & CDTI Study* for this accident (Reference 1) presents the results of using recorded Automatic Dependent Surveillance – Broadcast (ADS-B) and radar-based Traffic Information Service – Broadcast (TIS-B) data to calculate the position and orientation of each airplane in the minutes preceding the collision. This information is then used to simulate the Cockpit Display of Traffic Information (CDTI) data that could have been presented to the pilots had both airplanes been equipped to provide this information.

This *Cockpit Visibility Study* presents the results of using the positions and orientations of the airplanes as defined in Reference 1 to estimate the approximate location of each airplane in the other airplane pilot's field of view.

The sections that follow summarize the airplane movements documented in Reference 1, and describe the methods used to calculate cockpit visibility from this data. The results of the visibility calculations are presented in the various Figures throughout the *Study*. Hereafter, the DHC-2 (N4982U) will be referred to as the "Beaver," and the PA-12 (N2587M) will be referred to as the "Piper."

D. DETAILS OF THE INVESTIGATION

I. Airplane flight tracks and collision geometry, per Reference 1

Figure 1 depicts the airplane flight tracks based on the ADS-B data (for the Piper) and TIS-B data (for the Beaver), as presented in Reference 1. The tracks are plotted in a Cartesian coordinate system centered on the Soldotna Airport (PASX) runway 7 threshold, with axes extending east, north, and up from the center of the Earth. The coordinates of the PASX runway 7 threshold are:

Latitude: 60° 28' 29.8631" N
Longitude: 151° 03' 07.5236" W
Elevation: 95.4 ft. MSL

The north and east positions, and altitudes, of the Beaver and the Piper are presented as a function of time in Figures 2 and 3, which are taken from Reference 1. For the visibility study, the position and altitude of the Piper are depicted by the solid blue lines in Figures 1-3, and the position and altitude of the Beaver are depicted by the solid green lines. See Reference 1 for a description of the other data plotted in these Figures.

The flight tracks plotted in Figures 1-3 result in the following time and location of the collision:

Time of collision = 08:26:32.3 ADT
East coordinate = 1.78 nm east of PASX runway 7 threshold
North coordinate = 1.66 nm north of PASX runway 7 threshold
Altitude = 1,210 ft. MSL

Additional performance parameters computed for each airplane in Reference 1 are presented here in Figures 4-6, as follows:

Figure 4 shows the true airspeed, calibrated airspeed, groundspeed, and rate of climb calculated from the smooth trajectories for the Beaver and the Piper. Figure 4 indicates that at the time of the collision, the Beaver's groundspeed was about 78 knots, and the Piper's groundspeed was about 70 knots.

Figure 5 shows the separation distance between the two airplanes and the closure rate. The Figure indicates that the closure rate was about 140 knots at the time of the collision.

Figure 6 presents the pitch, flight path, roll, heading, and ground track angles calculated from the smooth tracks for the Beaver and the Piper.

See Reference 1 for a description of the derivation of these additional performance parameters from the recorded ADS-B data.

II. Cockpit visibility study

Azimuth and elevation angles of "target" aircraft relative to "viewer" aircraft

Once the position and orientation of each airplane has been determined, its position in the body axis system of the other airplane can be calculated. These relative positions then determine where the "target" aircraft will appear in the field of view of the pilot of the "viewer" aircraft.

For this S*tudy*, the relative positions of the two airplanes (and the visibility of each from the other) were calculated at 1-second intervals up to the collision, beginning at 08:25:39 (53 seconds before the collision), when the Piper was about 1.9 nm west-southwest of the Beaver.

The "visibility angles" from the "viewer" airplane to the "target" airplane correspond to the angular coordinates of the line of sight between the airplanes, measured in a coordinate system fixed to the viewer airplane (the viewer's "body axis" system), and consist of the azimuth angle and elevation angle (see Figure 7). The azimuth angle is the angle between the x-axis and the projection of the line of sight onto the x-y plane. The elevation angle is the angle between the line of sight itself, and its projection onto the x-y plane. At 0° elevation, 0° azimuth is straight ahead, and positive azimuth angles are to the right. 90° azimuth would be out the right window parallel to the y axis of the airplane. At 0° azimuth, 0° elevation is straight ahead, and positive elevation angles are up. 90° elevation would be straight up parallel to the z axis. The azimuth and elevation angles depend on both the position (east, north, and altitude coordinates) of the viewer and target airplanes, and the orientation (yaw, pitch, and bank angles) of the viewer. The azimuth and elevation angles of points on the target away from its center of gravity (CG) also depend on the orientation of the target.

The position, altitude, and orientation of the Piper and the Beaver are based on smoothed and interpolated ADS-B / TIS-B data, and so are sensitive to different ways of smoothing the data, and the possibility of multiple, slightly differing trajectories and Euler angles that all result in solutions within the uncertainty bounds of the data. Consequently, there is also some uncertainty in the visibility angles associated with any particular trajectory. The effects of these uncertainties on the visibility of each airplane from the other are considered below.

Azimuth and elevation angles of airplane structures from laser scans

The target airplane will be visible from the viewer airplane unless a non-transparent part of the viewer's structure lies in the line of sight between the two airplanes. To determine if this is the case, the azimuth and elevation coordinates of the boundaries of the viewer's transparent structures (windows) must be known, as well as the coordinates of the viewer's structure visible from the cockpit (such as the wings, nose, and wing struts). If the line of sight passes through a non-transparent structure (such as the instrument panel, a window post, or a wing), then the target airplane will be obscured from the viewer.

For this *Study*, the azimuth and elevation angles of the windows and structures of the Piper and the Beaver were determined from the interior and exterior dimensions of exemplar airplanes, as measured using a FARO laser scanner.[1] The laser scanner produces a "point cloud" generated by the reflection of laser light off objects in the laser's path, as the scanner sweeps through 360° of azimuth and approximately 150° of elevation. The 3-dimensional coordinates of each point in the

[1] Specifically, the FARO "Focus 3D" scanner; see http://www.faro.com/en-us/products/3d-surveying/faro-focus3d/overview.

cloud are known, and the coordinates of points from multiple scans (resulting from placing the scanner in different positions) are "merged" by the scanner software[2] into a common coordinate system. By placing the scanner in enough locations so that the scanner can "see" every part of the airplane, the complete exterior and interior geometry of the airplane can be defined.

For this *Study*, the scanner was placed in several locations to scan the exterior of the airplanes, and in the pilot seats to scan the interior of the airplanes. The scanner software was then used to identify the points defining the outline of the cockpit windows (from the interior scans) and exterior structures visible from the cockpit (from the exterior scans). The coordinates were transformed into the airplane's body axis system and, ultimately, into azimuth and elevations angles from the pilot's eye position. The transformation method is described in Appendix A.

The azimuth and elevation angles of the viewer airplane's windows and other structures are very sensitive to the pilot's eye location in the cockpit. If the pilot moves his head forward or aft, or from a position centered over his seat to one close to a window surface, the view out the window (and the azimuth and elevation angles of all the airplane's structures) change significantly. This potential variability in the pilot's eye position, and the consequent variability in the location of the window edges and airplane structures in the pilot's field of view, is by far the greatest source of uncertainty as to whether the target aircraft is obscured or not at a given time.

To evaluate the effect of varying eye position on the visibility of the target airplane, the azimuth and elevation angles of the cockpit windows and other airplane structures were computed for a matrix of eye positions displaced from the nominal eye positions, as described below. The pilots' "nominal" eye positions were identified by scanning an individual of approximately the same stature as the accident pilots seated in the cockpit of each airplane.[3]

In addition to the calculation of the visibility angles, this *Study* presents recreations of possible views from the pilots' seats (including simulation-based depictions of the outside world) constructed assuming the nominal eye positions as defined above.

Results: azimuth and elevation angle calculations

The azimuth and elevation angles from the "viewer" airplanes to the "target" airplanes are shown as a function of time in Figure 8. In the top plot, the Piper is the "viewer" and the Beaver is the "target," and in the bottom plot, the Beaver is the "viewer" and the Piper is the "target."

Plots of the "target" airplane elevation angle vs. azimuth angle for the 53 seconds preceding the collision are shown in Figures 9 and 10, along with the azimuth and elevation coordinates of the "viewer" airplane cockpit windows and other structures, as computed for the nominal pilot eye position from the pilots' seats. Figure 9 presents the view from the pilot's seat of the Piper to the Beaver. The trajectory of the Beaver in the Piper pilot's field of view is depicted by the multicolored line labeled "BEAVER N4982U" (the line labeled "SUN" is described below). Figure 10 presents the view from the pilot's seat of the Beaver to the Piper.

In Figures 9 and 10, the window edges are outlined with a black line, the cockpit structures are colored gray, and the windows are colored white. The trajectory of the "target" airplane over time is

[2] FARO SCENE software: see http://faro-3d-software.com/.
[3] The individual in the scans is 68" tall; the Piper pilot was 70" tall; and the Beaver pilot was 68" tall.

depicted by the multicolored line, where the color of the line at any point indicates the time corresponding to that point, per the color scale in the Figures. If the multicolored line passes through a shaded area of the plot, the "target" airplane is obscured from view by the "viewer" airplane structure. The symbols on the line depict the target airplane position at 1 second intervals.

To further clarify the cockpit geometry and scan points depicted in Figures 9 and 10, scanner images of the cockpits are presented in Figures 11 and 12. Figure 11 is an image of the full 360° scan from the pilot's seat of the exemplar Piper. Figure 12 is a similar image from the pilot's seat of the exemplar Beaver. The areas of interest plotted in Figures 9 and 10 are highlighted by the yellow rectangles in Figures 11 and 12.

The azimuth and elevation angles of the sun are also of interest, because sun glare can affect a pilot's ability to see other aircraft. The azimuth (relative to true north) and altitude angles of the sun at the time and location of the accident were 84.44° and 17.71°, respectively.[4] To compute the location (azimuth and elevation angles) of the sun in the Piper and Beaver pilots' fields of view, the coordinates of the sun in earth coordinates were computed (using the sun angles and an assumed very large distance to the sun), and then transformed into the airplane body axis coordinates using the Euler angles shown in Figure 6. The azimuth and elevation angles of the sun were then computed from its body axis coordinates.

The results of these calculations indicate that the sun would have been behind the Beaver pilot's head and out of view. The azimuth and elevation angles of the sun from the pilot's seat of the Piper are depicted in Figure 9 as the multicolored line labeled "SUN." Note that both the Beaver and the sun were east of the Piper, and the trajectory of the sun in the Piper pilot's field of view was parallel to, and about 20° degrees of elevation above, the trajectory of the Beaver. Consequently, to spot the Beaver, the Piper pilot would have had to be looking towards the sun. The 08:56 PASX METAR indicated a ceiling of 8,500 ft. overcast, and photographs taken from the Beaver during the accident flight and presented in Reference 2 depict a broken cloud cover. Consequently, the sun might have been shaded by clouds as the airplanes converged.

Figure 10 indicates that the Piper would have been unobscured and visible through the Beaver's left windshield throughout the 53-second period considered in this *Study*. Figure 9 indicates that the Beaver would have been unobscured and visible through the Piper's right window from the beginning of the period considered (08:25:39) to just before 08:25:51 (12 seconds), and then would have been obscured behind the Piper's right wing root until about 08:25:58. The Beaver would then have appeared on the right edge of, or been obscured by, a structural support tube inside the cockpit from about 08:25:58 to about 08:26:04 (6 seconds). From 08:26:04 to the collision at 08:26:32.3 (28.3 seconds), the Beaver would have been unobscured and visible in the Piper's windshield, just to the left of the support tube.

As noted above, the azimuth and elevation angles of the window and cockpit structures are sensitive to the position of the pilot's eyes in the cockpit. To determine how these angles change as the pilot's eye position changes (e.g., by leaning in different directions, or by a seat height adjustment), plots similar to Figures 9 and 10 were generated for the 27 different eye positions shown in Table 1. The positions are expressed as displacements from the nominal eye position along the three airplane body axes ($\{\Delta x_b, \Delta y_b, \Delta z_b\}$[5]).

[4] These sun angles are cited in Reference 2 as obtained from www.suncalc.net.
[5] The body axis system is illustrated in Figure 7.

Case name	Δx_b from nominal, in. (+ forward, - aft)	Δy_b from nominal, in. (+ right, - left)	Δz_b from nominal, in. (+ down, - up)
CCD	0	0	+1.5
FCD	+3	0	+1.5
ACD	-3	0	+1.5
FLD	+3	-3	+1.5
CLD	0	-3	+1.5
ALD	-3	-3	+1.5
FRD	+3	+3	+1.5
CRD	0	+3	+1.5
ARD	-3	+3	+1.5
CCC (nominal)	0	0	0
FCC	+3	0	0
ACC	-3	0	0
FLC	+3	-3	0
CLC	0	-3	0
ALC	-3	-3	0
FRC	+3	+3	0
CRC	0	+3	0
ARC	-3	+3	0
CCU	0	0	-1.5
FCU	+3	0	-1.5
ACU	-3	0	-1.5
FLU	+3	-3	-1.5
CLU	0	-3	-1.5
ALU	-3	-3	-1.5
FRU	+3	+3	-1.5
CRU	0	+3	-1.5
ARU	-3	+3	-1.5

Table 1. Matrix of eye positions for cockpit structure azimuth and elevation angle calculations.

The results of the calculations are presented in Figure 13 for the Piper pilot's field of view, and in Figure 14 for the Beaver pilot's field of view. The trajectory of each "target" airplane in these figures is depicted by the solid black line with yellow symbols.

As shown in Figures 13 and 14, variations in the pilot's eye position from the nominal position changes where the target airplane appears in the viewer's field of view, and how and when the target airplane might become obscured by the viewer airplane's structure. For example, Figure 13 shows that the position of the Beaver relative to the right support tube behind the Piper's windshield is very sensitive to movements of the Piper pilot's eye position. At some eye positions, the Beaver is temporarily obscured by the support tube, but at others, the tube never obscures the Beaver. However, and in contrast, Figure 14 shows that even though the position of the Piper in the Beaver's windshield changes with the Beaver pilot's eye position, the Piper remains unobscured in the Beaver windshield throughout the period studied, at all eye positions considered in Table 1.

Figure 13 indicates that the visibility of one aircraft from the other can be very sensitive to the position of the pilots' eyes relative to the window structures. This observation underscores the fact that scanning for traffic visually can be more effective if pilots move their heads as well as redirect their eyes, since head movements may bring otherwise obscured aircraft into view.

Simulated views from the Piper and Beaver cockpits

While Figures 9, 10, 12 and 13 depict where the "target" airplanes could have appeared in the "viewer" airplanes' windows, they do not provide a sense of the background against which the targets would appear, and against which the pilot of each airplane would have to see the target. To provide a rough approximation of these backgrounds and of how the view from each cockpit evolved over time, the views from the cockpits were recreated in the *Microsoft Flight Simulator X* (*FSX*) simulation program, using airplane, sky, and terrain graphics inherent in *FSX*.

The cockpit structures at the nominal pilots' eye points (based on the laser scans) were constructed in *FSX* as semi-transparent panels that "mask" the view from each cockpit (see Appendix B); the cockpit geometries built into the airplane models in the simulation were not used. Airplane models were only used to represent the exterior "target" airplane geometry in the recreated views. The airplane models were edited to better represent the colors of the accident airplanes. The position (latitude, longitude, and altitude) and attitude (heading, pitch, and roll) of each airplane were recreated in *FSX* using the *FS Recorder* program developed by Matthias Neusinger,[6] based on the final estimated position and attitude data for each airplane described in Reference 1.

FSX contains inherent options to customize the time, date, and weather depiction in the simulation. The time and date were set to those of the accident (08:27 ADT on July 31, 2020), which results in the correct placement of the sun in the sky. The weather option was set to unlimited visibility[7] with overcast (8/8) stratus clouds at 8,500 ft., based on the 08:56 PASX METAR report, and photographs taken from the Beaver during the accident flight shortly before the collision (see Reference 2).

The view depicted by *FSX* depends on the program's "camera" settings. In this *Study*, the *FSX* camera is equivalent to the pilot's eyes: the view from the cockpit depends on the camera's position, orientation (where it's pointed), and its "field of view" (i.e., the range of azimuth and elevation angles that can be "seen" by the camera). The widest field of view available in *FSX* is 90° horizontally and about 62° vertically.[8] Consequently, if the camera is pointed straight ahead (0° azimuth), then only azimuth angles between -45° and +45° will be visible in that view. If objects of interest (e.g., the target airplane) are beyond this range, then to "see" them the camera will have to be rotated away from 0° azimuth toward the object. However, in this case, a portion of the view straight-ahead will be lost, which may be unsatisfactory for the purpose of giving the viewer a good sense of the airplane's direction of travel and general situation relative to the outside world.

To see objects beyond ±45° of azimuth while at the same time preserving a field of view of at least ±45° of azimuth about the direction of travel, the view from two co-located cameras can be joined side-by-side: the first camera pointed away from 0° azimuth to capture the object, and the second camera pointed in such a way that the boundaries of the fields of view of the cameras coincide at a particular azimuth angle. For example, if one camera is rotated to -45° azimuth, the left boundary of its field of view will be at -45° - 45° = -90°, and the right boundary will be at -45° + 45° = 0°. If the second camera is rotated to +45° azimuth, its left boundary will be at +45° - 45° =0° (coinciding with

[6] This program used to be available at http://www.fs-recorder.net/, but the website is no longer operational.
[7] The 08:56 ADT PASX METAR reported the visibility as 10 statute miles, but to compensate for the limited resolution of the computer display (for which the size of distant but theoretically visible objects can be smaller than a pixel), the visibility in *FSX* was set to "unlimited" in order to display pixels representing the target airplanes as soon as possible.
[8] These values are for an *FSX* window with an aspect ratio of 1.6, at a "zoom" setting of 0.3.

the right boundary of the first camera), and its right boundary will be at +45° + 45° = +90°. Setting the views from the cameras side-by-side, a continuous field of view from -90° to +90° is obtained.

However, discontinuities (kinks) in straight lines may appear at the boundary of these views when they are viewed side-by-side on a flat surface (such as a computer screen), because the viewer will be viewing both from the same angle, whereas the view on the left is intended to be viewed at an angle rotated 90° from that on the right. The discontinuities can be removed if each view is presented on a separate surface (monitor), and then the surfaces are joined at a 90° angle. However, this solution may be impractical (and is impossible for presenting screenshots of these views in a single document), and so the line discontinuities at the boundaries of the views may simply need to be tolerated. At non-zero roll angles, the slope of the horizon line is discontinuous at the boundary between the views, but there is no break in the horizon line itself.

As shown in Figure 10, the Beaver appeared in the Piper pilot's field of view between azimuth angles of 10° to 70°. However, between 08:25:51 and 08:25:58, the Beaver would have been obscured by the Piper's right wing root, and so the period of most interest is the 34.3 seconds between 08:25:58 and the collision at 08:26:32.3, when the Beaver would have appeared in the Piper's windshield and might have been temporarily obscured by the support tube. Consequently, for this *Study* a single camera, pointed straight ahead (with azimuth and elevation angles of 0°) is used to depict the forward view from the Piper, covering azimuth angles between -45° and 45°. An identical camera is used to depict the view of the Piper from the Beaver.

Screenshots of the Piper cockpit recreation are presented in Figures 15a-h. The times of the screenshots correspond to the events listed in Table 2, which include the times corresponding to the simulated Cockpit Display of Traffic Information (CDTI) screens presented in Figures 13-17 of Reference 1. The simulated CDTI screens for the Piper presented in Reference 1 are reproduced here in Figure 15, together with the corresponding *FSX* cockpit view. See Reference 1 for a description of the CDTI screens, and the traffic alerts depicted on those screens. The locations of the Beaver in Figures 15a-h are highlighted by the yellow circles, though the airplane itself may be too small to be seen in some of the *FSX* images.

Screenshots of the Beaver cockpit recreation are presented in Figures 16a-h. The times of these screenshots are identical to those in Figure 15 (corresponding to the events listed in Table 2). The simulated CDTI screens for the Beaver presented in Reference 1 are reproduced here in Figure 16, together with the corresponding *FSX* cockpit view. The locations of the Piper in Figures 16a-h are highlighted by the yellow circles, though the airplane itself may be too small to be seen in some of the *FSX* images.

Time (ADT)	Time before collision (seconds)	Horizontal separation (nm)	Vertical separation (ft)	Closure rate (kt)	Simulated traffic alerts (See Reference 1)
08:25:51	41.3	1.58	281	97	
08:26:00	32.3	1.30	245	134	
08:26:06	26.3	1.06	204	146	1st ATAS alerts to both airplanes (PAZ alerts)
08:26:13	19.3	0.78	162	141	2nd ATAS alert to Beaver (CAZ alert)
08:26:23	9.3	0.37	110	155	2nd ATAS alert to Piper (CAZ alert)
08:26:27	5.3	0.21	65	143	
08:26:29	3.3	0.13 (785 ft.)	36	141	
08:26:31	1.3	0.05 (309 ft.)	12	140	

Table 2. Times corresponding to recreated cockpit views and CDTI displays in Figures 15 and 16.

A measure of the size of the "target" airplane in the field of view of the "viewer" is the difference in azimuth and elevation angles between different points on the "target." For this *Study*, the azimuth and elevation angles of the nose, tail, center, and left and right wingtips of the targets were computed (the angles plotted in Figures 9, 10, 13, and 14 correspond to the center of the targets). The difference in azimuth and elevation angles between the nose and the tail of the targets are presented as a function of time in Figure 17 as the lines labeled "Δ azimuth, fuselage" and "Δ elevation, fuselage." The difference in angles between the left and right wingtips are presented as the lines labeled "Δ azimuth, wings" and "Δ elevation, wings." In these calculations, the nose, tail, and wingtips are assumed to lie in a plane, and so the airplanes in this representation have zero thickness. Hence, the information in Figure 17 does not represent the size of the *area* of the target presented to the viewer (which is what makes the target visible), but only the extent of a subset of dimensions that contribute to the area. Nonetheless, Figure 17 does provide a measure of the target size, and of the very sudden increase in size (called the "blossom" effect) within a few seconds of the collision. Reference 3 indicates that on average, in ideal conditions people can see an object that spans at least 0.01° of the field of view, when looking directly at the object. However, the actual visual detection threshold depends on many factors, including viewer age, contrast, illumination, color, and the viewer's focus. Consequently, Figure 17 should not be used to determine a specific time at which the pilots "should" have been able to see the other airplane.

The yellow highlighted area in the top plot of Figure 17 indicates the time period (from 08:25:51 to 08:26:04) during which, with the Piper pilot's eyes at the nominal position, the center of the Beaver would have been obscured from the Piper pilot's view by the Piper's right wing root (from 08:25:51 to 08:25:58), and *might* have been obscured from view by the right support tube (from 08:25:58 to 08:26:04), consistent with Figure 9. At all other times, the Beaver would not have been obscured from the Piper pilot's view. The Piper would never have been obscured from the Beaver pilot's view.

During the 28.3 seconds prior to the collision (from 08:26:04 to 08:26:32.3), the Beaver would have appeared in the Piper pilot's view just to the left of the Piper's right support tube as a small object below the horizon, moving slowly against the background terrain. This complex background (compared to a sky background) might have made detecting the Beaver more difficult.

Throughout the 53-second period examined, the Piper would have appeared in the Beaver's windshield as a small object above the horizon, moving slowly within a small area and against a

background of sky and cloud. The light color of the Piper's fuselage might have provided little contrast against this background, making it more difficult to detect.

The ADS-B Traffic Advisory System (ATAS) alerts depicted in Figures 15 and 16 are described and discussed in Reference 1.

The circumstances of this accident underscore the difficultly in seeing airborne traffic (the foundation of the "see and avoid" concept in visual meteorological conditions (VMC)), particularly when the pilots have little or no warning of traffic in the vicinity. CDTI equipment with aural alerts can help to make pilots aware of surrounding traffic, and prompt them to look in the right direction for conflicting traffic. As stated in Reference 1,

> If both airplanes had been equipped with ADS-B Out and In, and with CDTI displays capable of ATAS alerts, it is possible that both pilots could have been made aware of the presence of the other airplane at least as soon as they were within line-of-sight of each other (say, by the time the Beaver climbed to 500 ft. MSL), or by 08:25:01 (about a minute and a half before the collision). Simulations of CDTI displays for both airplanes (that assume both airplanes were equipped as described above) indicate that at 08:26:06 (26.3 seconds before the collision), each airplane would have received an aural and visual ATAS alert concerning the other, as they penetrated each other's PAZ. The Beaver would also have received a second ATAS alert 19.3 seconds prior to the collision, as the ATAS algorithm predicted it would penetrate the Piper's CAZ, and the Piper would have received a second ATAS alert 9.3 seconds prior to the collision, as the ATAS algorithm predicted it would penetrate the Beaver's CAZ. The CDTI displays on both aircraft would have depicted the airplanes in alert status (solid yellow arrowheads enclosed in a yellow circle) converging on each other up until the collision.
>
> The Beaver was not equipped with ADS-B equipment or CDTI. However, the Piper was equipped with a Garmin G3X Touch system that included ADS-B Out and In capability and a CDTI capable of producing aural alerts (though the alerting algorithm and aural alert phraseology of the G3X Touch differ from those of the ATAS algorithm described in DO-317B). The pilot can disable traffic alerts on the system, and it is not known whether the alerts were enabled on the accident flight (though the alerts are automatically enabled with each power cycle). In addition, while the FAA confirmed that there was an opportunity for the Piper to have received TIS-B messages regarding the Beaver, it cannot be determined conclusively that the Piper in fact received those messages. If the Piper did receive the TIS-B messages and the G3X system was on with alerts enabled, then the system could have generated visual alerts and a single aural alert concerning the Beaver similar to those depicted in the CDTI simulations presented in this *Study*.

E. CONCLUSIONS

This *Cockpit Visibility Study* presents the results of using recorded ADS-B data and the airplane Euler angles computed in Reference 1 to estimate the approximate location of each airplane in the other airplane's windows during the 53 seconds prior to the collision. The time and coordinates of the collision determined in Reference 1 are:

Time of collision = 08:26:32.3 ADT
East coordinate = 1.78 nm east of PASX runway 7 threshold
North coordinate = 1.66 nm north of PASX runway 7 threshold
Altitude = 1,210 ft. MSL

The visibility of one airplane from another is sensitive to the position of the pilot's eyes relative to the cockpit windows. This sensitivity is illustrated in Figures 13 and 14, which underscore the fact that looking for traffic can be more effective if pilots move their heads as well as redirect their eyes, since

head movements may bring otherwise obscured aircraft into view. The descriptions of visibility that follow correspond to the pilots' eyes in their nominal positions, with the understanding that the views out the windows change if the pilots move their heads.

Figure 10 indicates that the Piper would have been unobscured and visible through the Beaver's left windshield throughout the 53-second period considered in this *Study*. Figure 9 indicates that the Beaver would have been unobscured and visible through the Piper's right window from the beginning of the period considered (08:25:39) to just before 08:25:51 (12 seconds), and then would have been obscured behind the Piper's right wing root until about 08:25:58. The Beaver would then have appeared on the right edge of, or been obscured by, a structural support tube inside the cockpit from about 08:25:58 to about 08:26:04 (6 seconds). From 08:26:04 to the collision at 08:26:32.3 (28.3 seconds), the Beaver would have been unobscured and visible in the Piper's windshield, just to the left of the support tube.

As the NTSB has noted in other mid-air collision investigations,[9] CDTI equipment can provide pilots with precise bearing, range, and altitude information about traffic targets, long before any target becomes a collision threat. Such timely and information-rich traffic presentations can help pilots to visually acquire other aircraft, and to avoid them using only slight course and / or altitude adjustments, without the need for aggressive maneuvering. In this accident, the Beaver was not equipped with ADS-B equipment or CDTI, but the Piper was equipped with a Garmin G3X Touch system that included ADS-B Out and In capability and a CDTI capable of producing aural alerts. However, it cannot be determined conclusively whether aural alerts were enabled in the Piper's Garmin G3X system, or whether the Piper in fact received traffic messages concerning the Beaver.

_____

John O'Callaghan
National Resource Specialist - Aircraft Performance
Office of Research and Engineering

[9] See References 4-8.

F. REFERENCES

1. National Transportation Safety Board, Office of Research and Engineering, *Aircraft Performance & CDTI Study, De Havilland DHC-2 Beaver N4982U / Piper PA-12 N2587M, Soldotna, Alaska, July 31, 2020, NTSB # ANC20LA074AB,* March 3, 2021. (Contact NTSB at pubinq@ntsb.gov.)
2. National Transportation Safety Board, Office of Aviation Safety, *Weather Factual Report, De Havilland DHC-2 Beaver N4982U / Piper PA-12 N2587M, Soldotna, Alaska, July 31, 2020, NTSB # ANC20LA074AB,* March 3, 2021. (Contact NTSB at pubinq@ntsb.gov.)
3. Velasco e Cruz, A. *Historical Roots of 20/20 as a (Wrong) Standard Value of Normal Visual Acuity*, Optometry and Vision Science Journal, Vol. 67, No.8, p. 661, March 30, 1990. Copyright © American Academy of Optometry.
4. National Transportation Safety Board, Office of Research and Engineering, *Aircraft Performance Radar & Cockpit Visibility Study, C150M N3601V / F-16CM 96-0085, Moncks Corner, SC, July 7, 2015, NTSB # ERA15MA259AB,* September 23, 2016. Available at: https://dms.ntsb.gov/public/59000-59499/59235/596875.pdf.
5. National Transportation Safety Board, Office of Research and Engineering, *Aircraft Performance Radar & Cockpit Visibility Study, C172M N1285U / NA265-60SC N442RM, San Diego, CA, August 16, 2015, NTSB # WPR15MA243AB,* October 11, 2016. Available at: https://dms.ntsb.gov/public/59000-59499/59067/596176.pdf.
6. National Transportation Safety Board, Office of Research and Engineering, *Aircraft Performance & Cockpit Visibility Study, C208B N752RV / PA-18-150 N82452, Russian Mission, AK, August 31, 2016, NTSB # ANC16FA061AB,* November 30, 2017. Available at: https://dms.ntsb.gov/public/61500-61999/61841/620464.pdf.
7. National Transportation Safety Board, Office of Research and Engineering, *Aircraft Performance & Cockpit Visibility Study, PA-34-200 N16281 / C172N N6428D, Miami, FL, July 17, 2018, NTSB # ERA18FA194AB,* April 22, 2019. Available at: https://dms.ntsb.gov/public/62500-62999/62604/626186.pdf.
8. National Transportation Safety Board, Office of Research and Engineering, *Aircraft Performance & Cockpit Visibility Study, De Haviland DHC-2 (Beaver) N952DB / De Havilland DHC-3 (Otter) N959PA, Ketchikan, Alaska, May 13, 2019, NTSB # CEN19MA141AB,* July 28, 2020. Available at: https://data.ntsb.gov/Docket/Document/docBLOB?ID=10009099&FileExtension=pdf&FileName=CEN19MA141AB_ADSB%20study%20E-Rel.pdf

FIGURES

ANC20LA074AB: Midair collision, DHC-2 Beaver N4982U / Piper PA-12 N2587M, Solotna, AK, 7/31/2020

Plan view of ADS-B and TIS-B data for Beaver and Piper (grid background)

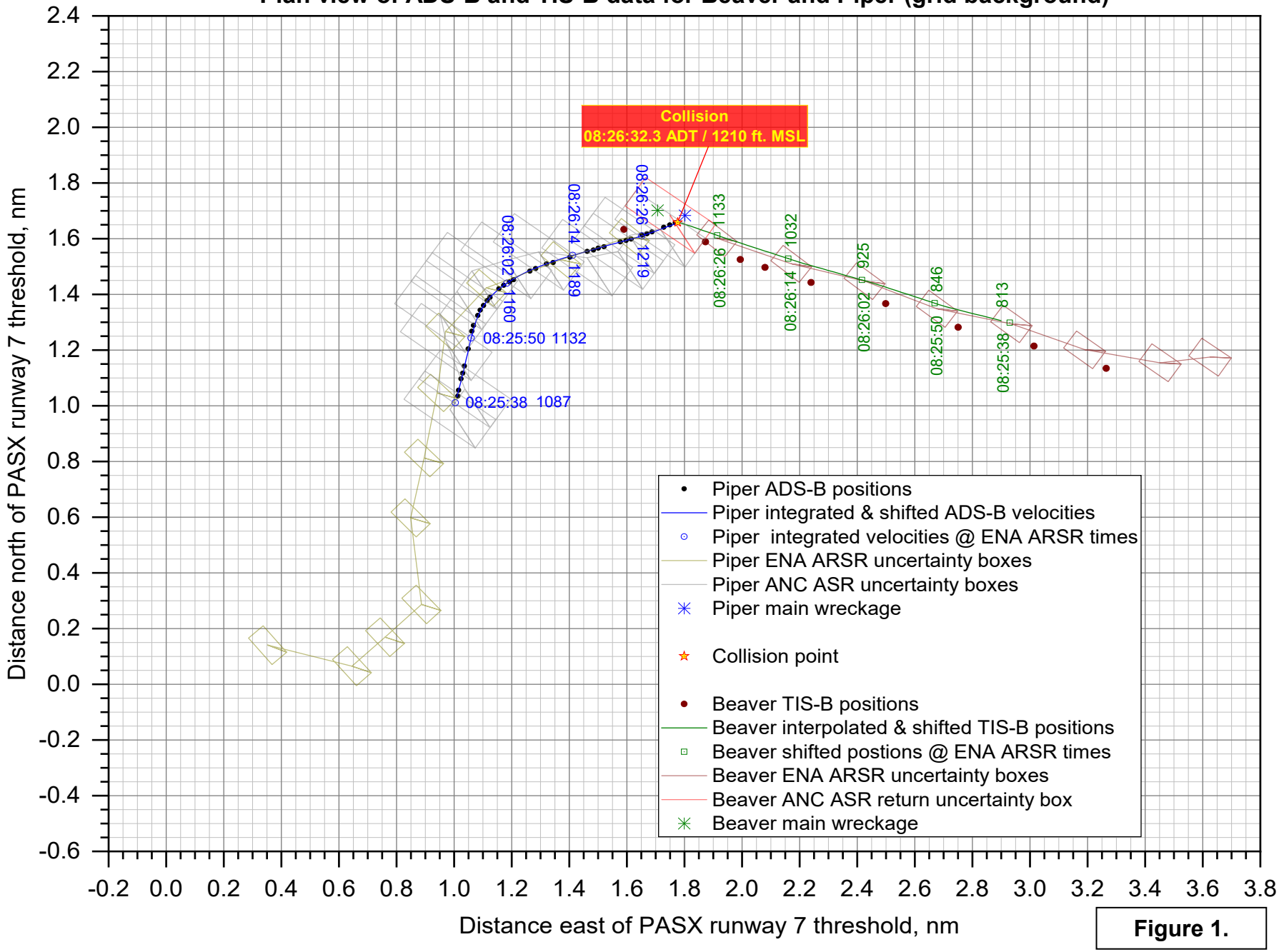

Figure 1.

ANC20LA074AB: Midair collision, Beaver N4982U / Piper N2587M, Solotna, AK, 7/31/2020

Beaver and Piper north and east coordinates vs. time

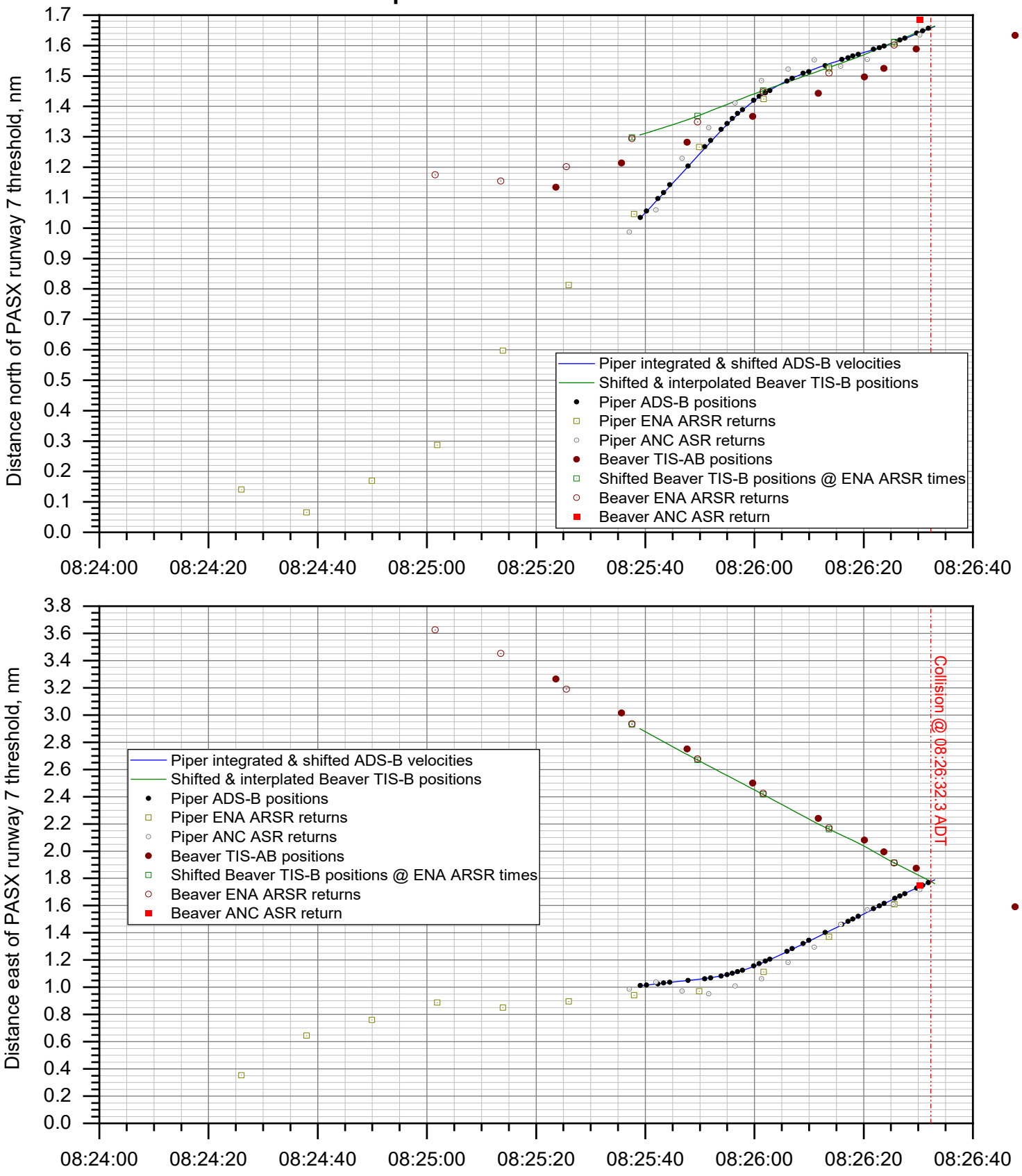

Figure 2.

ANC20LA074AB: Midair collision, DHC-2 Beaver N4982U / Piper PA-12 N2587M, Solotna, AK, 7/31/2020

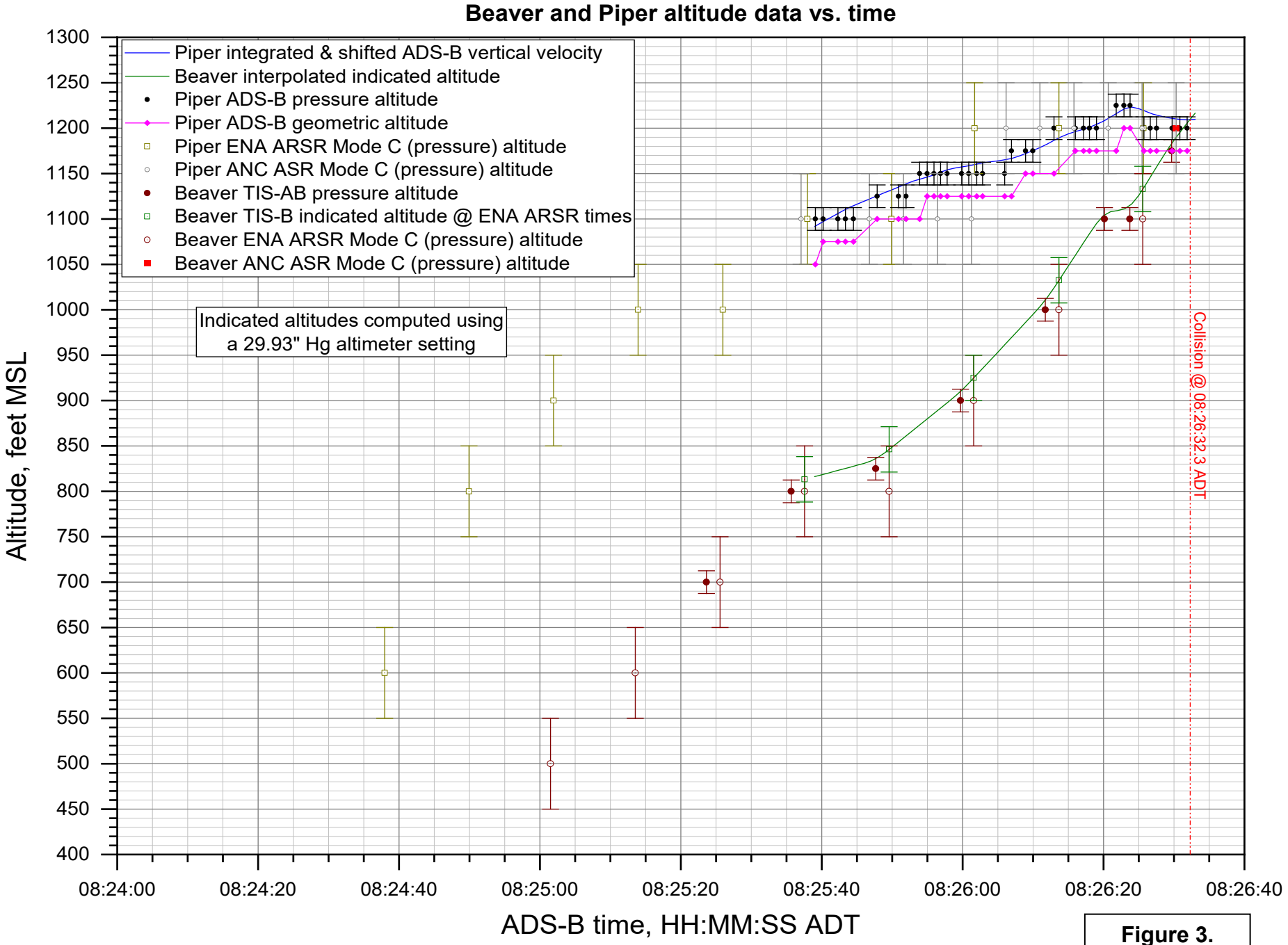

Figure 3.

ANC20LA074AB: Midair collision, Beaver N4982U / Piper N2587M, Solotna, AK, 7/31/2020

Beaver and Piper speeds and rate of climb

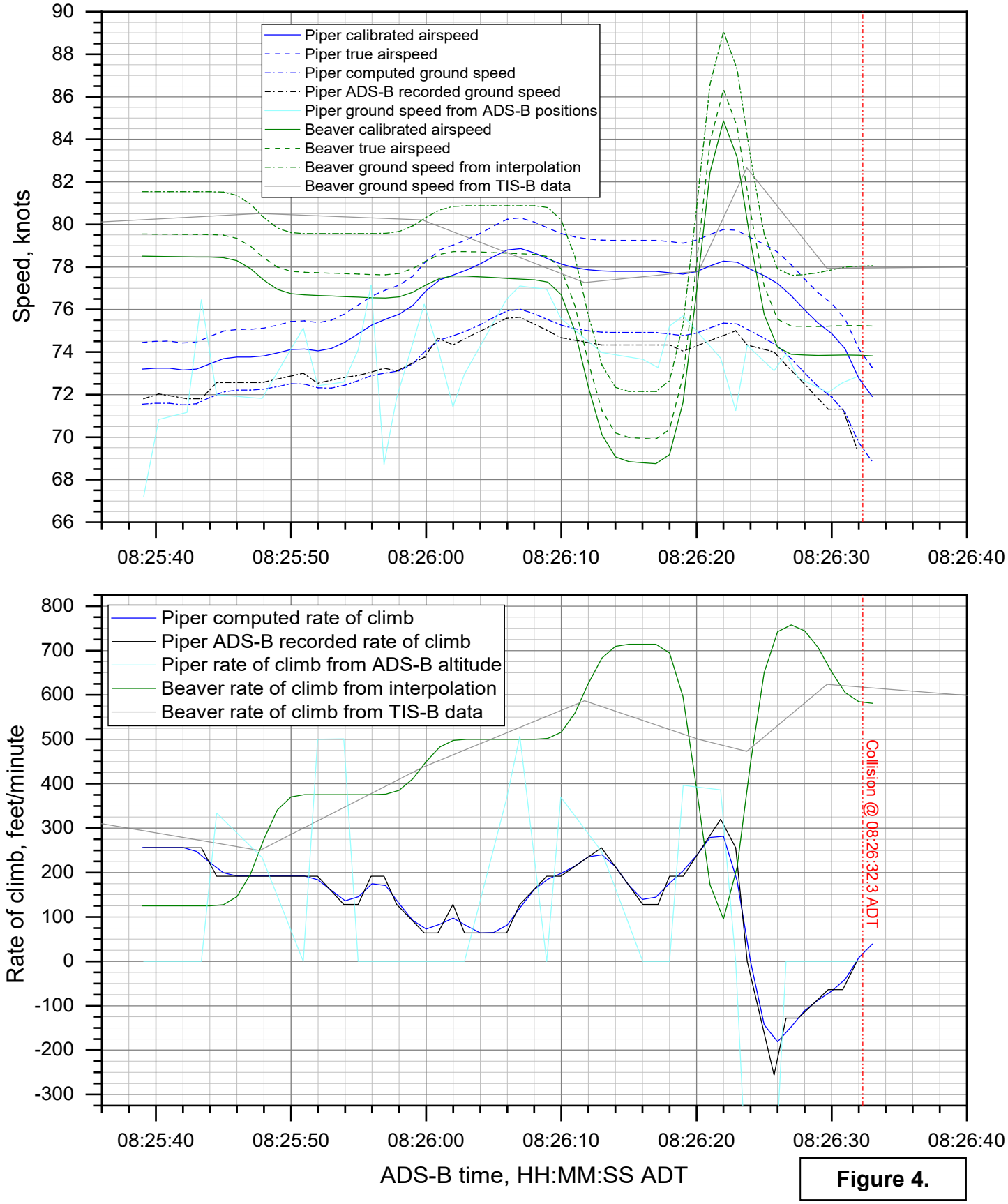

Figure 4.

ANC20LA074AB: Midair collision, Beaver N4982U / Piper N2587M, Solotna, AK, 7/31/2020

Beaver and Piper separation distance and closure rate

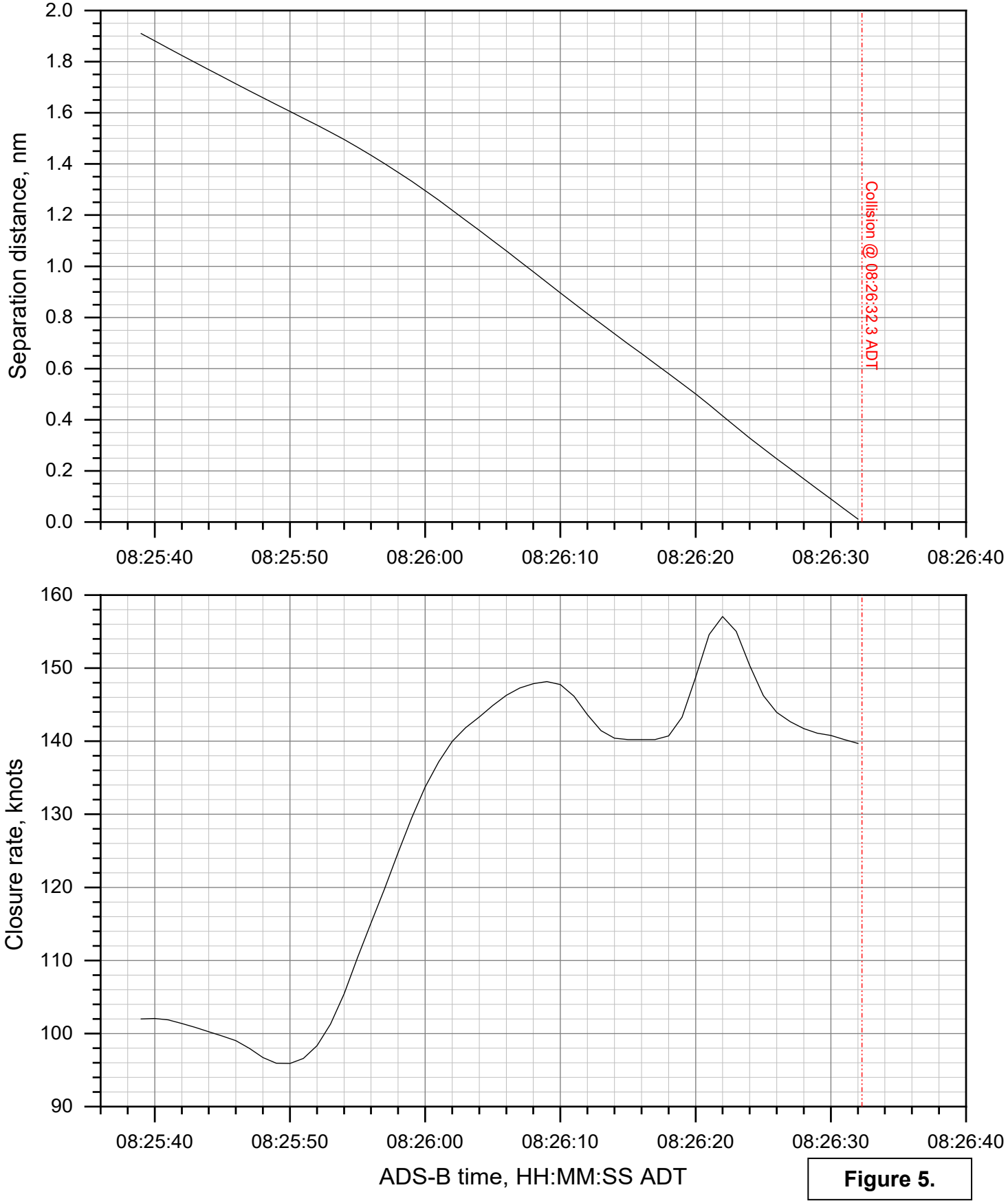

Figure 5.

ANC20LA074AB: Midair collision, Beaver N4982U / Piper N2587M, Solotna, AK, 7/31/2020

Beaver and Piper Euler angles

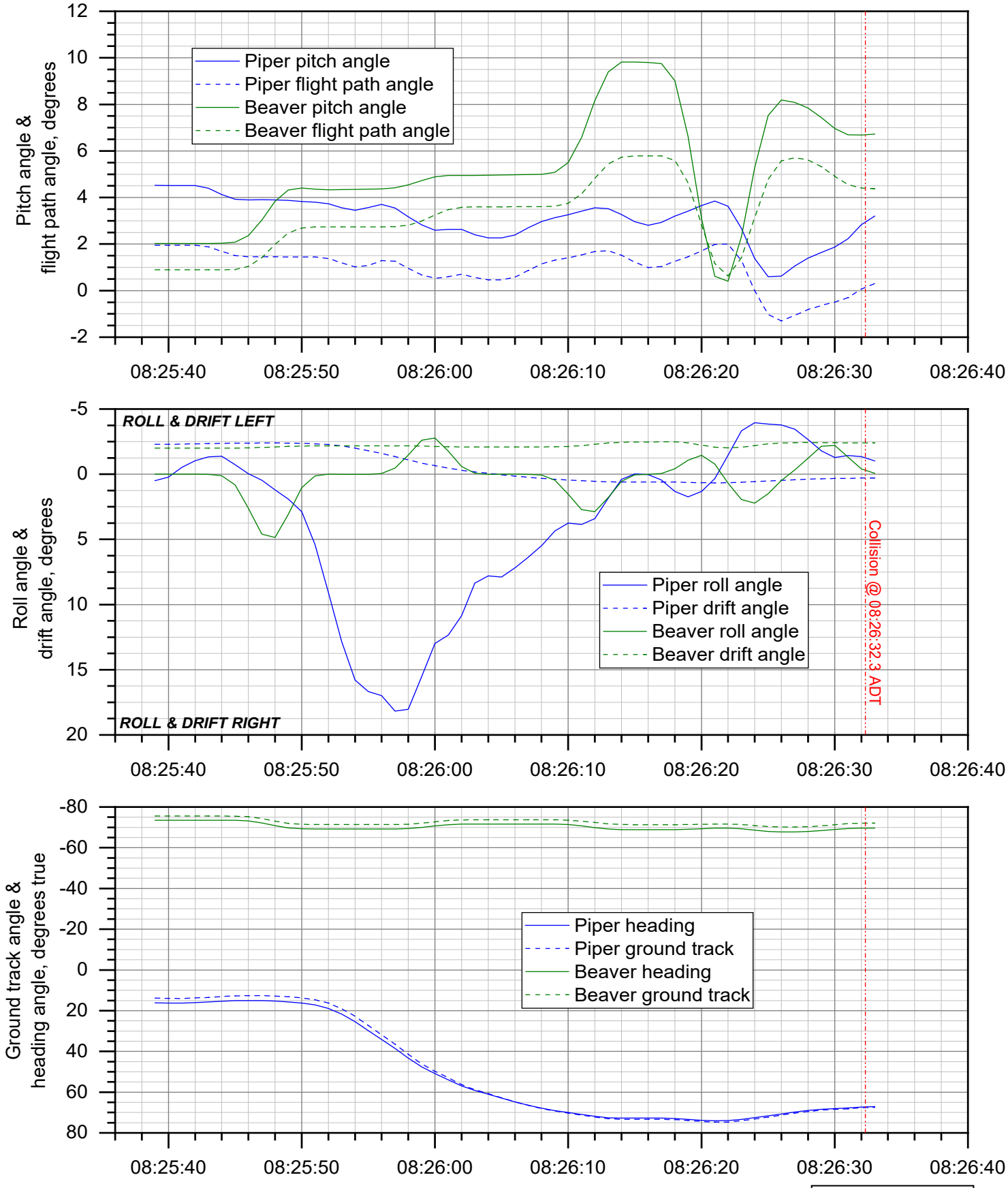

Figure 6.

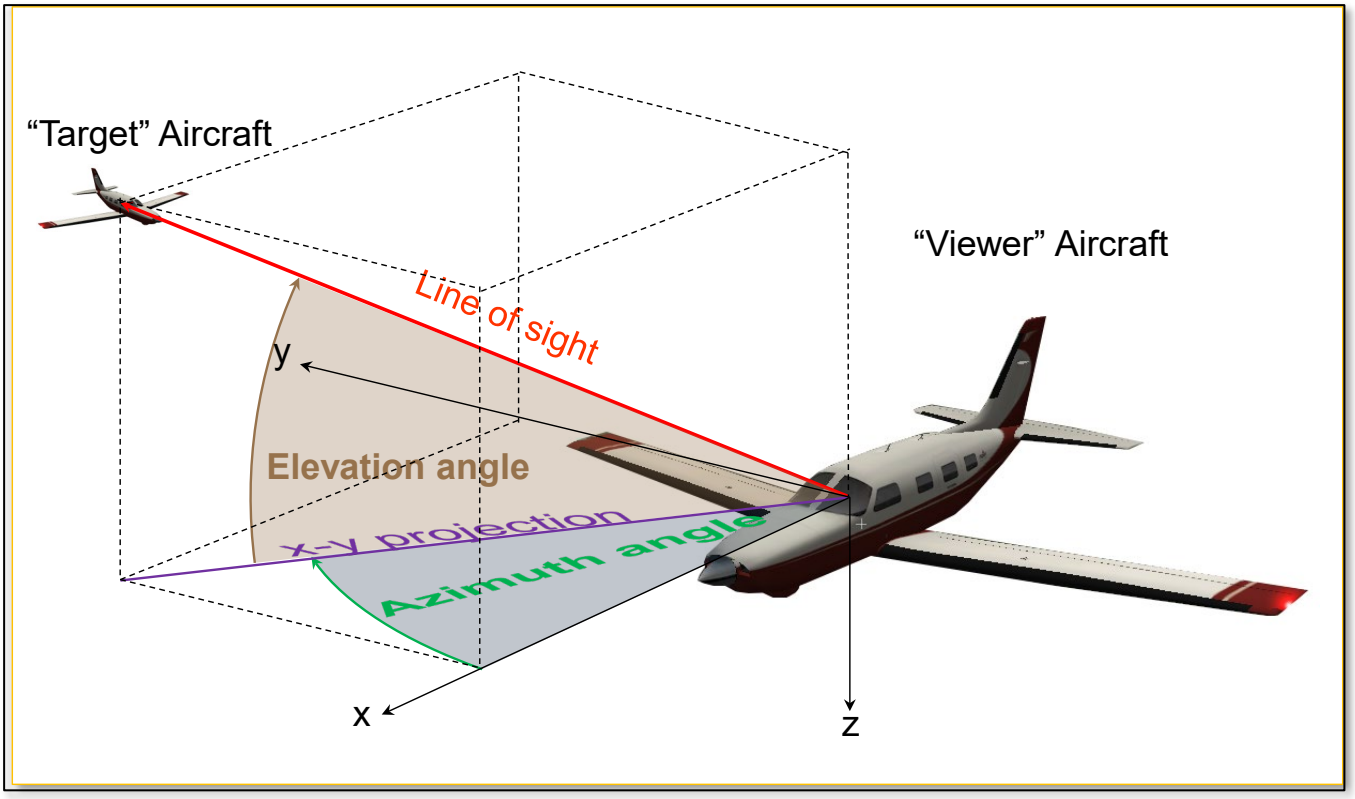

Figure 7. Azimuth and elevation angles from "viewer" airplane to "target" airplane.

ANC20LA074AB: Midair collision, Beaver N4982U / Piper N2587M, Solotna, AK, 7/31/2020

Beaver and Piper azimuth & elevation viewing angles vs. time

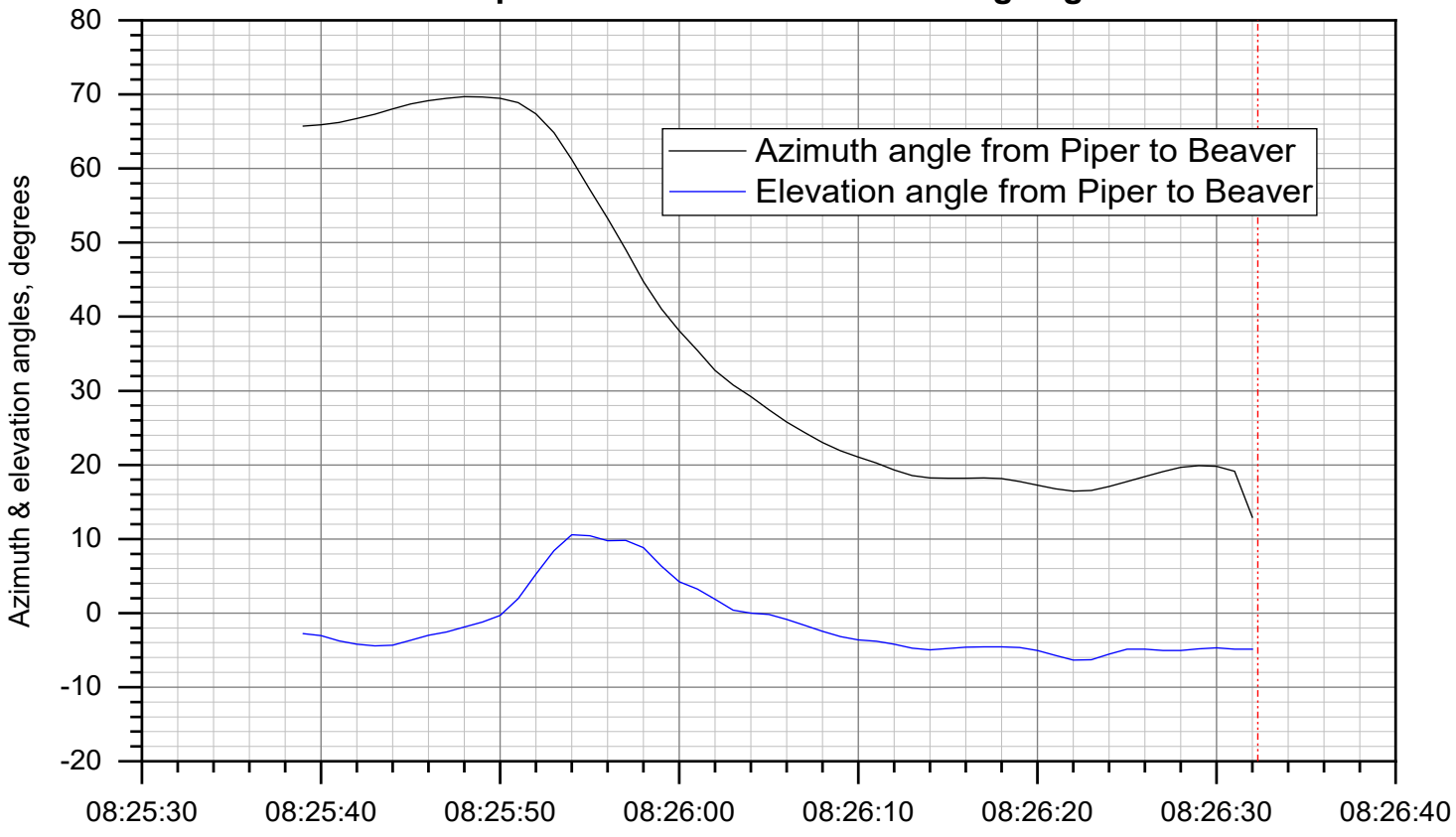

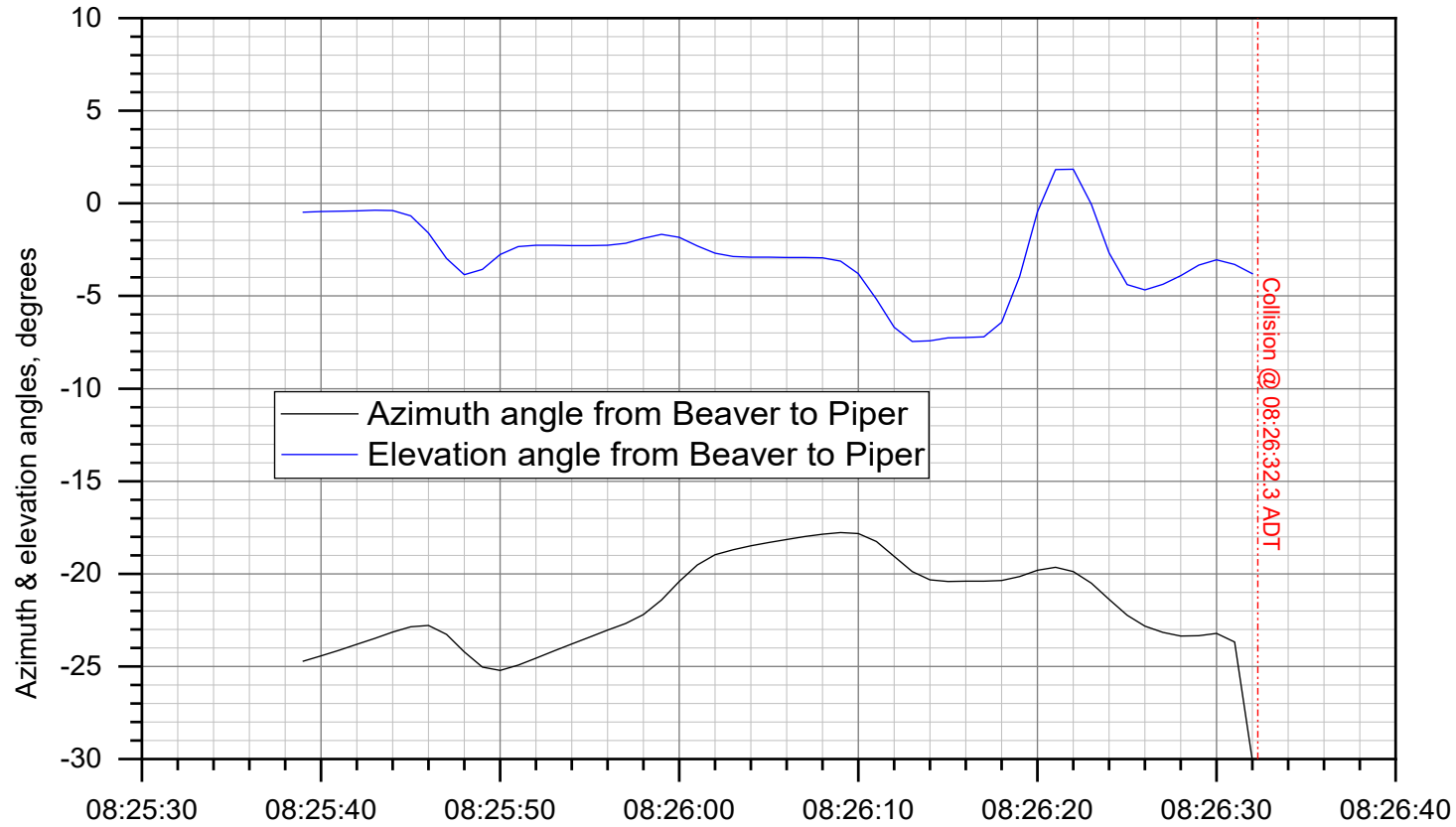

Figure 8.

ANC20LA074AB: Midair collision, Beaver N4982U / Piper N2587M, Solotna, AK, 7/31/2020

Elevation vs. azimuth viewing angles from pilot seat of Piper to Beaver

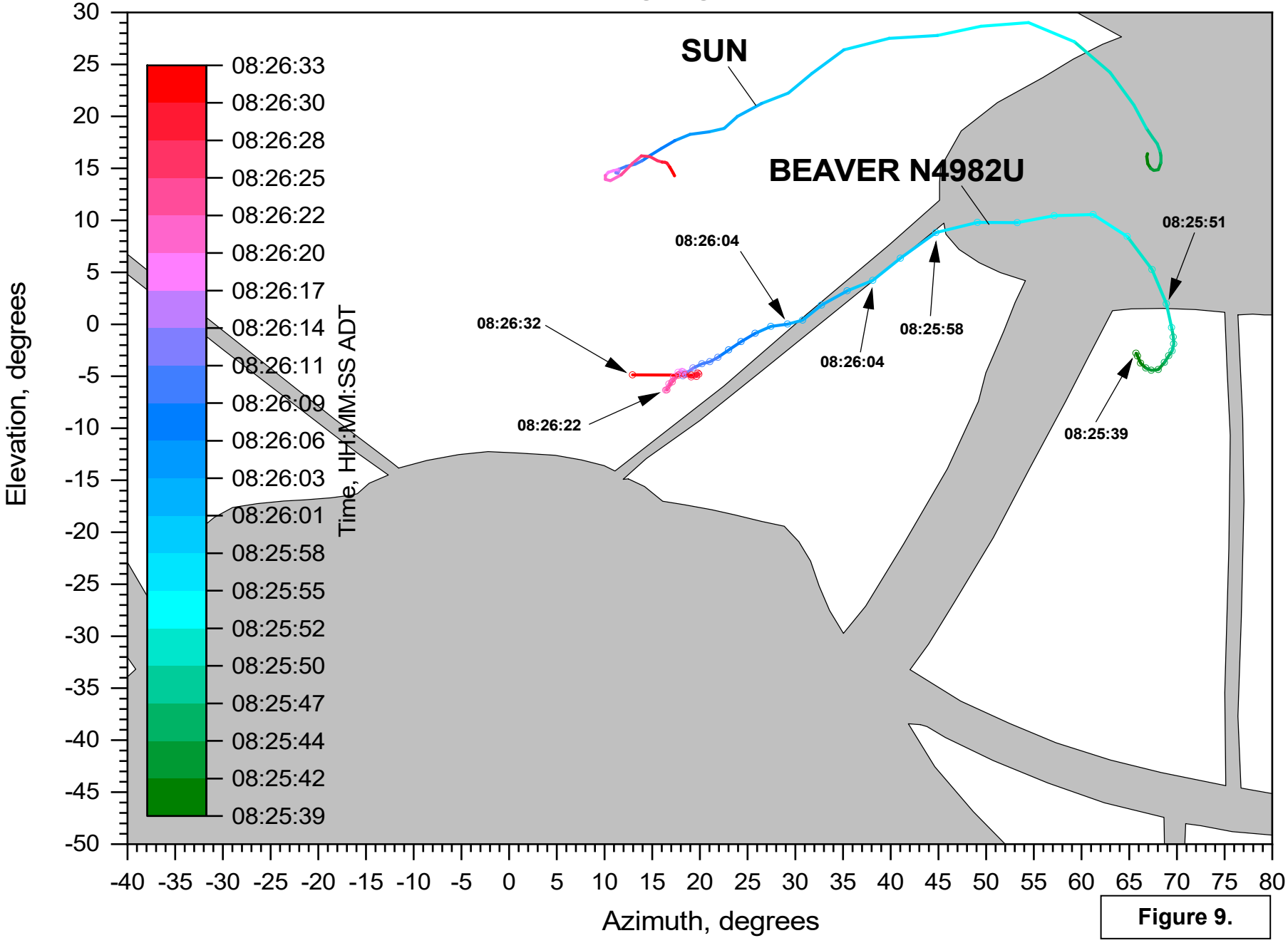

Figure 9.

ANC20LA074AB: Midair collision, Beaver N4982U / Piper N2587M, Solotna, AK, 7/31/2020

Elevation vs. azimuth viewing angles from pilot seat of Beaver to Piper

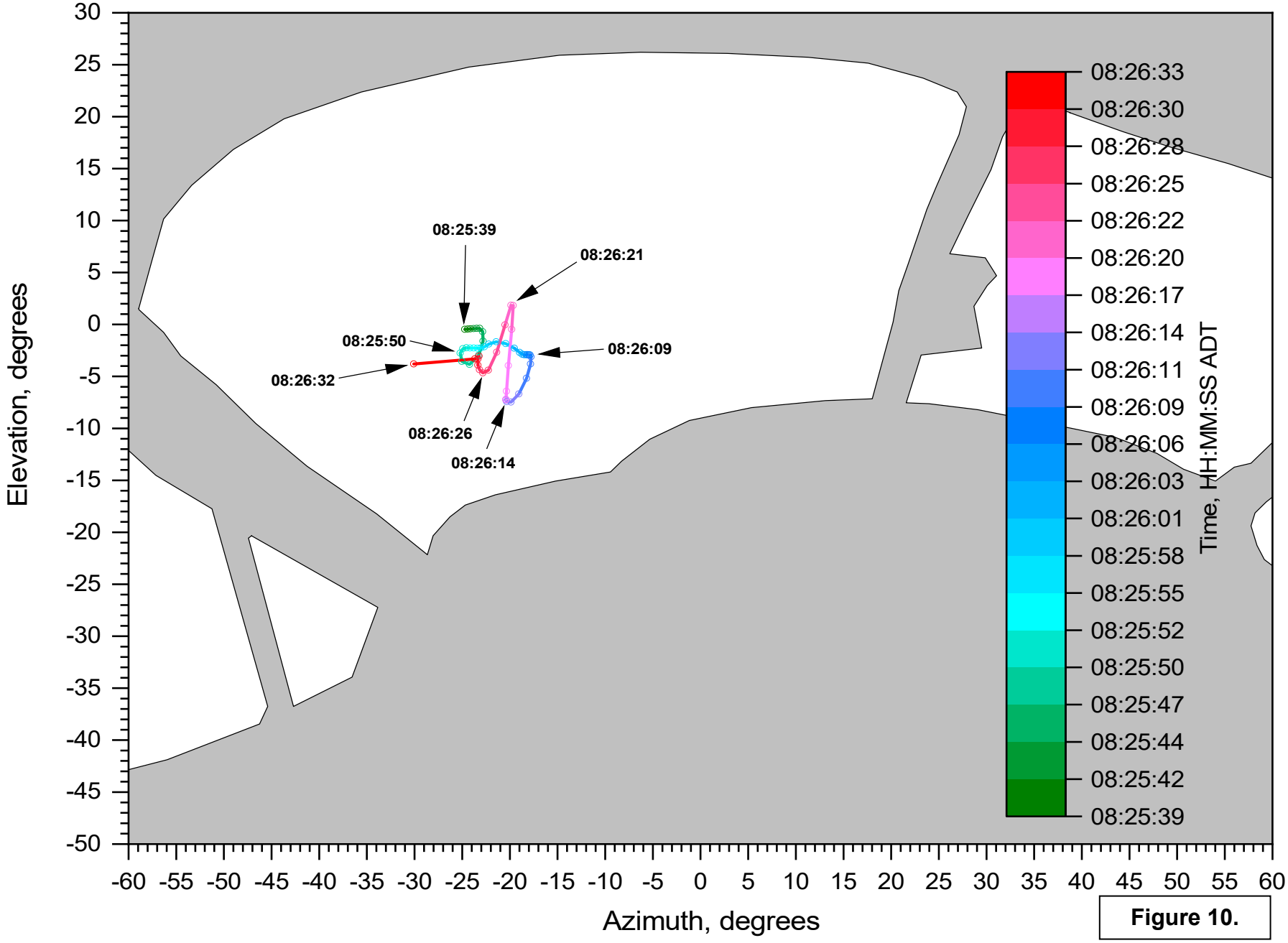

Figure 10.

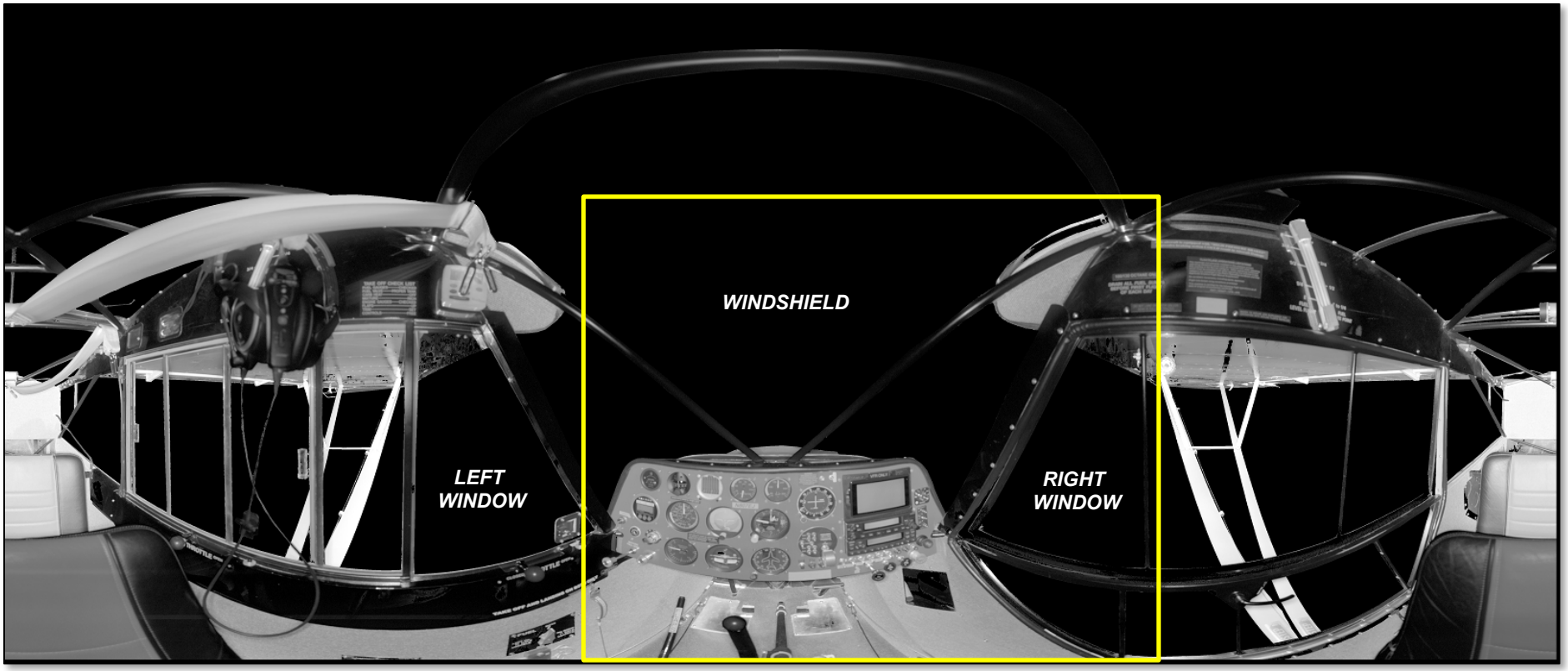

Figure 11. Image of the 360° laser scan from the pilot's seat of the exemplar Piper. The yellow box highlights the area depicted in Figure 9.

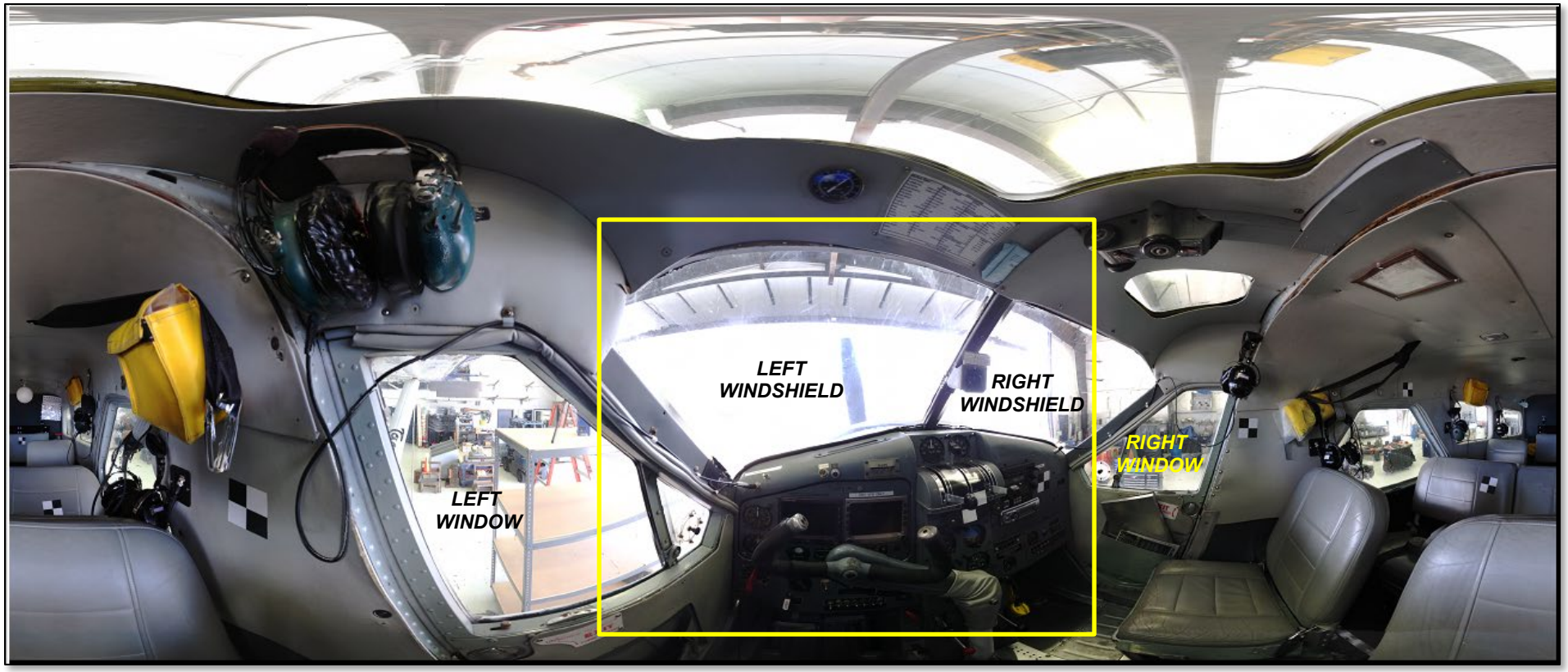

Figure 12. Color image of the 360° laser scan from the pilot's seat of the exemplar Beaver. The yellow box highlights the area depicted in Figure 10.

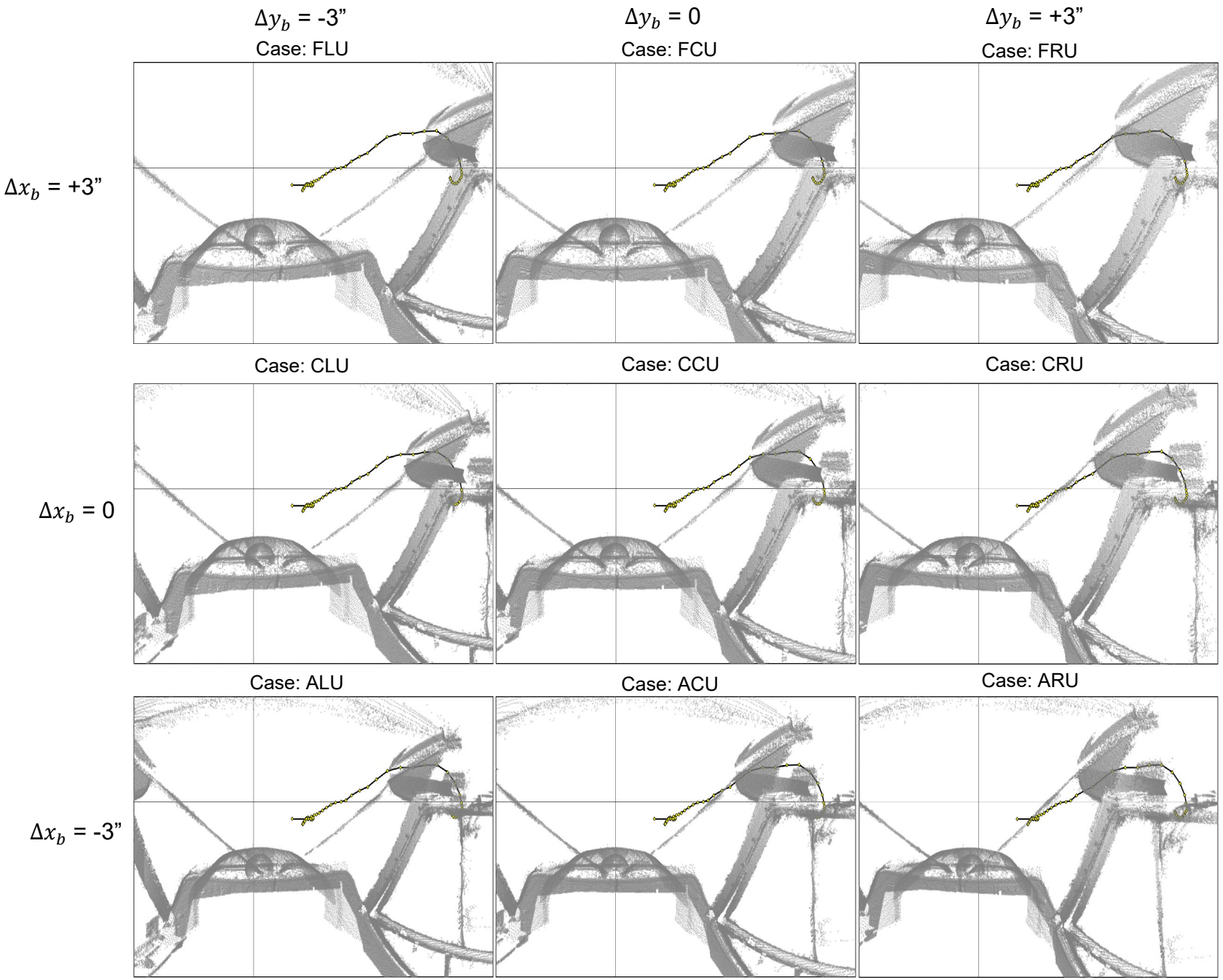

Figure 13a. Viewing angles for the Piper at Δz_b =-1.5” (i.e., up). Plots are elevation angle vs. azimuth angle.

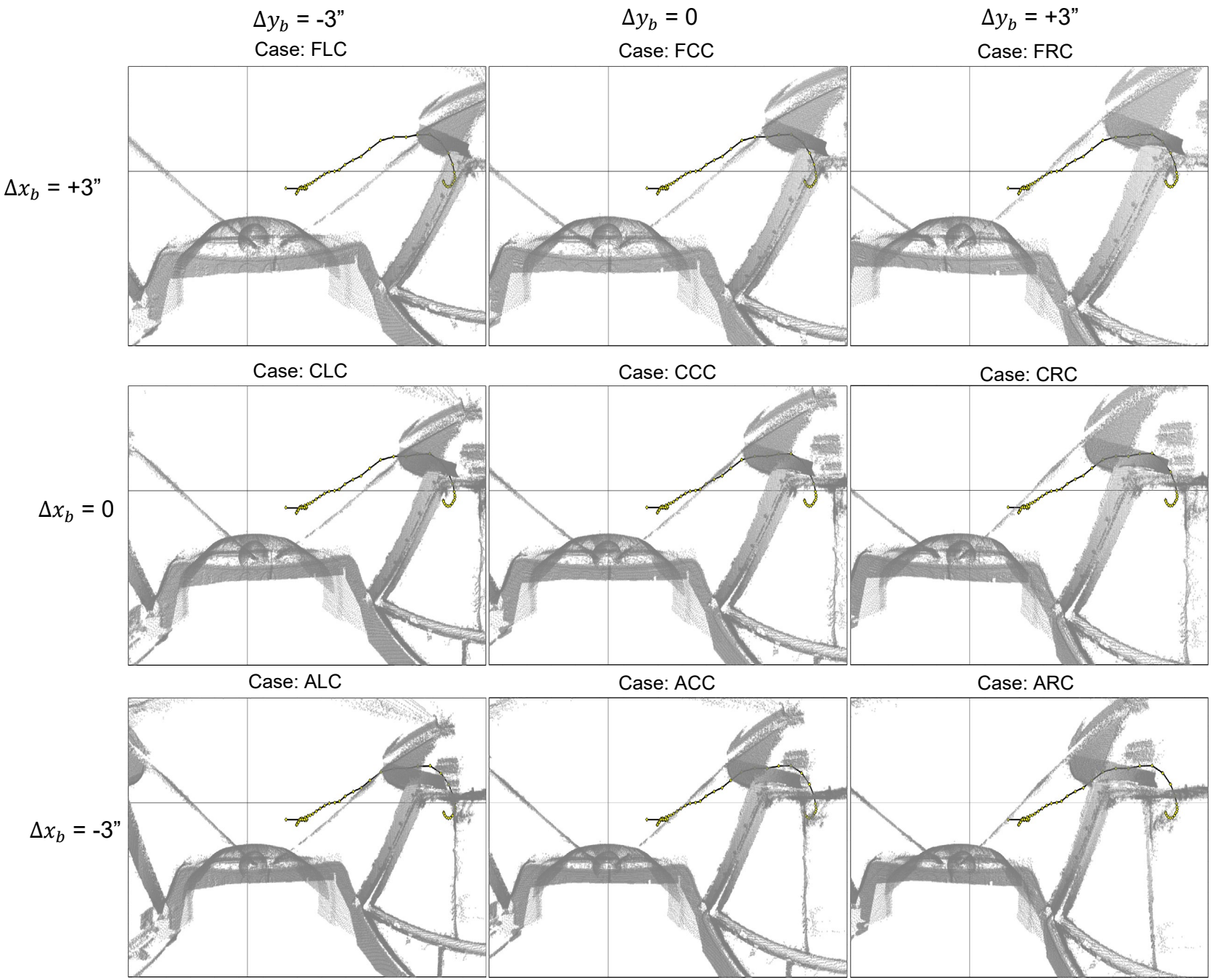

Figure 13b. Viewing angles for the Piper at Δz_b = 0. Plots are elevation angle vs. azimuth angle.

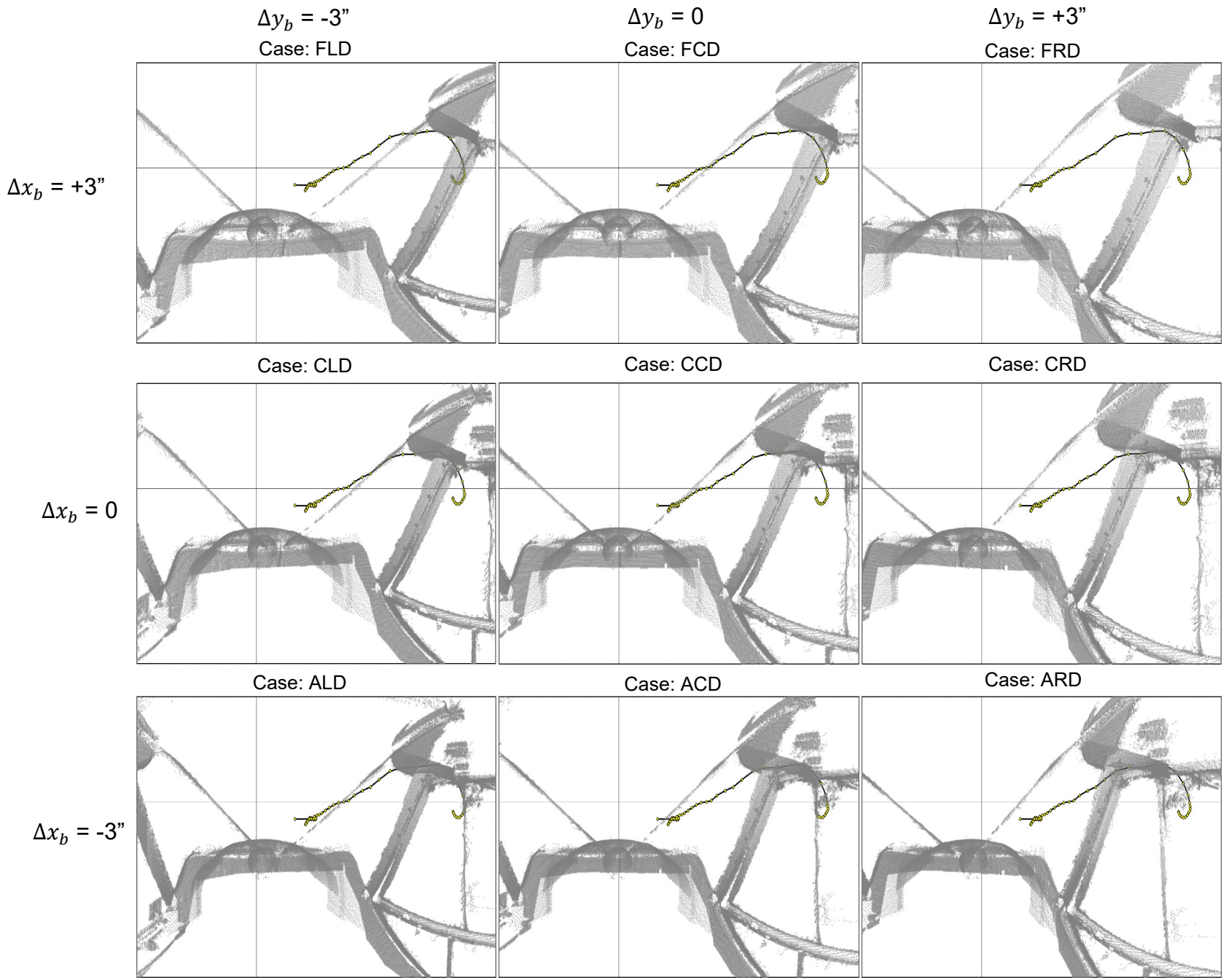

Figure 13c. Viewing angles for the Piper at Δz_b =+1.5” (i.e., down). Plots are elevation angle vs. azimuth angle.

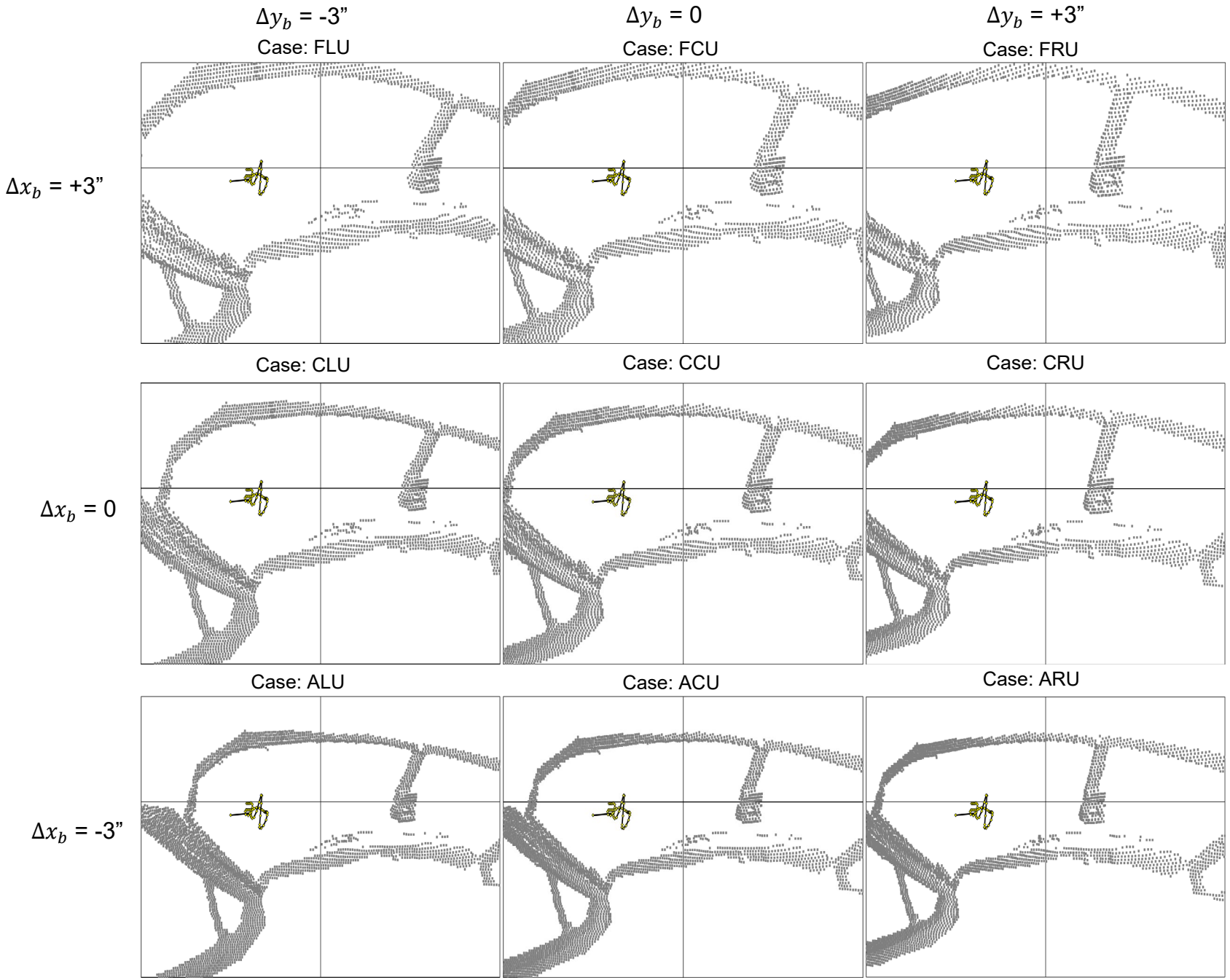

Figure 14a. Viewing angles for the Beaver at Δz_b =-1.5” (i.e., up). Plots are elevation angle vs. azimuth angle.

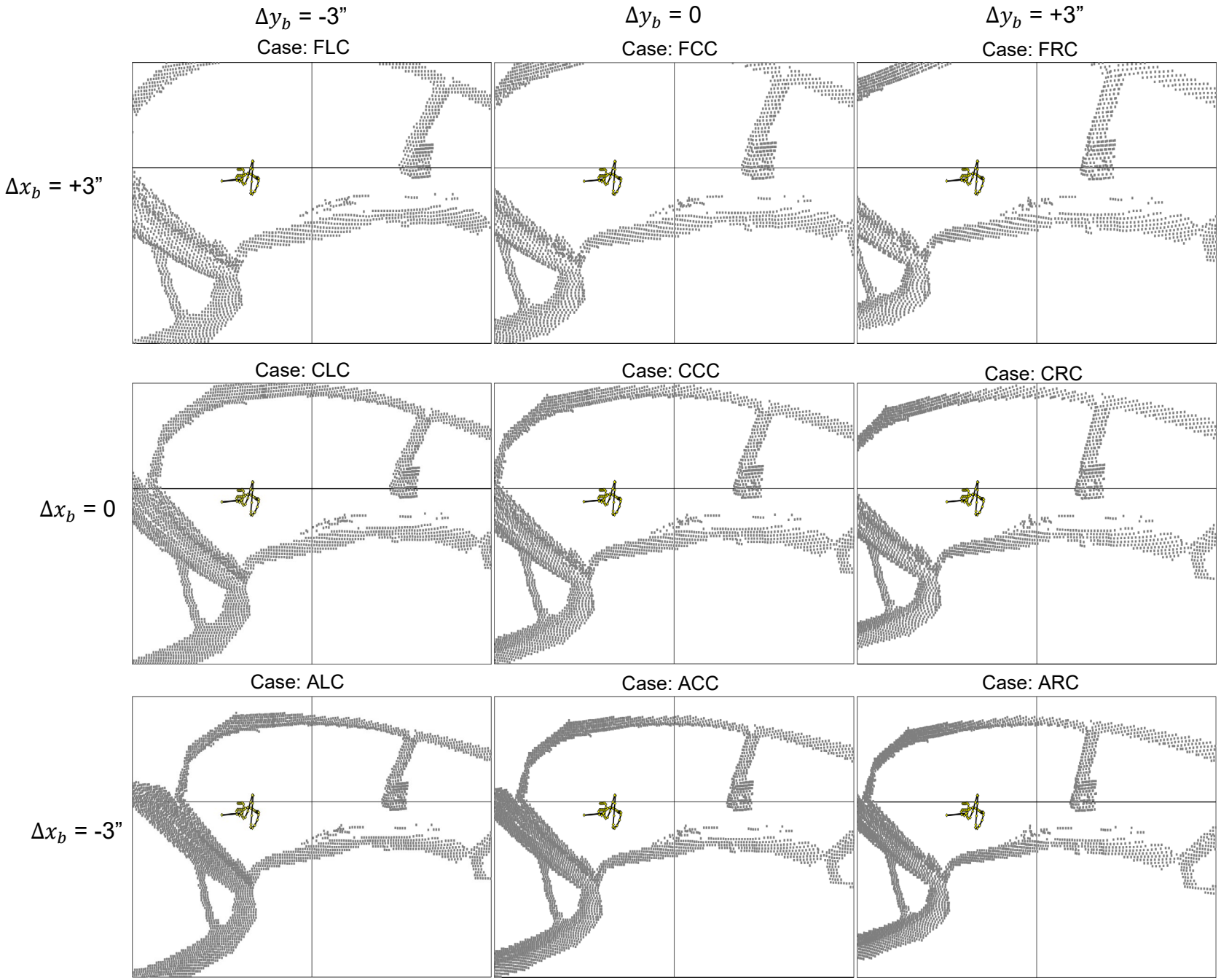

Figure 14b. Viewing angles for the Beaver at Δz_b = 0. Plots are elevation angle vs. azimuth angle.

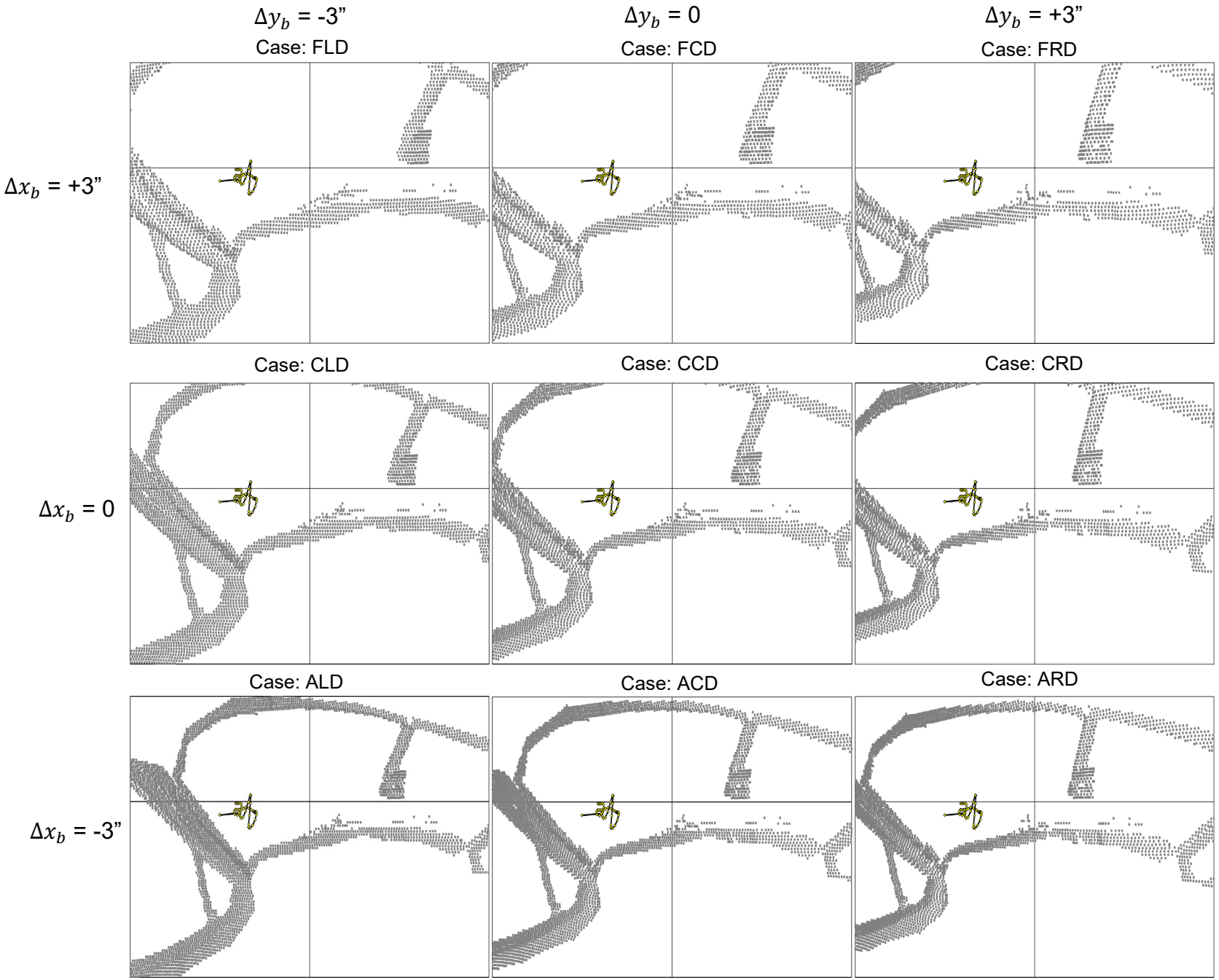

Figure 14c. Viewing angles for the Beaver at Δz_b =+1.5” (i.e., down). Plots are elevation angle vs. azimuth angle.

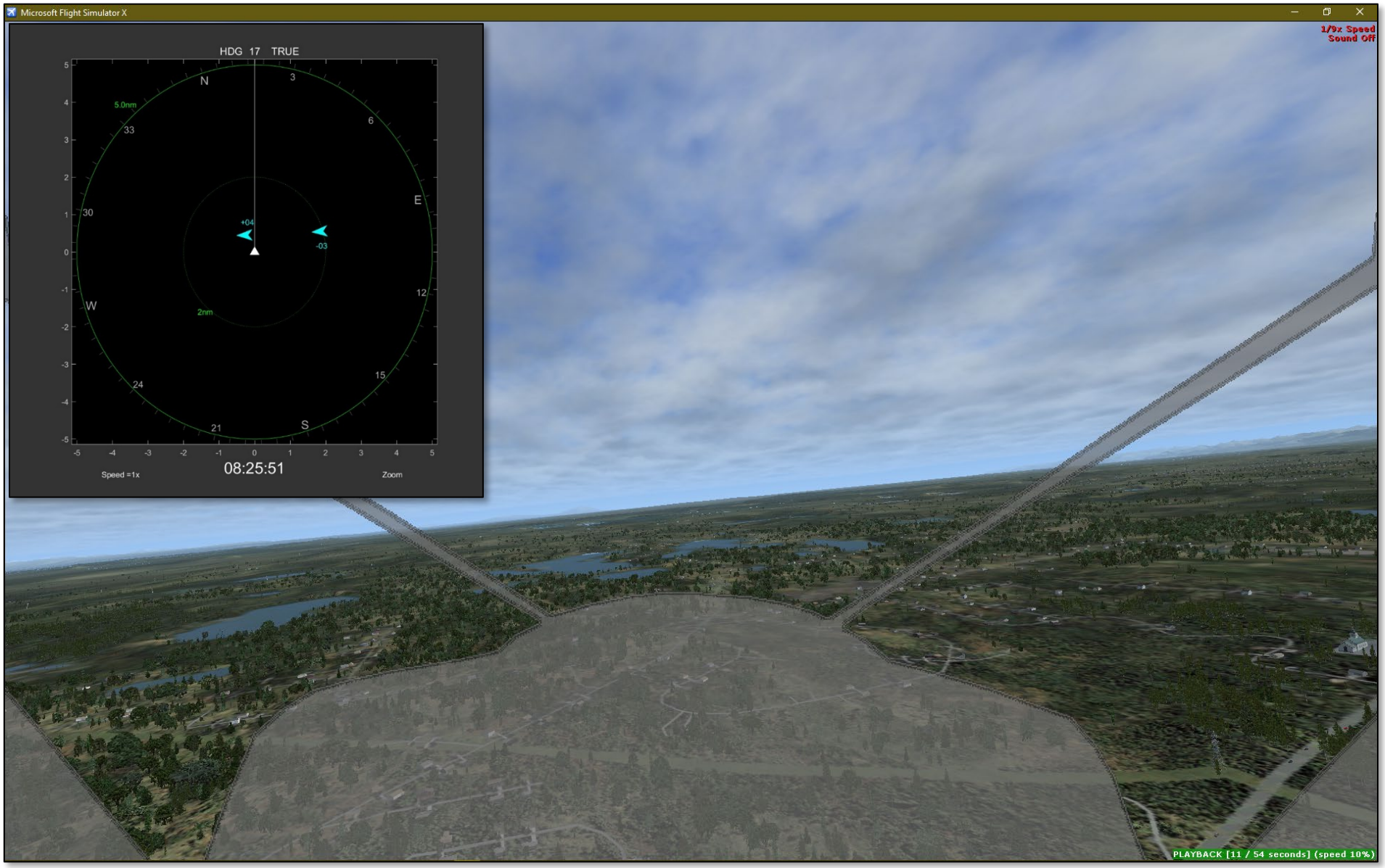

Figure 15a. Recreation of the view from the Piper cockpit and simulated CDTI display at 08:25:51 (41.3 seconds before the collision). The Beaver is out of view on the right, and obscured by the right window frame.

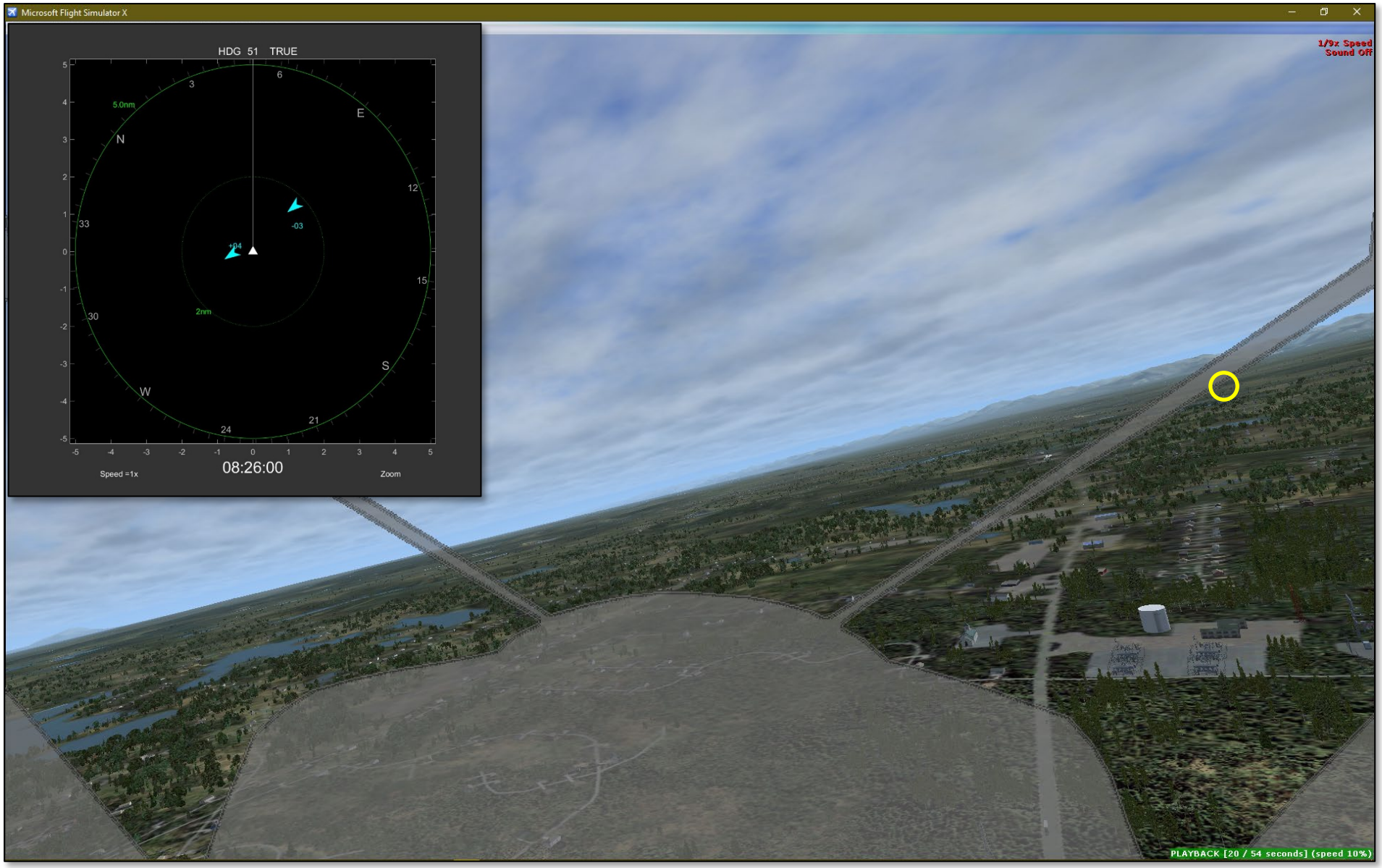

Figure 15b. Recreation of the view from the Piper cockpit and simulated CDTI display at 08:26:00 (32.3 seconds before the collision). The location of the Beaver is indicated by the yellow circle.

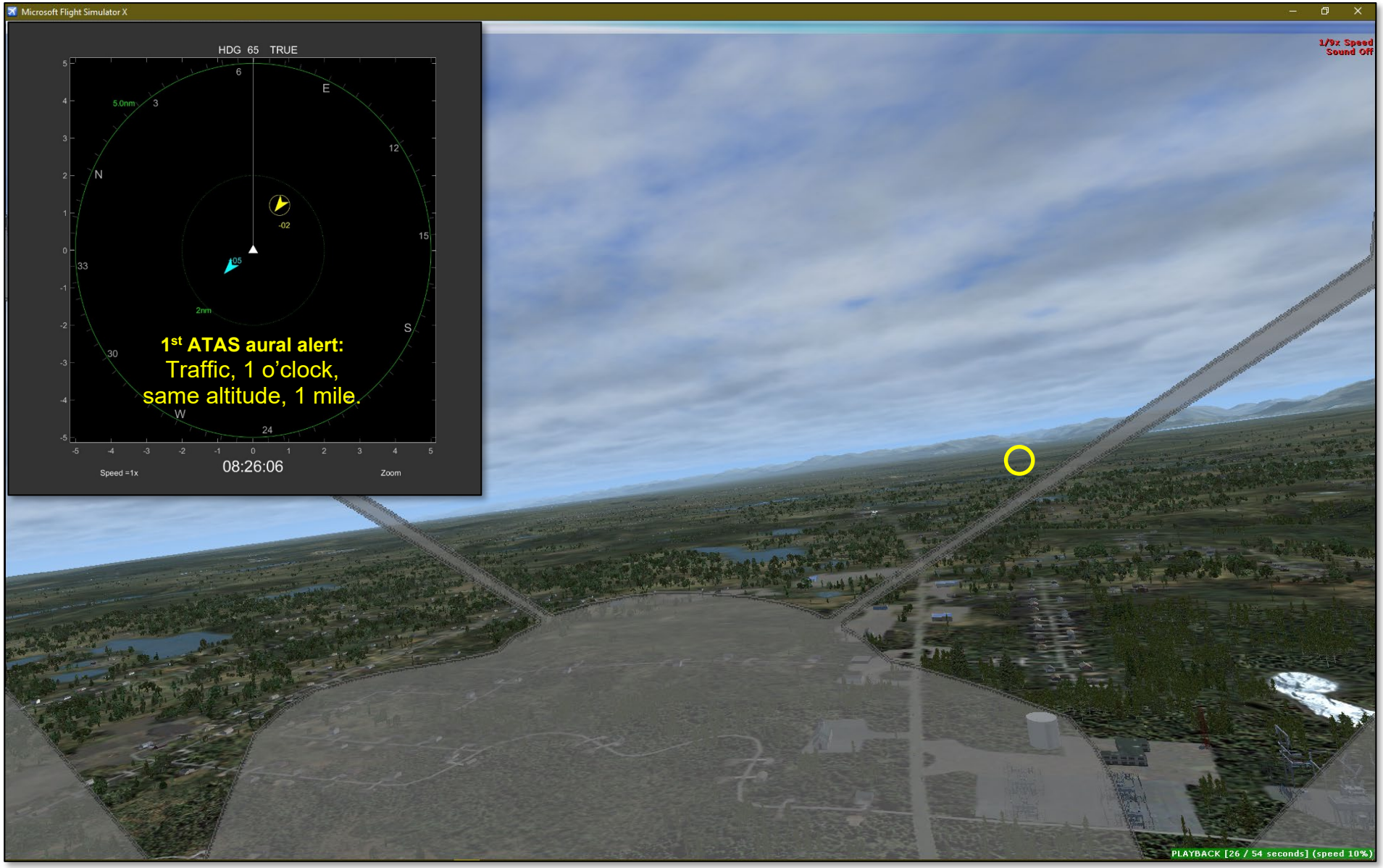

Figure 15c. Recreation of the view from the Piper cockpit and simulated CDTI display at 08:26:06 (26.3 seconds before the collision). The location of the Beaver is indicated by the yellow circle.

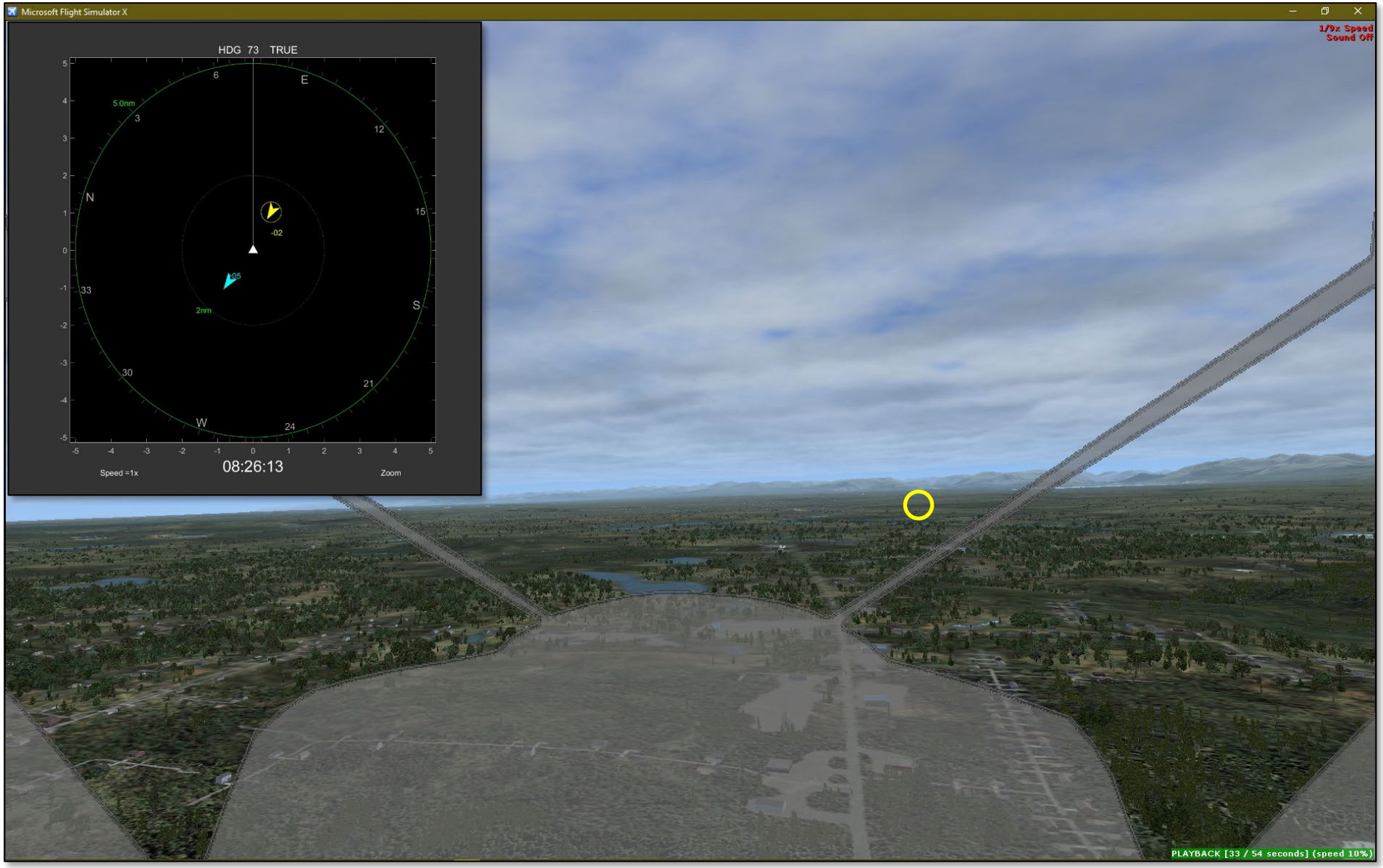

Figure 15d. Recreation of the view from the Piper cockpit and simulated CDTI display at 08:26:13 (19.3 seconds before the collision). The location of the Beaver is indicated by the yellow circle.

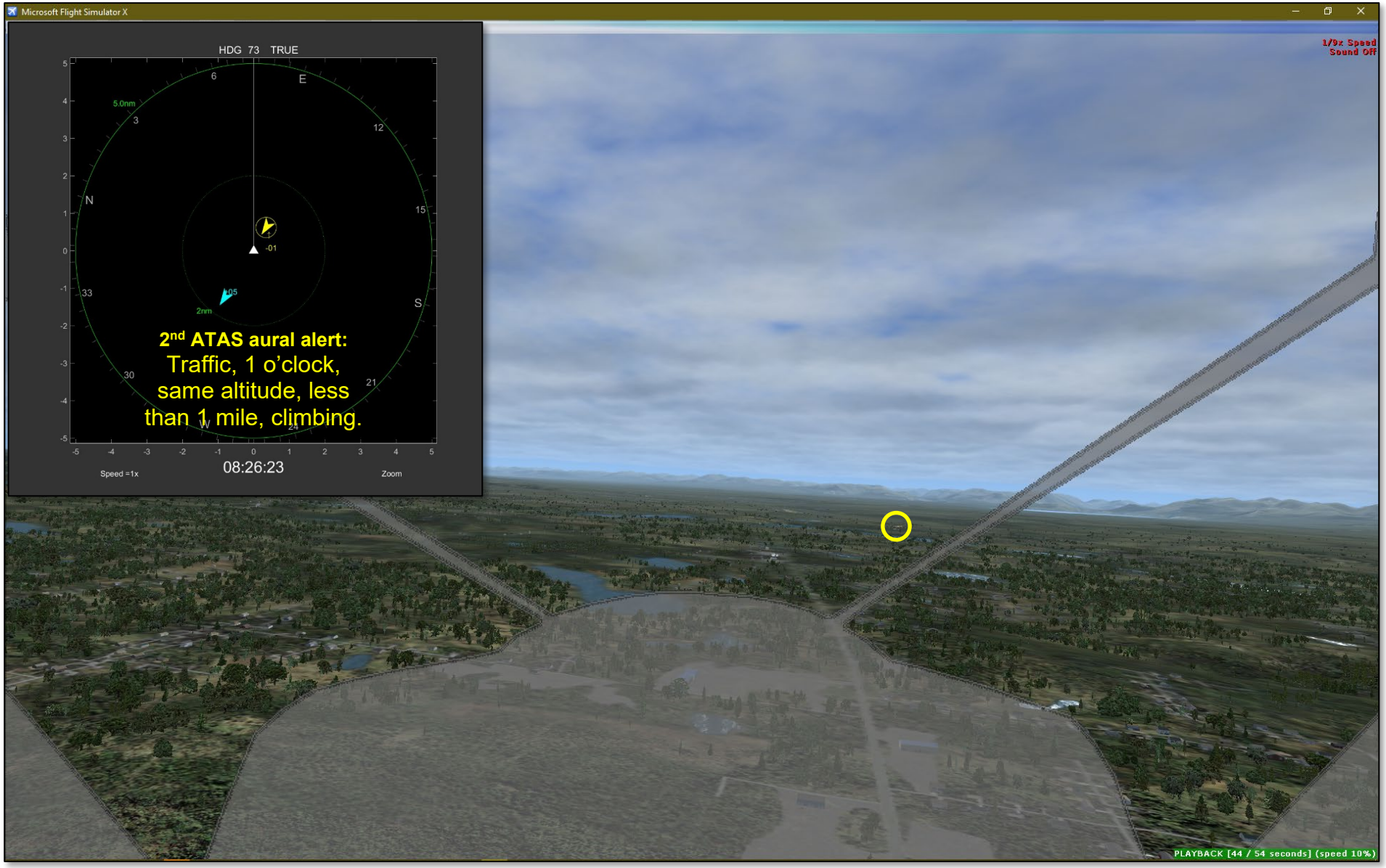

Figure 15e. Recreation of the view from the Piper cockpit and simulated CDTI display at 08:26:23 (9.3 seconds before the collision). The location of the Beaver is indicated by the yellow circle.

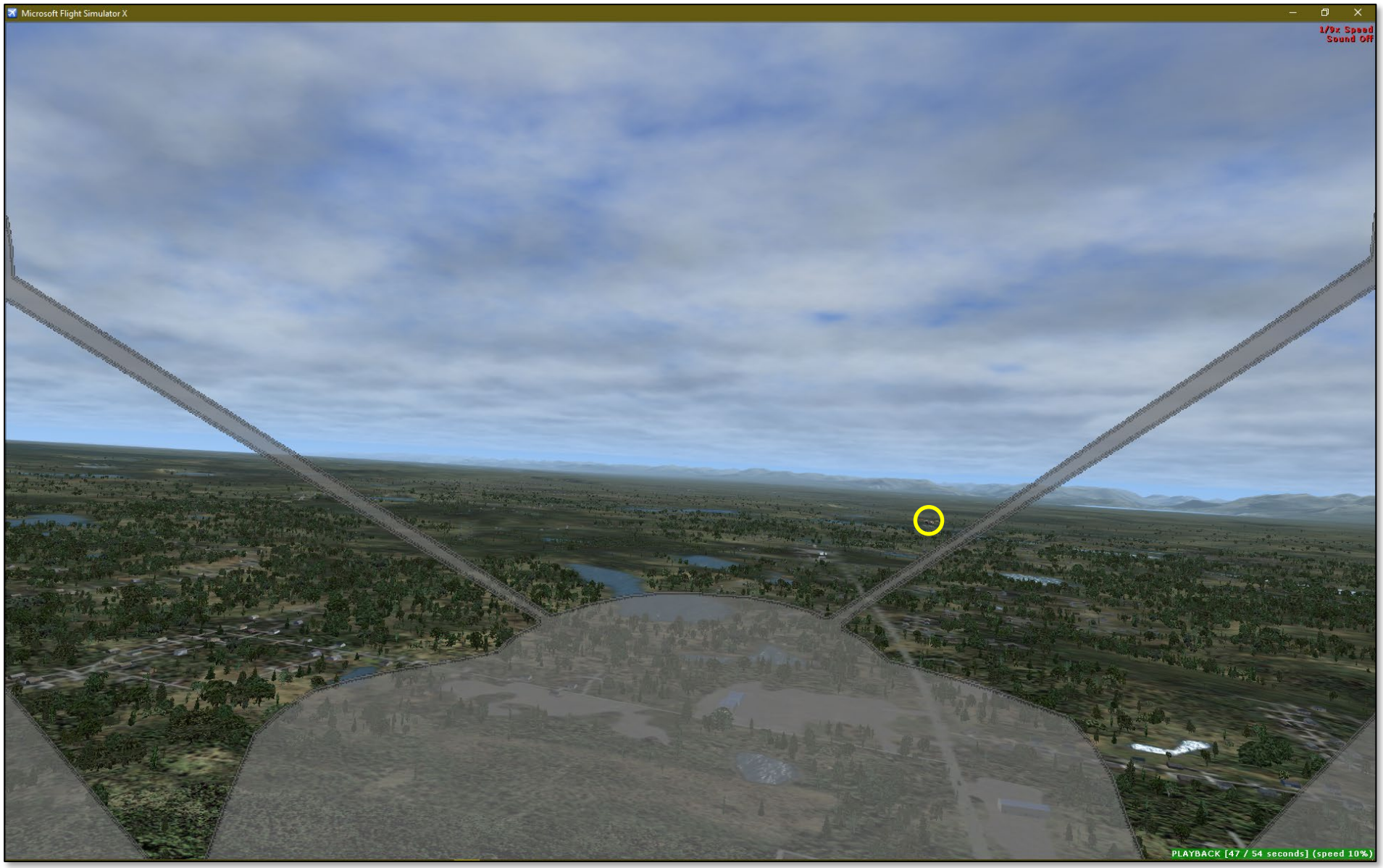

Figure 15f. Recreation of the view from the Piper cockpit at 08:26:27 (5.3 seconds before the collision). The location of the Beaver is indicated by the yellow circle.

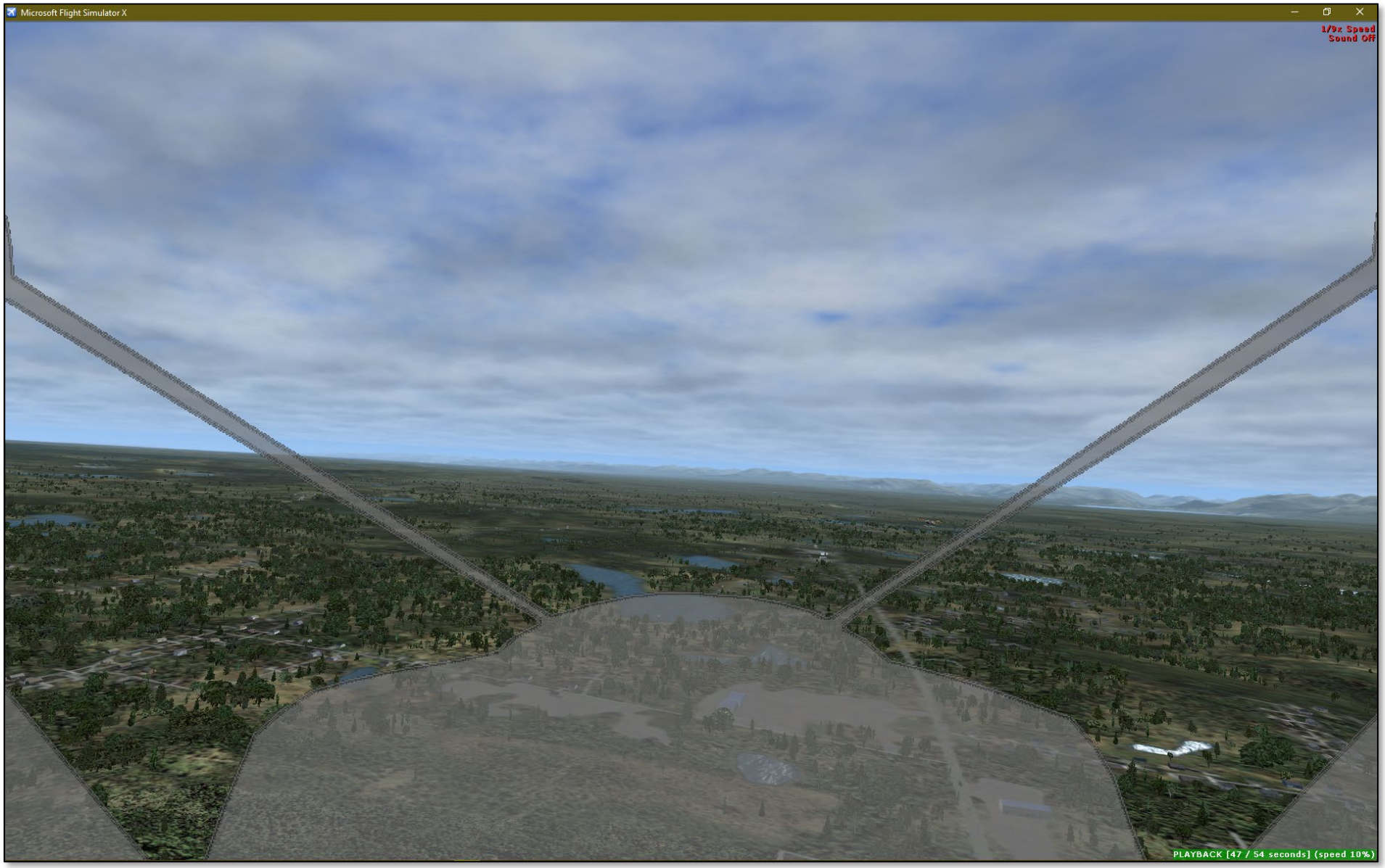

Figure 15g. Recreation of the view from the Piper cockpit at 08:26:29 (3.3 seconds before the collision).

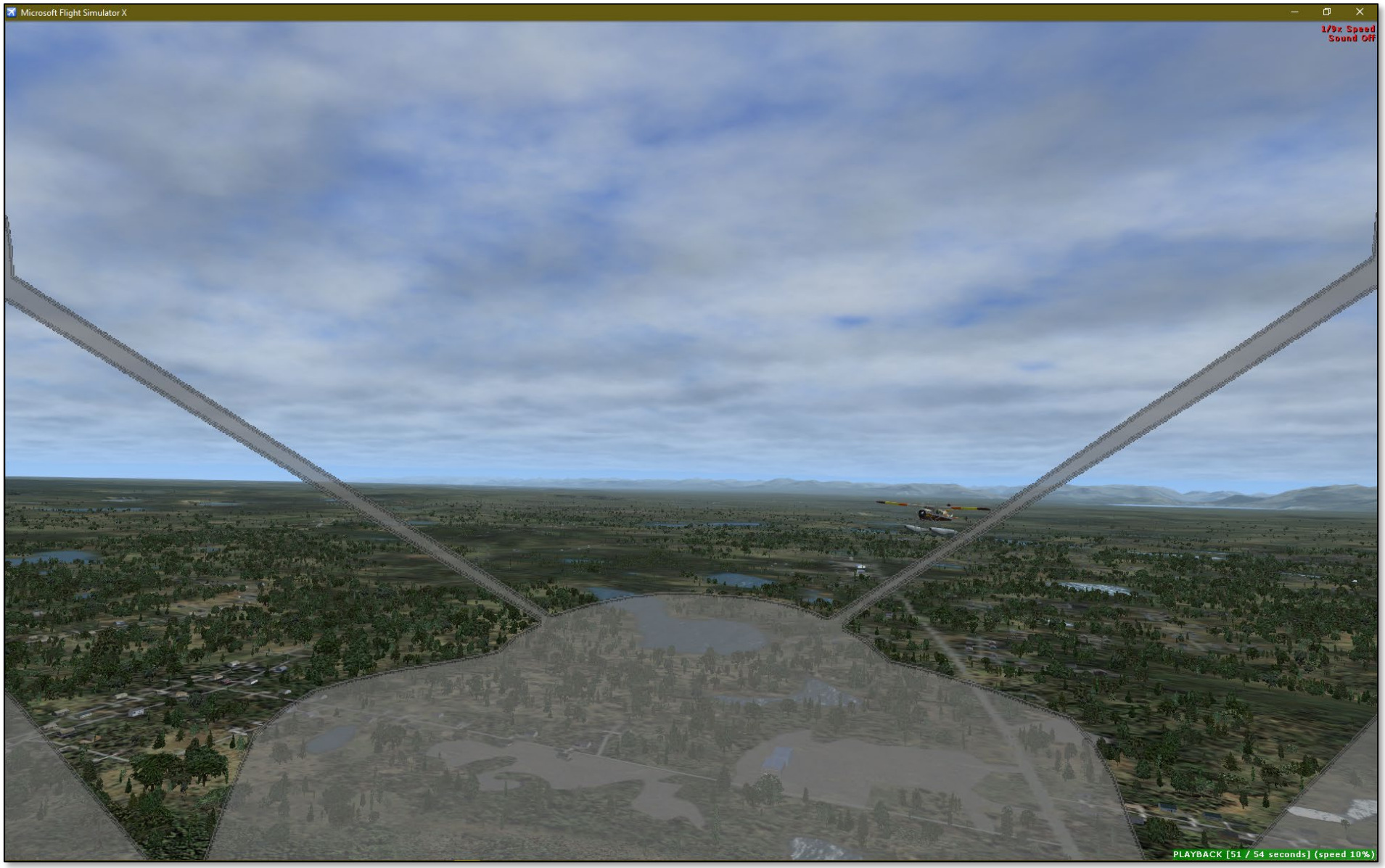

Figure 15h. Recreation of the view from the Piper cockpit at 08:26:31 (1.3 seconds before the collision).

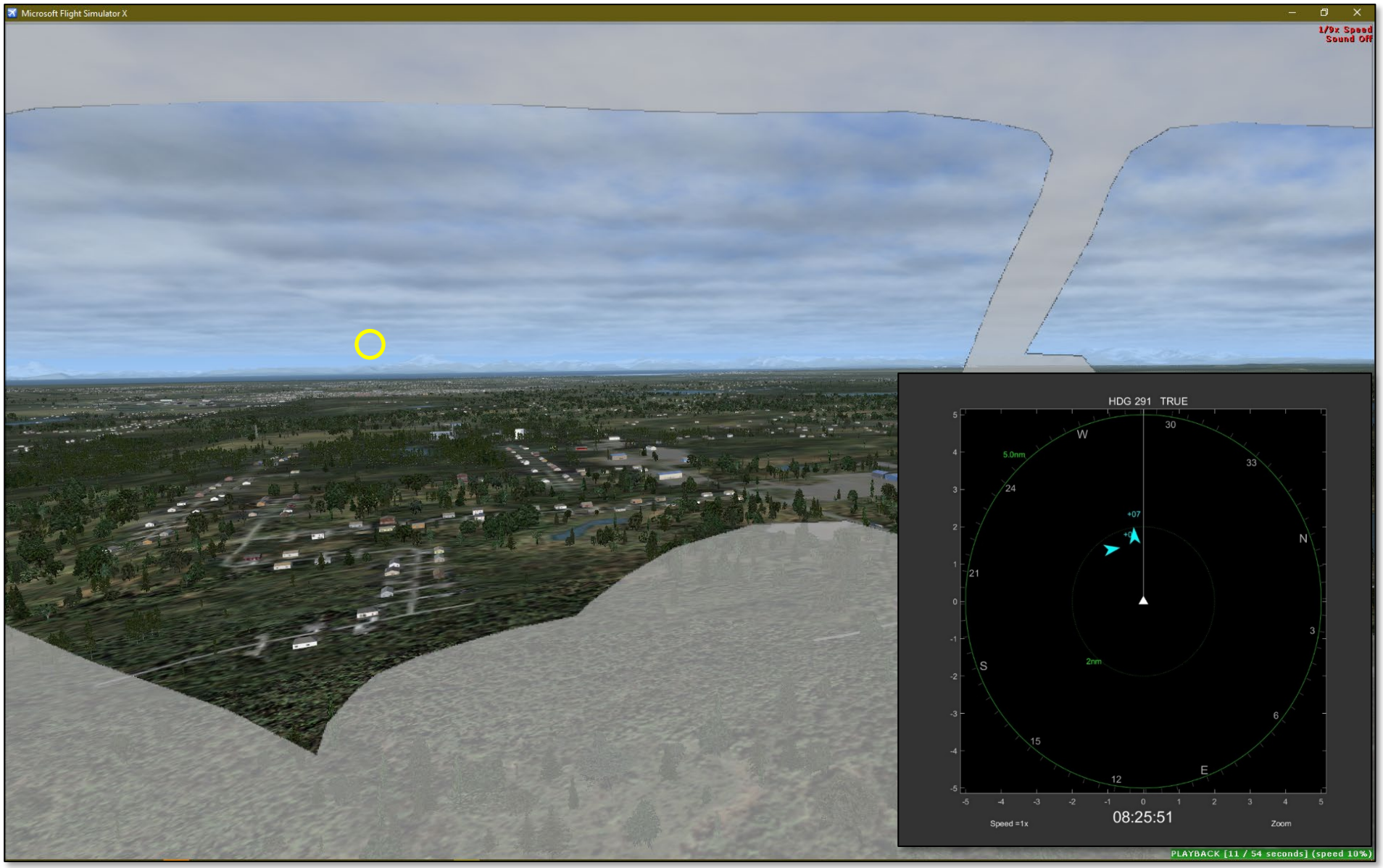

Figure 16a. Recreation of the view from the Beaver cockpit and simulated CDTI display at 08:25:51 (41.3 seconds before the collision). The location of the Piper is indicated by the yellow circle.

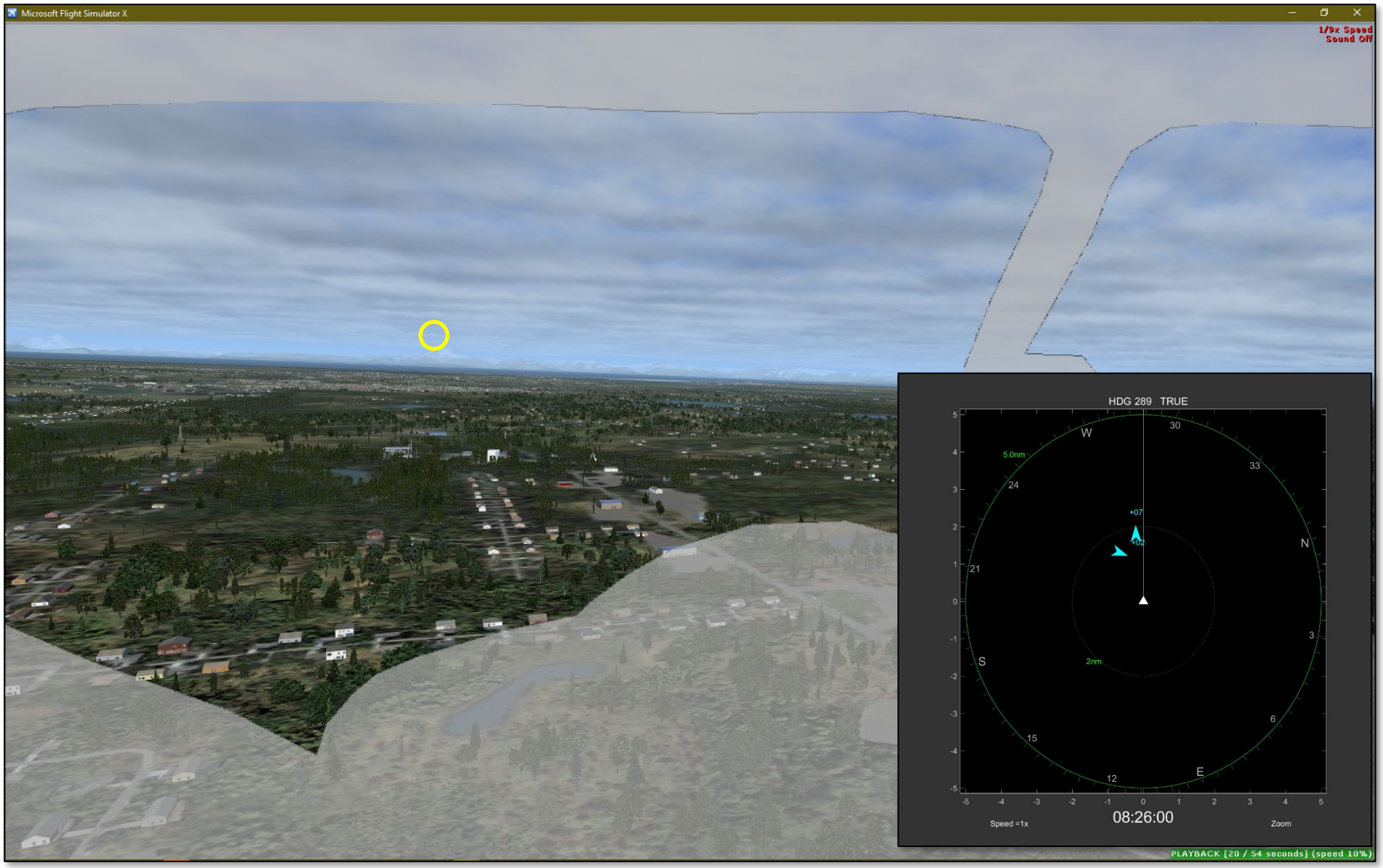

Figure 16b. Recreation of the view from the Beaver cockpit and simulated CDTI display at 08:26:00 (32.3 seconds before the collision). The location of the Piper is indicated by the yellow circle.

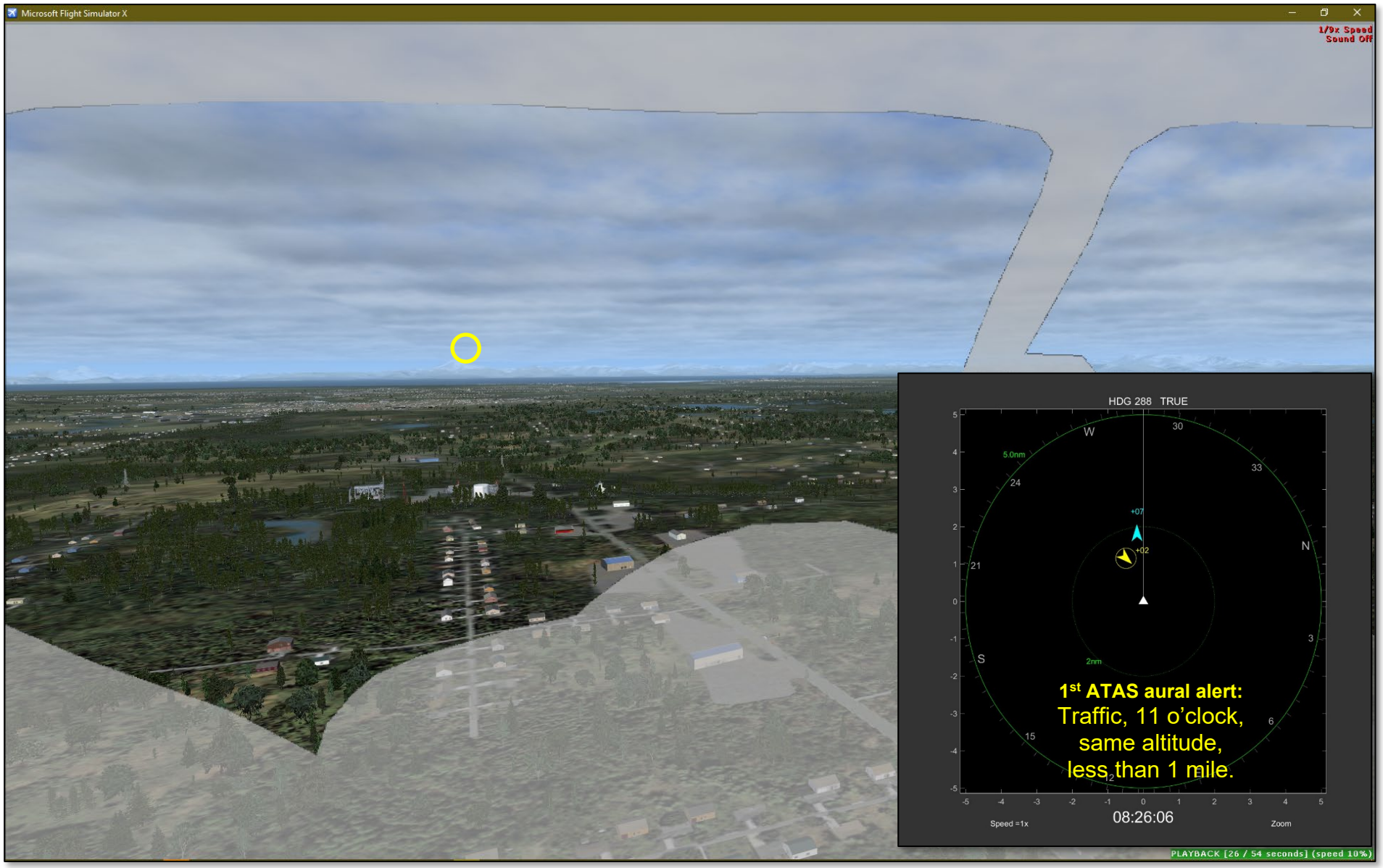

Figure 16c. Recreation of the view from the Beaver cockpit and simulated CDTI display at 08:26:06 (26.3 seconds before the collision). The location of the Piper is indicated by the yellow circle.

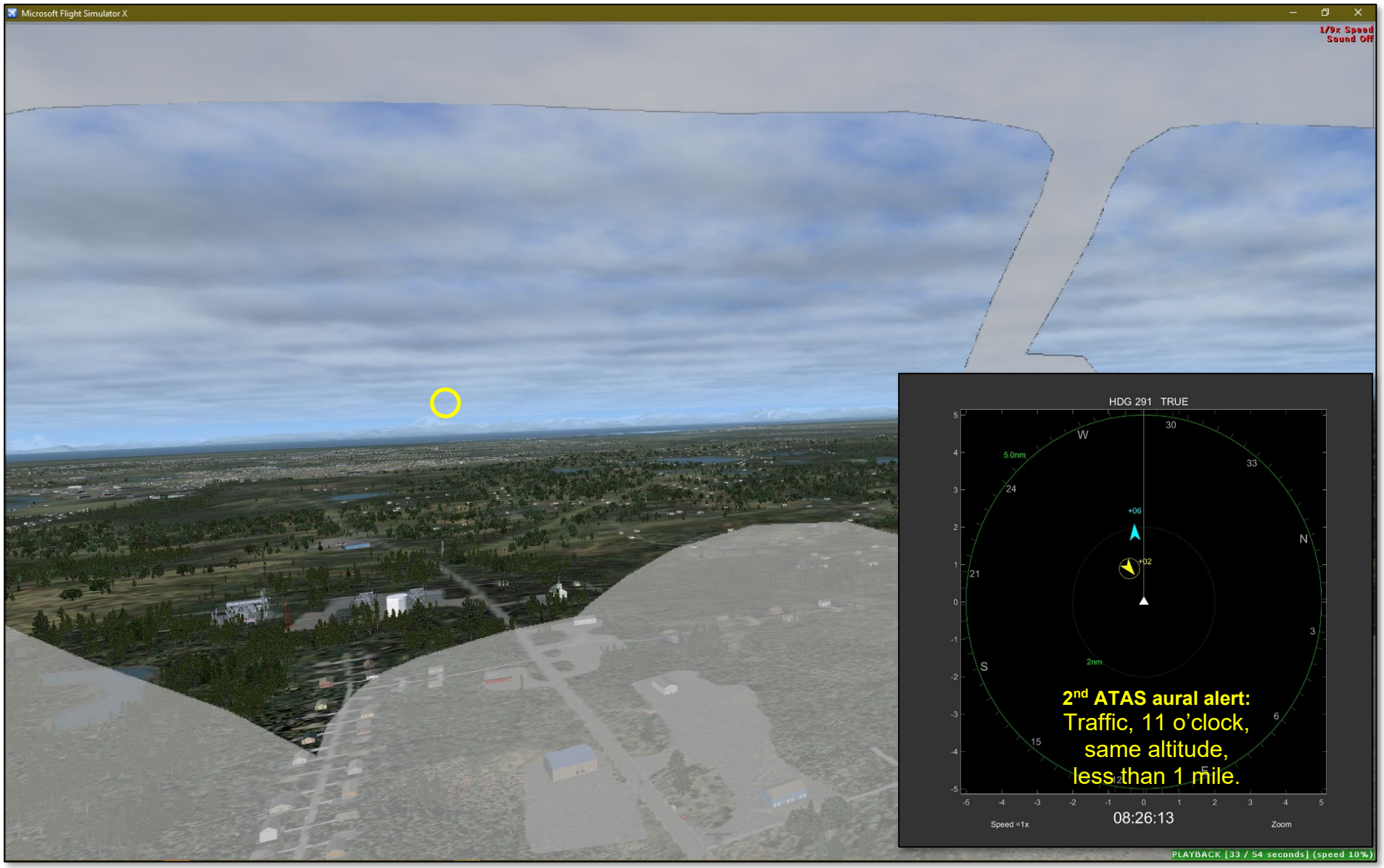

Figure 16d. Recreation of the view from the Beaver cockpit and simulated CDTI display at 08:26:13 (19.3 seconds before the collision). The location of the Piper is indicated by the yellow circle.

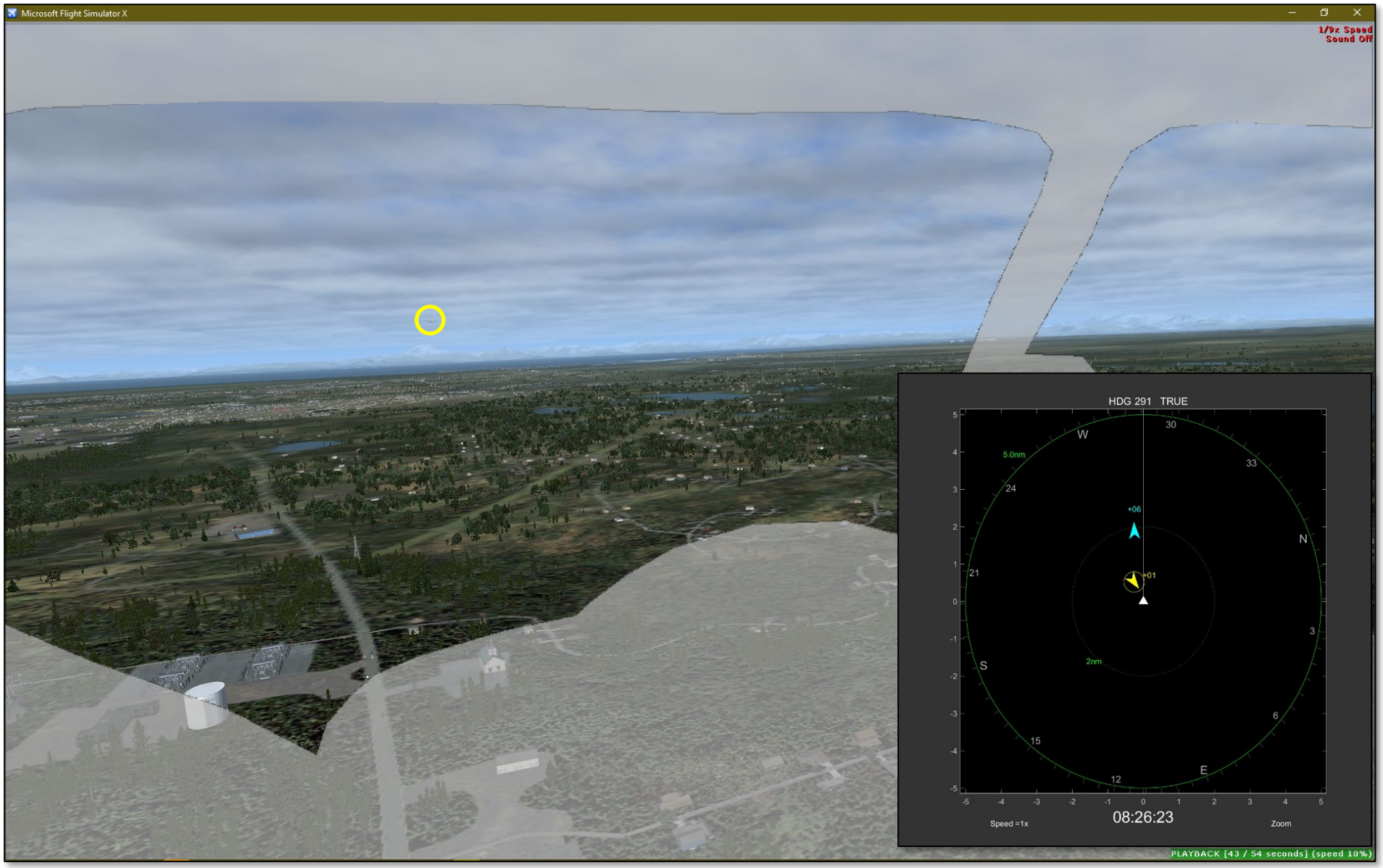

Figure 16e. Recreation of the view from the Beaver cockpit and simulated CDTI display at 08:26:23 (9.3 seconds before the collision). The location of the Piper is indicated by the yellow circle.

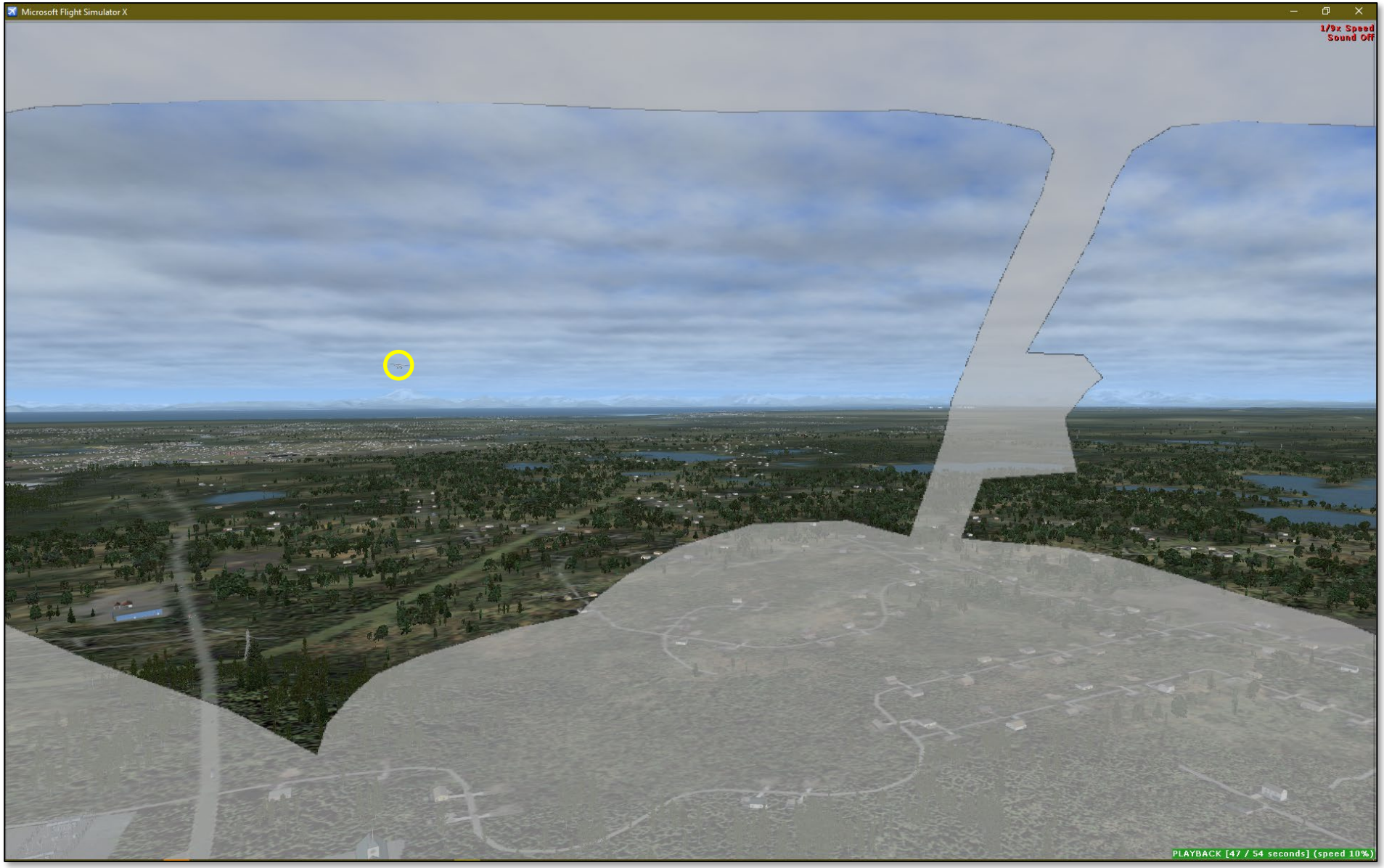

Figure 16f. Recreation of the view from the Beaver cockpit at 08:26:27 (5.3 seconds before the collision). The location of the Piper is indicated by the yellow circle.

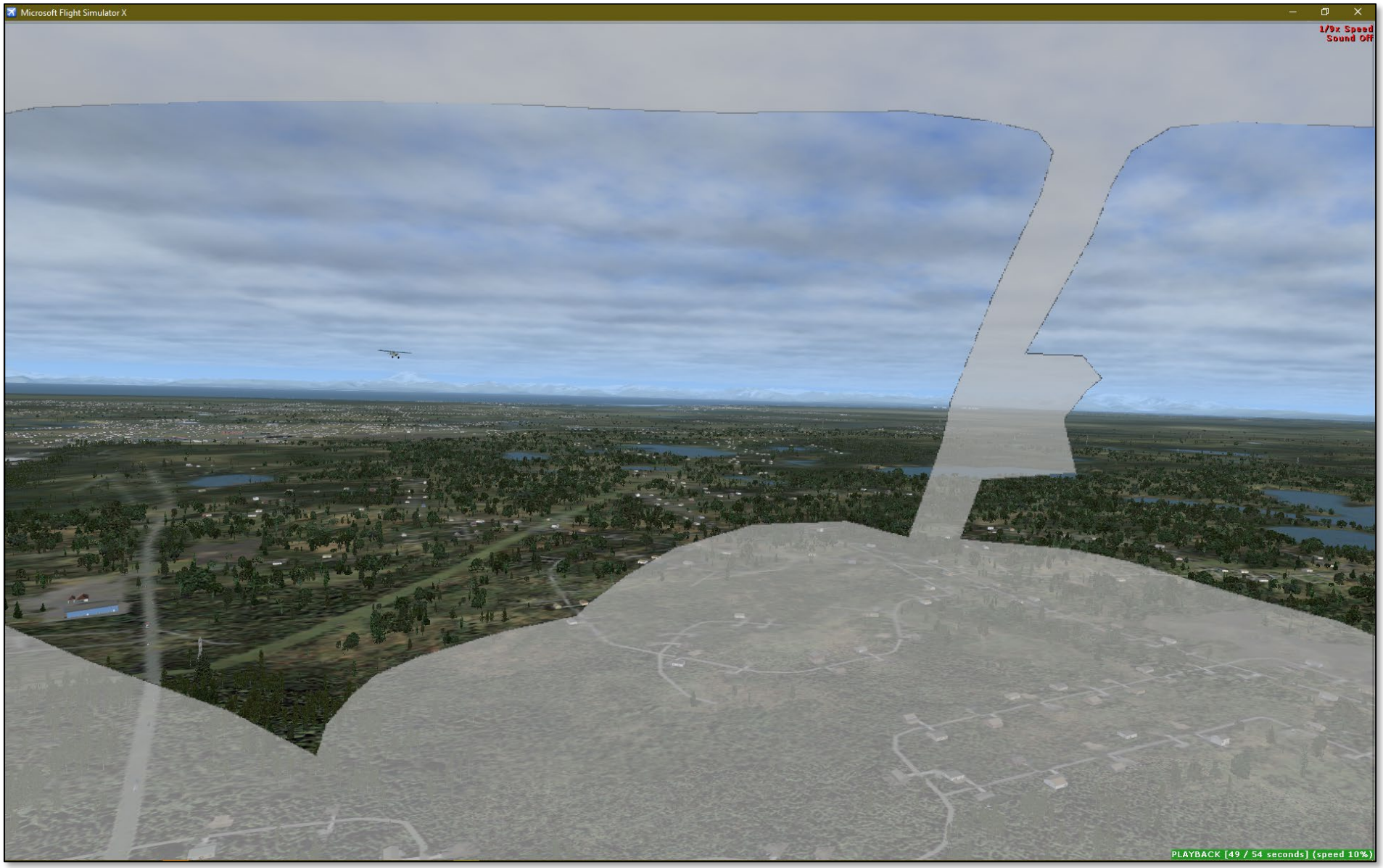

Figure 16g. Recreation of the view from the Beaver cockpit at 08:26:29 (3.3 seconds before the collision).

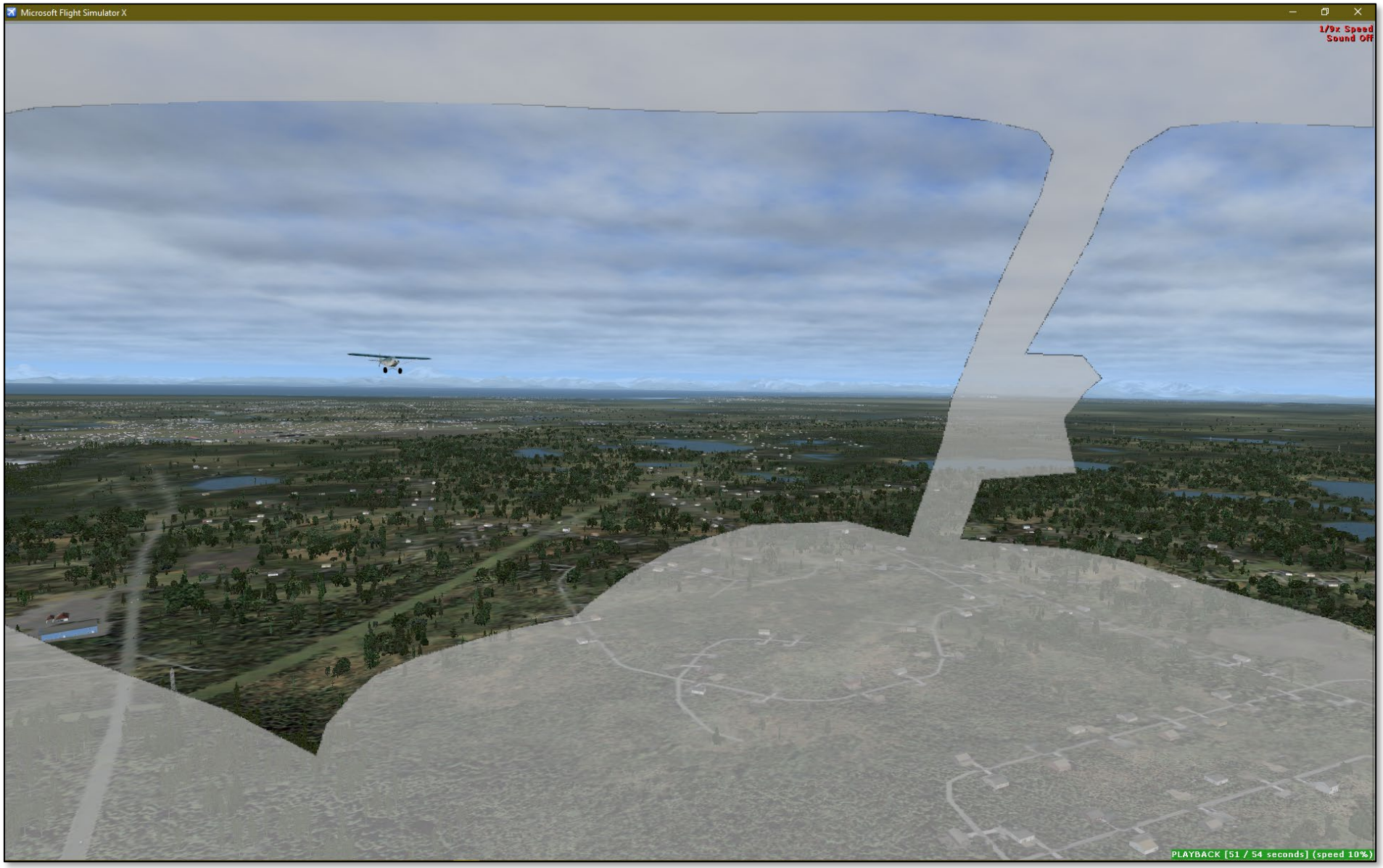

Figure 16h. Recreation of the view from the Beaver cockpit at 08:26:31 (1.3 seconds before the collision).

ANC20LA074AB: Midair collision, Beaver N4982U / Piper N2587M, Solotna, AK, 7/31/2020

"Target" airplane size growth vs. time

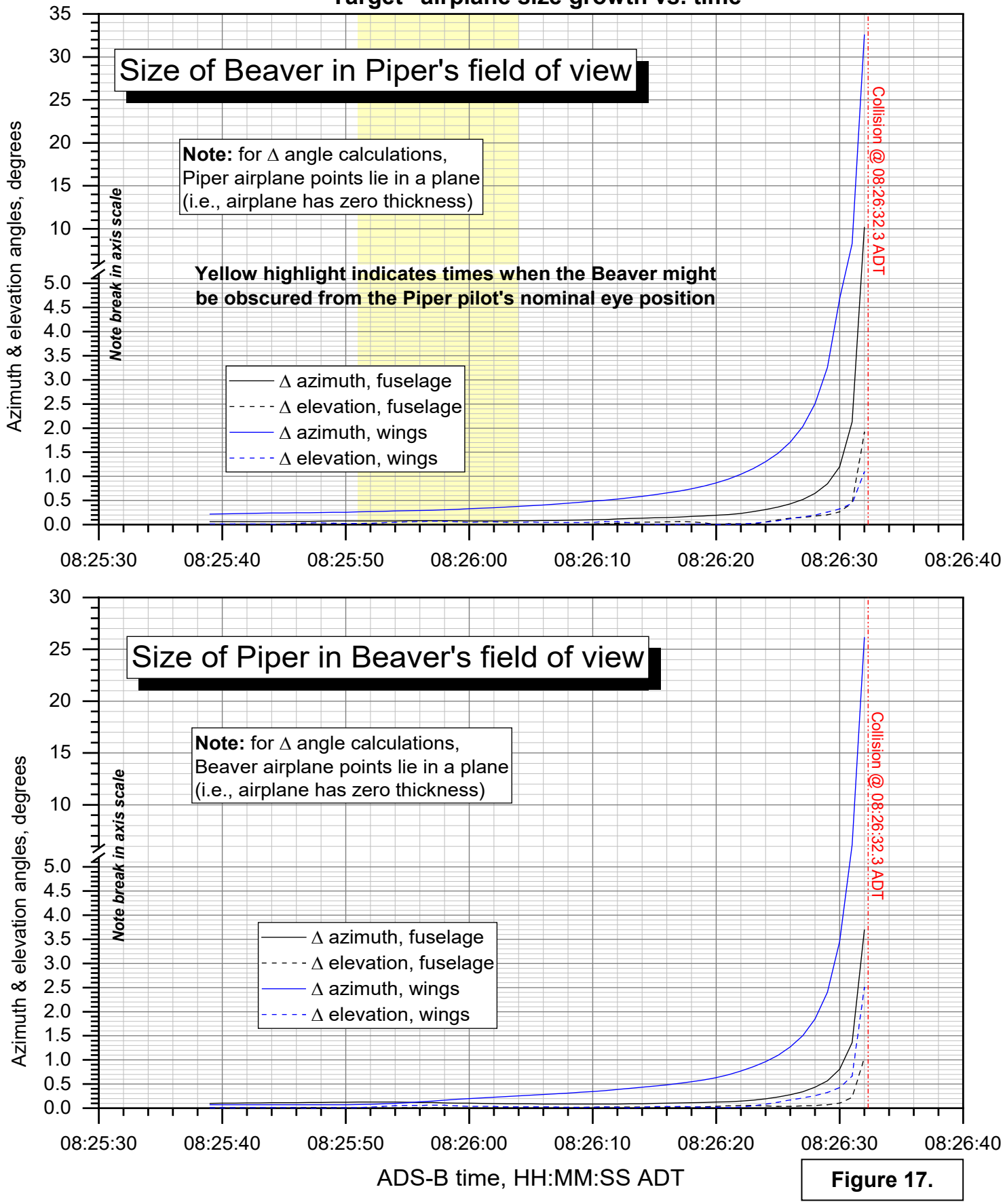

Figure 17.

APPENDIX A

Computing the Azimuth and Elevation Angles of Airplane Cockpit Windows and other Structures from Laser Scans

APPENDIX A: Computing the Azimuth and Elevation Angles of Airplane Cockpit Windows and other Structures from Laser Scans

Azimuth and elevations of "target" aircraft relative to "viewer" aircraft

The "visibility angles" from the "viewer" airplane to the "target" airplane correspond to the angular coordinates of the line of sight between the airplanes, measured in a coordinate system fixed to the viewer airplane (the viewer's "body axis" system), and consist of the azimuth angle and elevation angle (see Figure A1). The azimuth angle is the angle between the x-axis and the projection of the line of sight onto the x-y plane. The elevation angle is the angle between the line of sight itself, and its projection onto the x-y plane. At 0° elevation, 0° azimuth is straight ahead, and positive azimuth angles are to the right. 90° azimuth would be out the right window parallel to the y axis of the airplane. At 0° azimuth, 0° elevation is straight ahead, and positive elevation angles are up. 90° elevation would be straight up parallel to the z axis. The azimuth and elevation angles depend on both the position of the viewer and target airplanes, and the orientation (yaw, pitch, and bank angles) of the viewer.

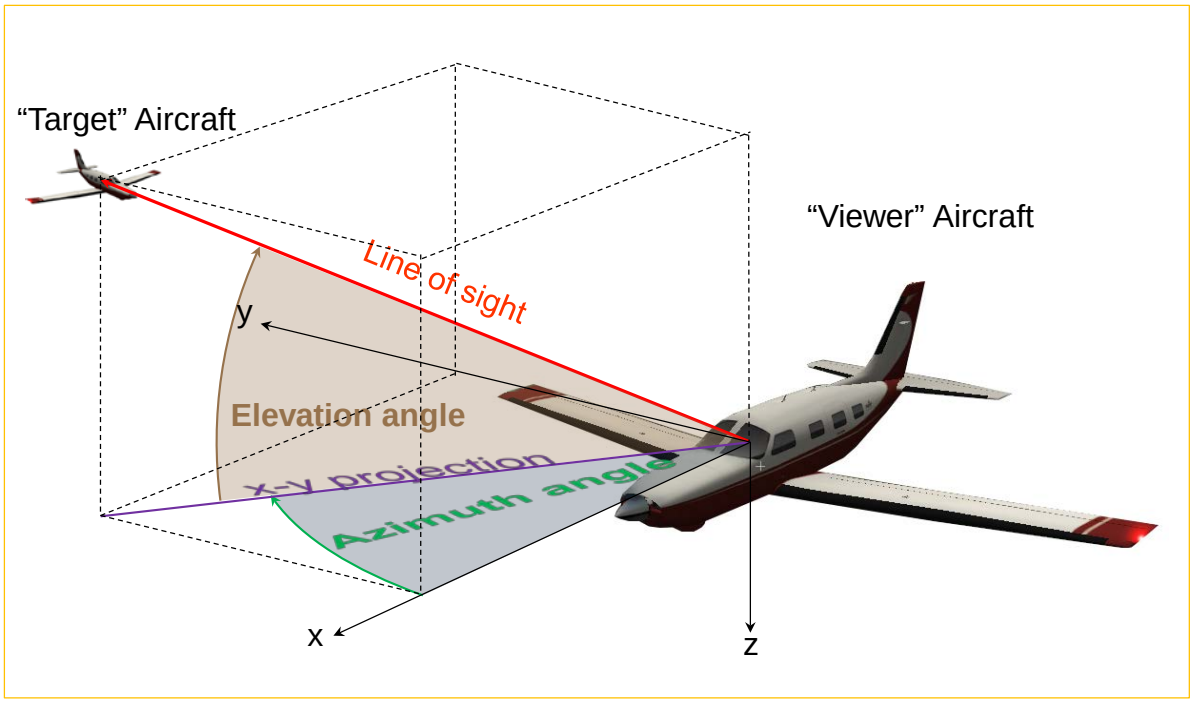

Figure A1. Azimuth and elevation angles from "viewer" airplane to "target" airplane.

The target airplane will be visible from the viewer airplane unless a non-transparent part of the viewer's structure lies in the line of sight between the two airplanes. To determine if this is the case, the azimuth and elevation coordinates of the boundaries of the viewer's transparent structures (windows) must be known, as well as the coordinates of the viewer's structure visible from the cockpit (such as the wings). If the line of sight passes through a non-transparent structure (such as the instrument panel, a window post, or a wing), then the target airplane will be obscured from the viewer.

Azimuth and elevation angles of airplane structures from laser scans

The azimuth and elevation angles of the window boundaries and other structures of the airplane of interest can be determined from the interior and exterior dimensions of the airplane, as measured using a FARO laser scanner.[1] The laser scanner produces a "point cloud" generated by the reflection of laser light off of objects in the laser's path, as the scanner sweeps through 360° of azimuth and approximately 150° of elevation. The 3-dimensional coordinates of each point in the cloud are known, and the coordinates of points from multiple scans (resulting from placing the scanner in different positions) are "merged" by the scanner software[2] into a common coordinate system. By placing the scanner in a sufficient number of locations so that the scanner can "see" every part of the airplane, the complete exterior and interior geometry of the airplane can be defined.

Coordinate transformations: scanner axes to body axes

The scanner software merges the point clouds from multiple scans into a single, "global" coordinate system. By default, this coordinate system is centered at the first scan location, which in general will not be coincident or aligned with the airplane body axis system. Hence, to compute azimuth and elevation angles of the scanned points relative to the pilot's eyes, the following transformations must be accomplished:

1. Translate the scanner global coordinates to the origin of the airplane body axis system.

2. Transform the translated scanner global coordinates into the airplane body axis system using a transformation matrix defined by the three rotations required to align the scanner axis system with the body axis system.

3. Determine the location of the pilot's eyes in the body axis system.

4. Determine the positions of the scanned points relative to the pilot's eyes in the body axis system.

5. Compute the azimuth and elevation angles from the pilot's eyes to the scanned points.

[1] Specifically, the FARO "Focus 3D" scanner; see http://www.faro.com/focus/us.
[2] FARO SCENE software: see http://www.faro.com/focus/us/software.

Note that to accomplish these steps, the following must also be known:

- The scanner global coordinates of the origin of the body axis system
- The three rotation angles between the scanner global coordinates and the body axis system

As will be shown below, these items can be determined from the scanned geometry of the airplane and the following known points:

- The scanner global coordinates at which the body x axis passes through the front and back of the airplane
- The body x coordinates of these points
- The scanner global coordinates of the left and right wingtips
- The body (x,y,z) coordinates of the wingtips

The body coordinates of the points listed above can be determined from technical or scaled drawings of the airplane.

The transformation equations and details of the steps outlined above can be derived starting from the sketch shown in Figure A2, where:

$\vec{R}_{sb}$ = Vector from the origin of the scanner global axis system to the origin of the airplane body axis system

$\vec{R}_{s}$ = Vector from the origin of the scanner global axis system to point *P*

$\vec{R}_{b}$ = Vector from the origin of the airplane body axis system to point *P*

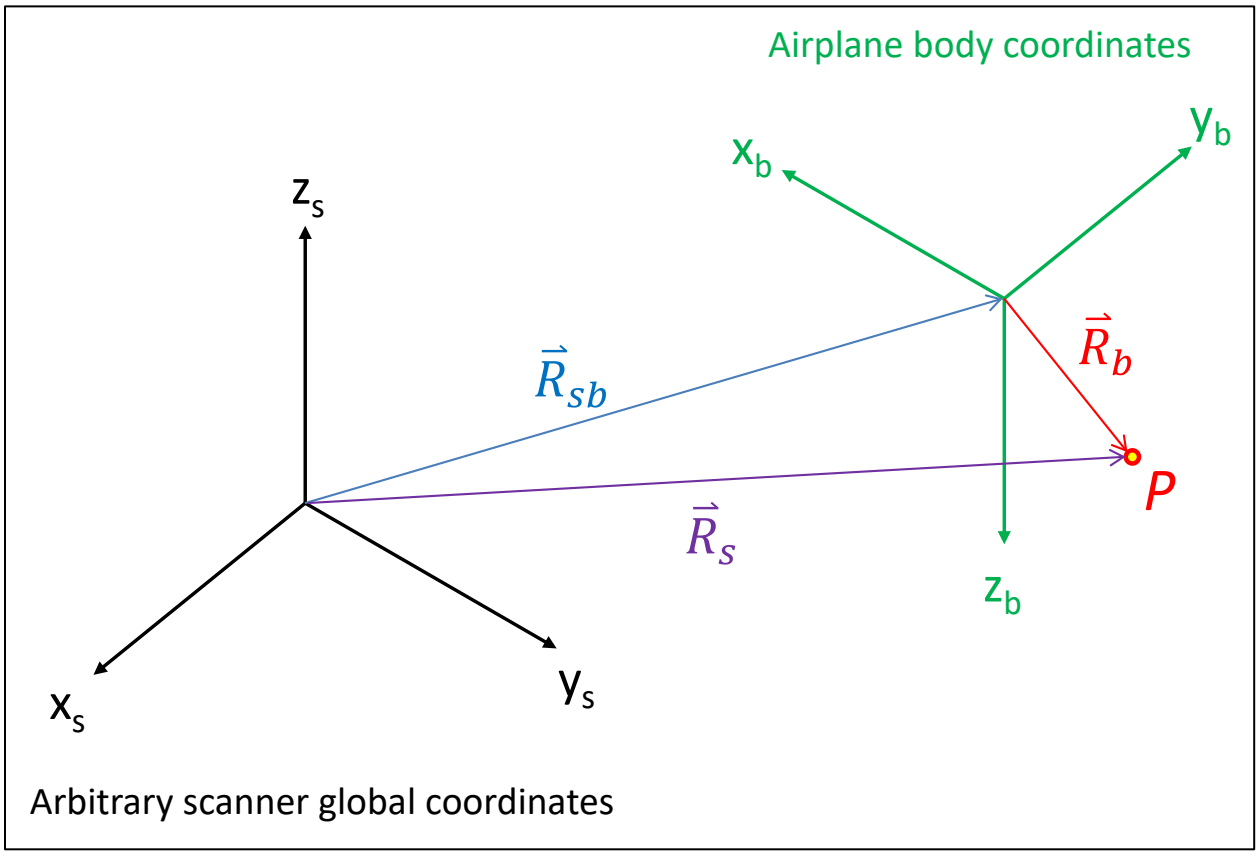

Figure A2. Vectors used to determine coordinates of point P in body axes coordinates.

The vectors $\vec{R}_{sb}$, $\vec{R}_s$, and $\vec{R}_b$ are expressed in the scanner global coordinates. We would like to know the coordinates of point *P* in body axis coordinates; let $\vec{r}_b$ be the vector from the origin of the body axis system to point *P*, expressed in body coordinates. Then, $\vec{r}_b$ is simply $\vec{R}_b$ transformed from scanner global coordinates to body axis coordinates. This transformation can be computed as follows. First, note that:

$\vec{r}_b = \begin{Bmatrix} x \\ y \\ z \end{Bmatrix}_b$ = coordinates of point *P* from body axis origin, in body axes

$\vec{R}_b = \begin{Bmatrix} x \\ y \\ z \end{Bmatrix}_s$ = coordinates of point *P* from body axis origin, in scanner axes

$\vec{R}_s = \begin{Bmatrix} x_s \\ y_s \\ z_s \end{Bmatrix}_s$ = coordinates of point *P* from scanner axis origin, in scanner axes

$\vec{R}_{sb} = \begin{Bmatrix} x_{sb} \\ y_{sb} \\ z_{sb} \end{Bmatrix}_s$ = coordinates of body axis origin from scanner axis origin, in scanner axes

From Figure A2,

$$\vec{R}_b = \vec{R}_s - \vec{R}_{sb} = \begin{Bmatrix} x_s \\ y_s \\ z_s \end{Bmatrix}_s - \begin{Bmatrix} x_{sb} \\ y_{sb} \\ z_{sb} \end{Bmatrix}_s = \begin{Bmatrix} x \\ y \\ z \end{Bmatrix}_s \quad \text{[A1]}$$

Equation [A1] translates the coordinates of point *P* from the origin of the scanner axis system to the origin of the body axis system, which is step 1 in the procedure outlined above. The coordinates are transformed into the body axis system (step 2 in the procedure) using a transformation matrix:

$$\vec{r}_b = [T_{sb}]\vec{R}_b \quad \text{[A2a]}$$

Or, equivalently,

$$\begin{Bmatrix} x \\ y \\ z \end{Bmatrix}_b = [T_{sb}] \begin{Bmatrix} x \\ y \\ z \end{Bmatrix}_s \quad \text{[A2b]}$$

Where $[T_{sb}]$ is the transformation matrix from the scanner axis system to the body axis system. This transformation matrix is defined by a series of three rotations of the scanner axis system, in the following order:

1. A rotation about the z_s axis through the angle ψ, yielding axes $(x_s', y_s', z_s' = z_s)$.
2. A rotation about the y_s' axis through the angle θ, yielding axes $(x_s'', y_s'' = y_s', z_s'')$.
3. A rotation about the x_s'' axis through the angle ϕ, yielding axes $(x_b = x_s'', y_b, z_b)$.

There is a transformation matrix associated with each of these rotations; the elements of the matrices are sines or cosines of the rotation angles involved. Combining these transformations through matrix multiplication yields the final transformation matrix $[T_{sb}]$:

$$[T_{sb}] = \begin{bmatrix} \cos\theta\cos\psi & \cos\theta\sin\psi & -\sin\theta \\ \sin\phi\sin\theta\cos\psi - \cos\phi\sin\psi & \sin\phi\sin\theta\sin\psi + \cos\phi\cos\psi & \sin\phi\cos\theta \\ \cos\phi\sin\theta\cos\psi + \sin\phi\sin\psi & \cos\phi\sin\theta\sin\psi - \sin\phi\cos\psi & \cos\phi\cos\theta \end{bmatrix} \quad \text{[A3]}$$

The details of these operations can be found in textbooks about airplane dynamics (or other subjects associated with rigid body dynamics and coordinate transformations).[3]

[3] See, for example, Roskam, Jan: Airplane Flight Dynamics and Automatic Flight Controls, Part I (Roskam Aviation and Engineering Corporation, 1979), pp. 24-27.

The reverse transformation (from airplane body axes to scanner axes) follows from Equations [A2a] and [A2b]:

$$\vec{R}_b = [T_{sb}]^{-1}\vec{r}_b = [T_{sb}]^T\vec{r}_b \qquad \text{[A4a]}$$

$$\begin{Bmatrix} x \\ y \\ z \end{Bmatrix}_s = [T_{sb}]^{-1}\begin{Bmatrix} x \\ y \\ z \end{Bmatrix}_b = [T_{sb}]^T\begin{Bmatrix} x \\ y \\ z \end{Bmatrix}_b \qquad \text{[A4b]}$$

Because the transformation matrix $[T_{sb}]$ is orthogonal, its inverse is equal to its transpose.

Note that Equations [A1], [A2b] and [A3] involve the coordinates of the origin of the body axis system in scanner axes $\{x_{sb}, y_{sb}, z_{sb}\}_s$, and the three rotation angles ψ, θ, and ϕ, which are all unknown and must be determined.

The coordinates $\{x_{sb}, y_{sb}, z_{sb}\}_s$ can be determined from the body axis coordinates of the points where the body x axis intersects the front and back of the airplane. It is assumed that these points are known from technical drawings of the airplane. It is also assumed that the location of these points can also be identified in the scanned point cloud by comparing the scan results to the technical drawings of the airplane, and that therefore the scanner coordinates $\{x_s, y_s, z_s\}_s$ of the points, measured from the scanner axis origin, can be determined using the scanner software.

Let $\{x_{sn}, y_{sn}, z_{sn}\}_s$ be the coordinates of the intersection of the body x axis with the front (nose) of the airplane, measured from the scanner axis origin, in scanner axes, as determined from the examination of the scanned point cloud using the scanner software.

Let $\{x_{st}, y_{st}, z_{st}\}_s$ be the coordinates of the intersection of the body x axis with the back (tail) of the airplane, measured from the scanner axis origin, in scanner axes, as determined from the examination of the scanned point cloud using the canner software.

The distance along the body x axis from nose to tail is then

$$l_{nt} = \sqrt{(x_{sn} - x_{st})_s^2 + (y_{sn} - y_{st})_s^2 + (z_{sn} - z_{st})_s^2} \qquad \text{[A5]}$$

Since the ratio of the distance between the body axis origin and the nose (i.e., $(x_n)_b$) to l_{nt} is the same in both the scanner and body axis coordinate systems, the scanner coordinates of the body axis origin, measured from the scanner axis origin, are given by

$$\begin{Bmatrix} x_{sb} \\ y_{sb} \\ z_{sb} \end{Bmatrix}_s = \begin{Bmatrix} x_{sn} \\ y_{sn} \\ z_{sn} \end{Bmatrix}_s + \left[\begin{Bmatrix} x_{st} \\ y_{st} \\ z_{st} \end{Bmatrix}_s - \begin{Bmatrix} x_{sn} \\ y_{sn} \\ z_{sn} \end{Bmatrix}_s \right] \frac{(x_n)_b}{l_{nt}} \quad [A6]$$

There remains to determine the rotation angles ψ, θ, and ϕ. From Equation [A4b],

$$\begin{Bmatrix} x_n \\ y_n \\ z_n \end{Bmatrix}_s = \begin{Bmatrix} x_{sn} \\ y_{sn} \\ z_{sn} \end{Bmatrix}_s - \begin{Bmatrix} x_{sb} \\ y_{sb} \\ z_{sb} \end{Bmatrix}_s = [T_{sb}]^T \begin{Bmatrix} x_n \\ y_n \\ z_n \end{Bmatrix}_b \quad [A7]$$

Where $\{x_n, y_n, z_n\}_s$ are the coordinates of the nose measured from the body origin in scanner axes, and $\{x_n, y_n, z_n\}_b$ are the coordinates of the nose measured from the body origin in body axes. From Equations [A7] and [A3],

$$\{z_{sn} - z_{sb}\}_s = (-\sin\theta)\{x_n\}_b + (\sin\phi\cos\theta)\{y_n\}_b + (\cos\phi\cos\theta)\{z_n\}_b \quad [A8]$$

Since by definition the "nose" lies on the x body axis, $(y_n)_b = (z_n)_b = 0$, and Equation [A8] gives

$$\theta = \sin^{-1}\left(\frac{-\{z_{sn} - z_{sb}\}_s}{\{x_n\}_b}\right) \quad [A9]$$

Similarly, Equations [A7] and [A3] with $(y_n)_b = (z_n)_b = 0$ give

$$\{x_{sn} - x_{sb}\}_s = (\cos\theta\cos\psi)\{x_n\}_b \quad [A10]$$

$$\{y_{sn} - y_{sb}\}_s = (\cos\theta\sin\psi)\{x_n\}_b \quad [A11]$$

And therefore

$$\psi = \cos^{-1}\left(\frac{\{x_{sn} - x_{sb}\}_s}{\{x_n\}_b\cos\theta}\right) \quad [A12]$$

$$\psi = \sin^{-1}\left(\frac{\{y_{sn} - y_{sb}\}_s}{\{x_n\}_b\cos\theta}\right) \quad [A13]$$

These two equations for ψ allow the proper quadrant for ψ to be determined.

To solve for the remaining rotation angle (ϕ), the coordinates of the wingtips can be used. Let $\{x_{sl}, y_{sl}, z_{sl}\}_s$ be the coordinates of the left wingtip, measured from the scanner axis origin, in scanner axes, as determined from the examination of the scanned point cloud

using the scanner software. Similarly, let $\{x_{sr}, y_{sr}, z_{sr}\}_s$ be the corresponding coordinates for the right wing. The coordinates of the wingtips in body coordinates, measured from the body axis origin, are

$\begin{Bmatrix} x_r \\ y_r \\ z_r \end{Bmatrix}_b = \begin{Bmatrix} x_w \\ y_w \\ z_w \end{Bmatrix}_b$ for the right wing, and

$\begin{Bmatrix} x_l \\ y_l \\ z_l \end{Bmatrix}_b = \begin{Bmatrix} x_w \\ -y_w \\ z_w \end{Bmatrix}_b$ for the left wing.

From Equation [A4b],

$$\begin{Bmatrix} x_r \\ y_r \\ z_r \end{Bmatrix}_s = \begin{Bmatrix} x_{sr} \\ y_{sr} \\ z_{sr} \end{Bmatrix}_s - \begin{Bmatrix} x_{sb} \\ y_{sb} \\ z_{sb} \end{Bmatrix}_s = [T_{sb}]^T \begin{Bmatrix} x_w \\ y_w \\ z_w \end{Bmatrix}_b \quad [A14]$$

$$\begin{Bmatrix} x_l \\ y_l \\ z_l \end{Bmatrix}_s = \begin{Bmatrix} x_{sl} \\ y_{sl} \\ z_{sl} \end{Bmatrix}_s - \begin{Bmatrix} x_{sb} \\ y_{sb} \\ z_{sb} \end{Bmatrix}_s = [T_{sb}]^T \begin{Bmatrix} x_w \\ -y_w \\ z_w \end{Bmatrix}_b \quad [A15]$$

Then, from Equations [A14], [A15], and [A3],

$$\{z_{sr} - z_{sb}\}_s = (-\sin\theta)\{x_w\}_b + (\sin\phi\cos\theta)\{y_w\}_b + (\cos\phi\cos\theta)\{z_w\}_b \quad [A16]$$

$$\{z_{sl} - z_{sb}\}_s = (-\sin\theta)\{x_w\}_b + (\sin\phi\cos\theta)\{-y_w\}_b + (\cos\phi\cos\theta)\{z_w\}_b \quad [A17]$$

Solving Equations [A16] and [A17] for $\cos\phi$ gives

$$\cos\phi = \frac{\{z_{sl}-z_{sb}\}_s+\{z_{sr}-z_{sb}\}_s+2(\sin\theta)\{x_w\}_b}{2(\cos\theta)\{z_w\}_b} \quad [A18]$$

Solving Equations [A16] and [A17] for $\sin\phi$ gives

$$\sin\phi = \frac{\{z_{sr}-z_{sl}\}_s}{2(\cos\theta)\{y_w\}_b} \quad [A19]$$

$\cos\phi$ and $\sin\phi$ then define the proper quadrant for ϕ, and ϕ itself. Now, Equations [A1], [A2b] and [A3] can be used to compute the body axis coordinates of any scanned point, starting from the scanner coordinates of that point.

Azimuth and elevation angles from body axis coordinates

Once the coordinates of the scanned points are available in the body axis system, the azimuth and elevation angles of these points relative to the pilot's eye position can be computed. In keeping with the previous notation, let $\{x_e, y_e, z_e\}_b$ be the body-axis coordinates of one of the pilot's eyes,[4] and $\{x_P, y_P, z_P\}_b$ be the body-axis coordinates of a point *P*. Then the distance from the eye to point *P* is

$$l_{eP} = \sqrt{(x_P - x_e)_b^2 + (y_P - y_e)_b^2 + (z_P - z_e)_b^2} \quad \text{[A20]}$$

The azimuth angle from the eye to the point *P* is

$$\Psi = \tan^{-1}\left[\frac{(y_P - y_e)}{(x_P - x_e)}\right] \quad \text{[A21]}$$

The elevation angle from the eye to the point *P* is

$$\Theta = -\sin^{-1}\left[\frac{(z_P - z_e)}{l_{eP}}\right] \quad \text{[A22]}$$

[4] Note that the pilot's left and right eyes are in slightly different positions, so these calculations should be made for each eye.

APPENDIX B

Creating Geometrically Correct Cockpit Window “Masks” in Microsoft Flight Simulator X (*FSX*)

APPENDIX B: Creating Geometrically Correct Cockpit Window "Masks" in Microsoft Flight Simulator X (*FSX*)

Field of view vs. FSX screen display coordinates

The geometry of an airplane's cockpit windows and other structures can be defined in terms of their azimuth and elevation angles (Ψ and Θ, respectively) from the pilot's eyes. The visual systems of flight simulation programs, such as *FSX*, include a "cockpit view" that similarly displays the cockpit and other airplane structures from the "pilot's point of view." The *FSX "*virtual cockpit,*"* in particular, depicts a 3-dimensional model of the airplane interior from the pilot's seat (or any other point at which a "camera" is placed). The 3D model can be explored by rotating and / or translating the camera from the pilot's eye position.

While many airplane models for *FSX* include "virtual cockpits" that are very convincing and satisfactory for gaming or flight training purposes, the geometrical accuracy of these models is unknown, and so they are not suitable for determining whether outside objects would be visible or obscured in the real airplane in any particular scenario. *FSX* also includes a simple "2D cockpit" view, which presents a forward-looking scene of the outside world, overlaid with an instrument panel that is a compromise between realism, and the desire to have all the necessary flight instruments (and a sufficiently large out-the-window view) visible to the user at the same time, given limited screen real estate. These "2D cockpits" are necessarily less representative of the real airplane than the "virtual cockpits." However, the default 2D cockpit instrument panel can be substituted with a user-created "panel" that correctly represents the pilot's view of the cockpit and airplane structures in the real airplane, as determined from the airplane geometry measured with a laser scanner (see Appendix A). This "geometrically correct" panel can be used to determine whether an object outside the airplane is obstructed from the pilot's view.

The custom panel created by the user is a whole-screen instrument panel that contains transparent and non-tranparent areas. The transparent areas correspond to areas of the windows that offer unobstructed views of the outside world; the non-transparent areas correspond to everything else (cockpit structure, and exterior structure visible from the cockpit that obstructs the outside view). The "panel" is simply a 1024 x 768 bitmap image file, in which transparent areas are defined by assigning pixels a particular color (e.g., black) that *FSX* interprets as "transparent." Hence, the coordinates and color of the pixels in the bitmap file define the shapes of the panel transparent and non-transparent areas.

However, while the scope of the scene of the outside world displayed on the screen is defined in terms of angular and vertical “fields of view,” the screen coordinates of objects “seen” by the camera (including the cockpit windows) are not simply proportional to the angular Ψ and Θ coordinates of those objects from the camera positon. Instead, the screen coordinates of an object correspond to the points where the line of sight from the camera to the object intercepts a flat surface (the screen) placed some distance R between the camera and the object, as shown in Figure B1 (this Figure, and the discussion below, is adapted from Reference B1).

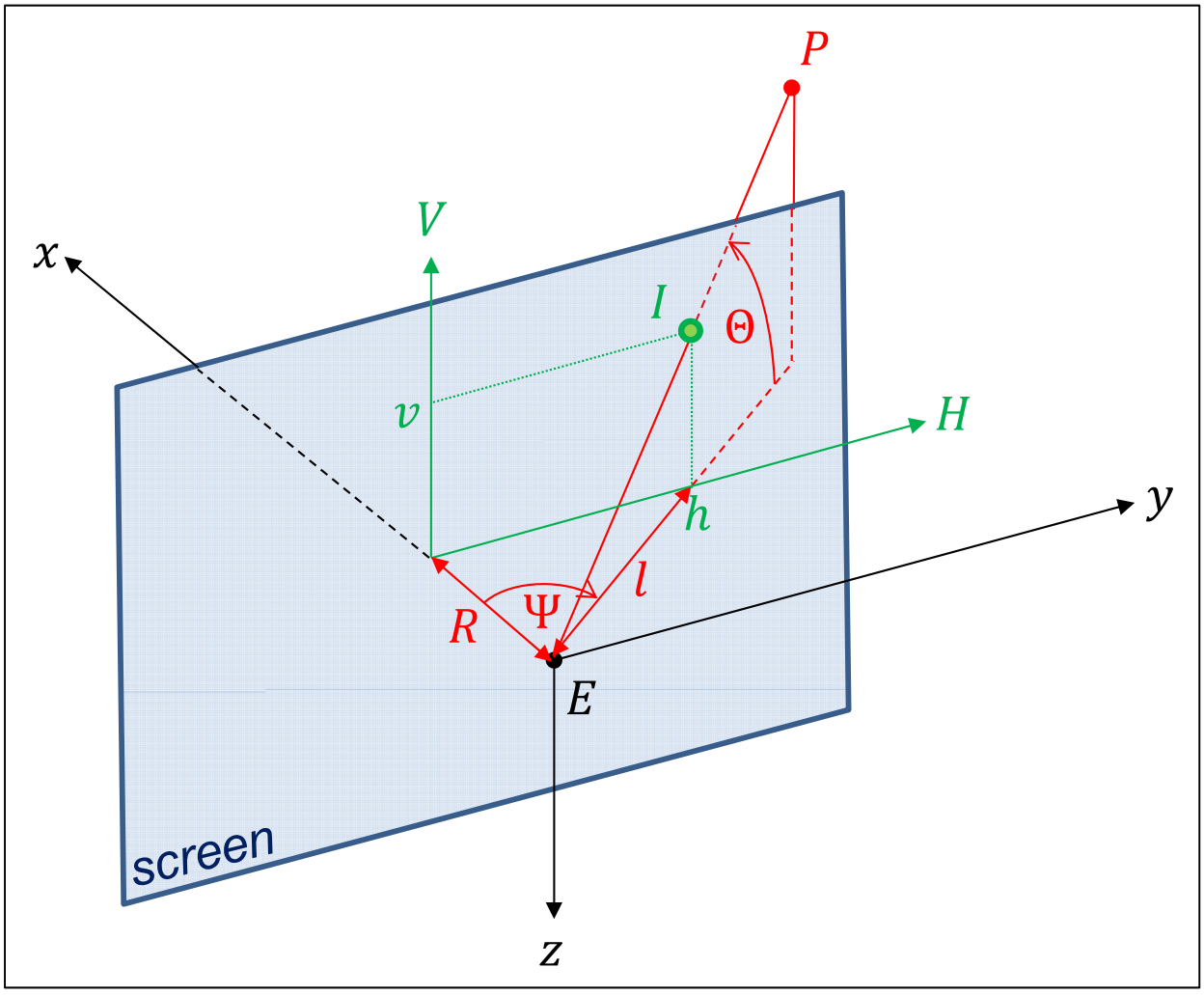

Figure B1. Relationships between the (Ψ, Θ) viewing angles of the line of sight from E to P (EP), and the (h, v) screen coordinates of the point I, where EP intersects the screen.

In Figure B1,

E = location of viewer's eye point (i.e., the camera location in *FSX*);
(x, y, z) = airplane body axis system with origin at E;
P = location of point or object to be drawn on the screen;
EP = line of sight from E to P;
Ψ = azimuth angle of EP;
Θ = elevation angle of EP;
I = point where EP intersects a flat screen placed in the yz plane between E and P;
R = x coordinate of I (i.e., the distance from E to the screen along x axis);
(H, V) = screen horizontal and vertical axis coordinate system, originating where the x body axis intersects the screen;
(h, v) = screen coordinates of I;
l = distance from E to the point defined by screen coordinates $(h, 0)$.

We seek to find the screen coordinates (h, v) at which a point P should be drawn, given the viewing angles (Ψ, Θ) from E to P.

From the geometry of Figure B1,

$$h = R \tan \Psi \qquad \text{[B1]}$$

$$l = \sqrt{R^2 + h^2} = \sqrt{R^2 + R^2 \tan^2 \Psi} = R\sqrt{1 + \tan^2 \Psi} \qquad \text{[B2]}$$

$$v = l \tan \Theta = R \tan \Theta \sqrt{1 + \tan^2 \Psi} \qquad \text{[B3]}$$

Consequently, (h, v) can be computed from (Ψ, Θ) once the distance R is known. R can be determined in *FSX* if the angular range of the horizontal field of view ($HFOV$) and the width of the screen in pixels (w) are known. For example, at the right edge of the screen, $h = w/2$, and $\Psi = HFOV/2$. Then, from Equation [B1],

$$R = \frac{(w/2)}{\tan(HFOV/2)} \qquad \text{[B4]}$$

Unfortunately, determining the exact $HFOV$ in *FSX* is not straightforward. $HFOV$ is modified by the *FSX* "zoom" level (smaller zoom yields greater $HFOV$), but the quantitative relationship between the zoom and $HFOV$ is not specified in any *FSX* documentation. However, both the $HFOV$ and vertical $VFOV$ in *FSX* can be determined by experiment, using a method presented in Reference 2 and described below.

Determining the field of view in FSX

Reference 2 describes how to modify *FSX* .FLT files to customize the geometry (size, shape, and screen location) of *FSX* windows (in which visual scenes are displayed), and to control the cameras used to view the world in each window. Significantly, the camera position, orientation, and zoom level can be defined in the .FLT files.

The field of view of a window of a given shape and zoom level can be determined by creating a second window of similar shape and zoom level adjacent to the first. The camera in the second window is then rotated until the scene at the edge where the two windows meet match. The rotation of the camera required to accomplish this is known. Furthermore, the azimuth angle from the second camera to the common edge is half of the $HFOV$, and since the two windows are the same size, it is also half of the camera rotation angle. Hence, the $HFOV$ is simply the rotation angle of the camera required to match the scene at the window edges (see Figure B2). This method can also be used to determine the $VFOV$.

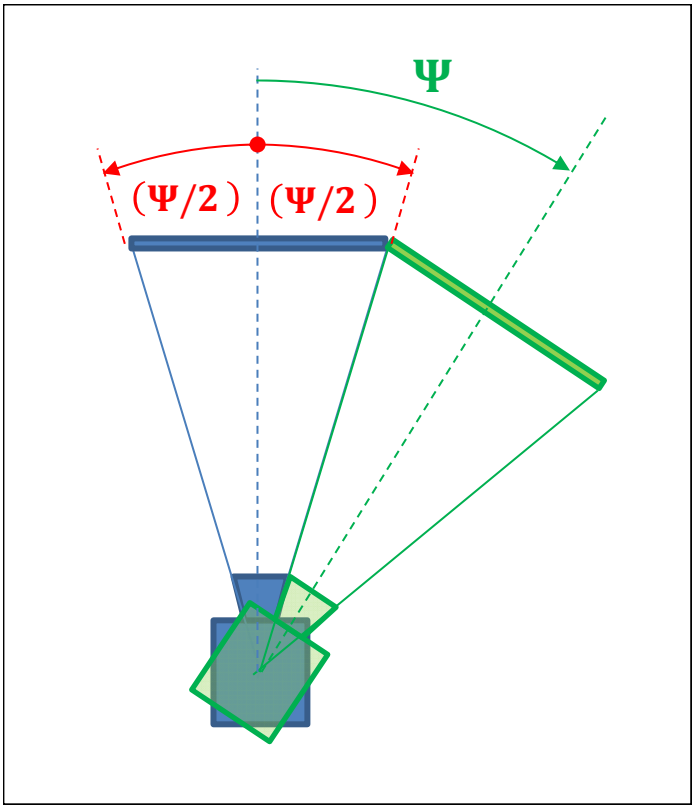

Figure B2. Determining the $HFOV$ by rotating a second (green) camera through angle Ψ to match the scene at the boundary of the view from the first (blue) camera.

Experiments with this method indicate that the $HFOV$ in *FSX* is a function of the window aspect ratio (width / height), as well as the *FSX* zoom level. Results using a window of aspect ratio of 1.6 and a zoom of 0.3 are shown in Figure B3. In this case, the $HFOV$ is 90° and the $VFOV$ is 61.8°. Per Equation [B4], R in this case would be equal to $w/2$.

Creating the FSX *instrument panel "mask" bitmap file*

With the value of R determined as described above, Equations [B1] and [B3] can be used to convert the (Ψ, Θ) viewing angles of the cockpit window structures into the (h, v) screen coordinates at which they should be drawn in order to be consistent with the outside scenery drawn by *FSX*. Once the (h, v) coordinates are in hand, the bitmap file defining the full-screen instrument panel "mask" can be created.

These bitmaps were created for this *Study* as follows.

1. First, the (h, v) coordinates of the windows were plotted into a graph with boundaries set equal to the horizontal and vertical resolution of the computer screen (i.e., the horizontal scale ranged from $-w/2$ to $+w/2$, and the vertical scale ranged from $-h/2$ to $+h/2$, where w is the screen width in pixels and h is the screen height in pixels); see Figure B4.
2. An image of the plot created in step 1 was pasted into Microsoft *PowerPoint*, and the graphical tools in *PowerPoint* were used to create a grey background covering the entire plot area, with black-filled polygons depicting the unobstructed areas of the window transparencies (see Figure B5).
3. The *PowerPoint* image was pasted into the *GIMP2* image-manipulation program, and resized to 1024 x 768, as required by *FSX.*
4. The *FastStone Photo Resizer 3.2* program was used to change the color depth of the bitmap to "4 (2 bit)." This step successfully compresses the bitmap into an "8 bit file," as required by *FSX*.
5. The bitmap is specified in the *FSX panel.cfg* file for the desired airplane model. In addition, the windows that are to use the panel (with camera rotations defined to be consistent with the view created in the bitmap file) are created in the *FSX .FLT* files for the "flight" corresponding to the project. Details concerning configuring the *panel.cfg* and .FLT files can be found in the *FSX* Software Development Kit (SDK) documentation, and in Reference 2.

The instrument panel mask constructed per the steps illustrated in Figures B4 and B5 is shown in its finished form within *FSX* in Figure B6.

Figure B3. Application of the method for determining the $HFOV$ illustrated in Figure B2.

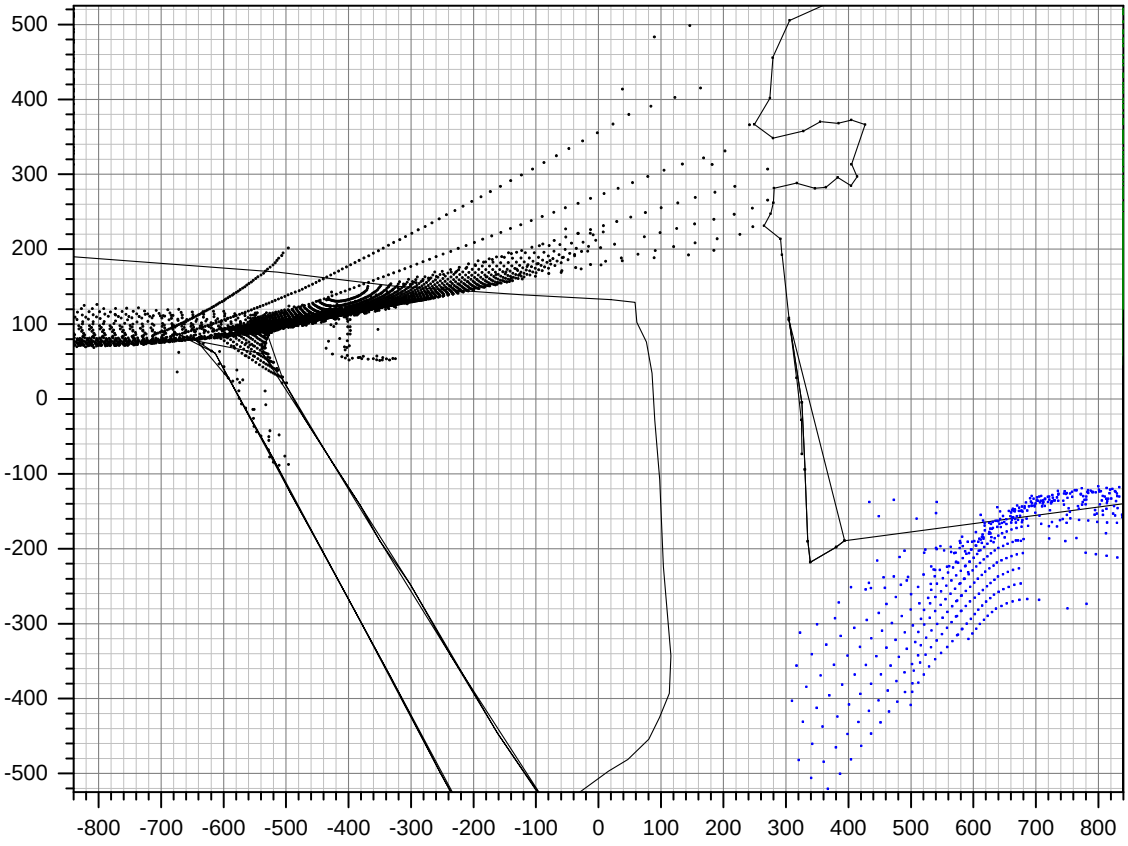

Figure B4. Plot of window v vs. h screen coordinates. The axis scales correspond to screen height and width.

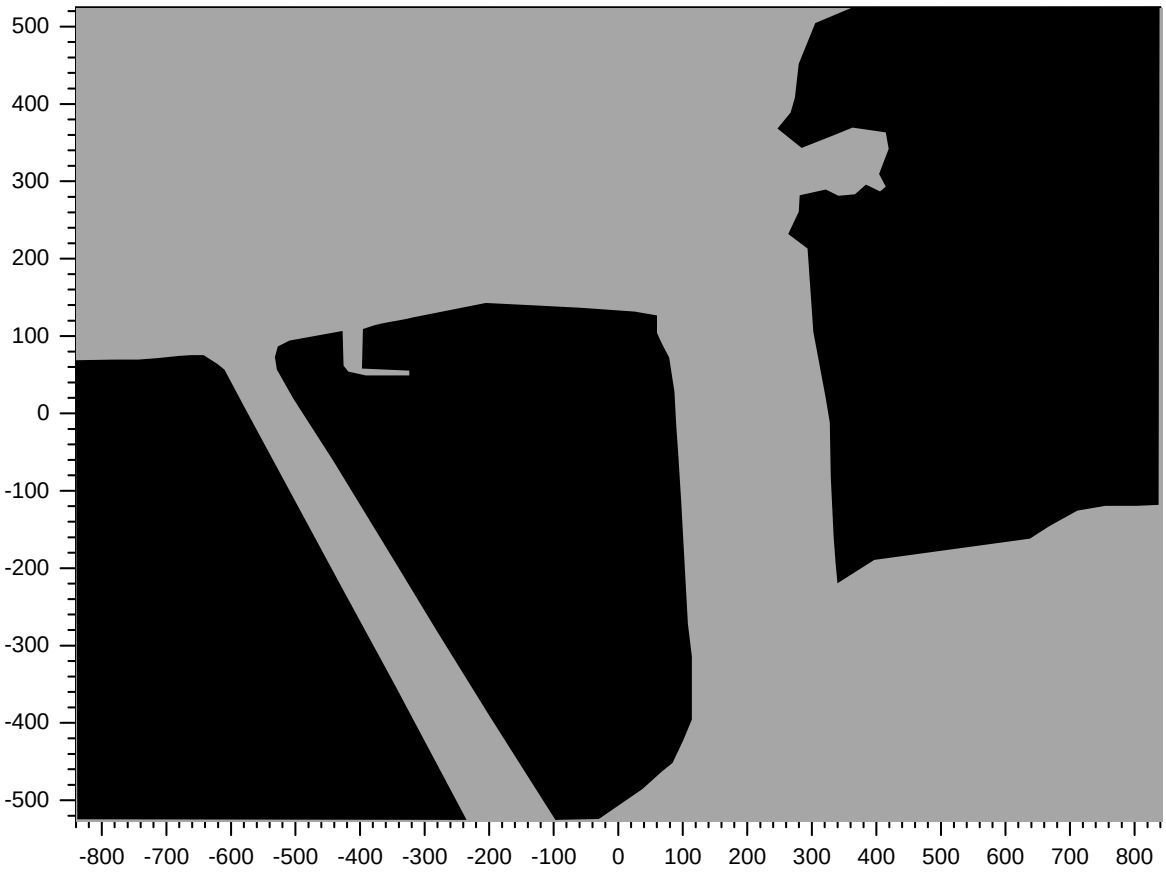

Figure B5. Black color applied to plot of Figure B4 to denote unobstructed window transparencies.

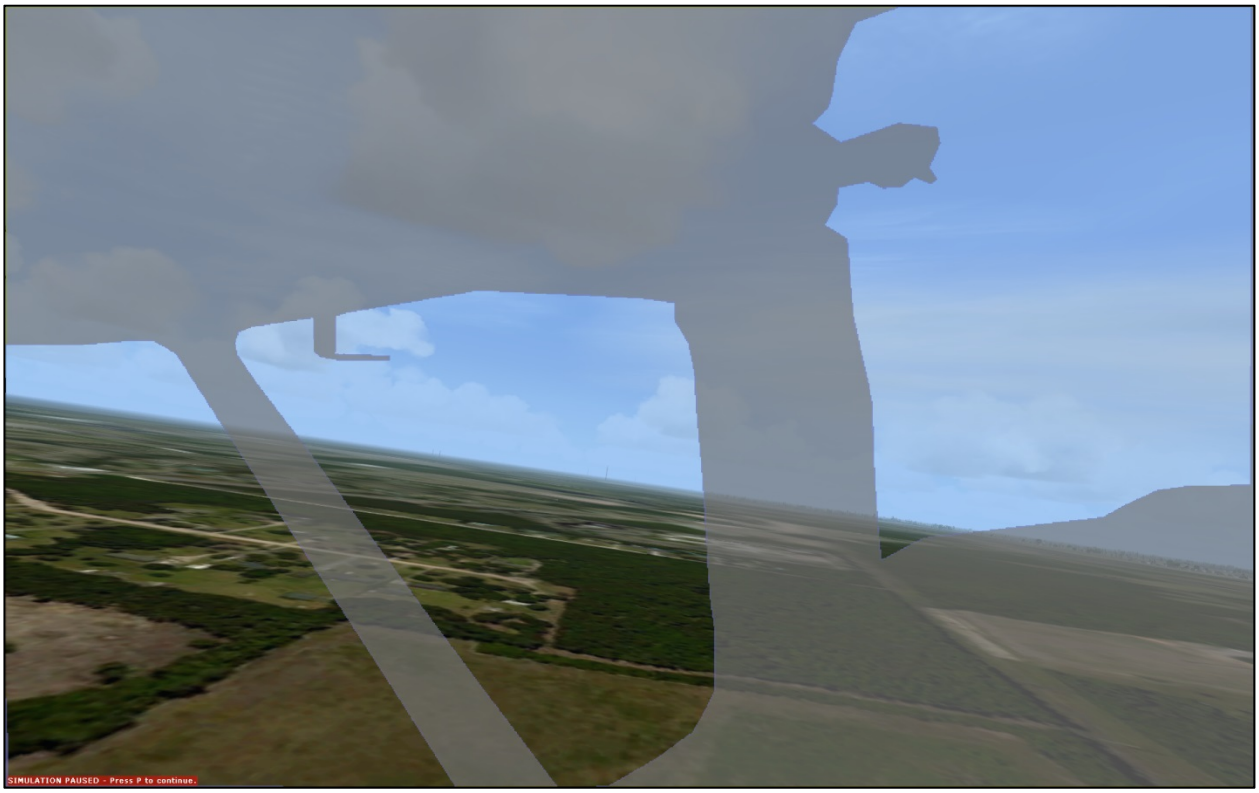

Figure B6. Finished instrument panel mask as it appears in *FSX*, with panel transparency set to 34%.

Joining windows in FSX to create larger field of view

As noted above, the maximum field of view available in a single *FSX* window is 90°, corresponding to the minimum available zoom level of 0.3. In this view, objects beyond an azimuth angle Ψ of ±45° (for a camera pointed straight ahead) will be outside the field of view and not visible.

To see objects beyond ±45° of azimuth while at the same time preserving a field of view of at least ±45° of azimuth about the direction of travel, the view from two co-located cameras can be joined side-by-side, with the second camera pointed in such a way that the boundaries of the fields of view of the cameras coincide at a particular azimuth angle. This method is illustrated in the top two images of Figure B3. In this Figure, the camera in the left image is pointed straight ahead (Ψ = 0°), and the right boundary of its field of view is at Ψ = +45°. The camera in the right image is rotated to Ψ = +90°, and its left boundary is at +90° - 45° = +45° (coinciding with the right boundary of the image on the left). By setting the views from the cameras side-by-side, a continuous field of view from -45° to +135° is obtained.

However, discontinuities (kinks) in straight lines may appear at the boundary of these views when they are viewed side-by-side on a flat surface (such as a computer screen), because the viewer will be viewing both from the same angle, whereas one of the views is intended to be viewed at an angle rotated relative to the other. The discontinuities can be removed if each view is presented on a separate surface (monitor), and then the surfaces are joined at an angle equal to the relative rotation between the cameras (though this may be impractical). The discontinuities are apparent in Figure B3.

To use this method to increase the total field of view, and also use the user-defined instrument panel masks described above, a separate mask must be created for each camera view. In addition, the airplane *model.cfg FSX* file must be modified to comment out the line specifying the airplane interior model, so that this model does not get drawn and the instrument panel masks appear over a scene that only depicts the outside world.

References

1. Diston, Dominic J., *Computational Modeling and Simulation of Aircraft and the Environment, Vol. 1: Platform Kinematics and Synthetic Environment,* p. 58. Copyright © 2009, John Wiley & Sons, Ltd.

2. Hestnes, Ivar, *Visual System Tutorial, Rev. 1.0.* Available at *http://www.google.com/url?sa=t&rct=j&q=&esrc=s&source=web&cd=1&cad=rja&uact=8&ved=0ahUKEwiFkpCX-PDOAhVG7B4KHfVCCtAQFggcMAA&url=http%3A%2F%2Fwww.flightdeck737.be%2Fwp-content%2Fuploads%2F2011%2F03%2FVisual-system-tutorial.pdf&usg=AFQjCNFHJq7T3TRTvT4ylwOAm1PpzJc-Eg*